Mechanical & Aerospace Engineering Theses & Dissertations

Mechanical & Aerospace Engineering

Spring 1987

Finite Element Methodology for Nonlinear Free and Harmonic Forced Vibrations of Beam and Plate Structures

Kamolphan Decha-Umphai
Old Dominion University

FINITE ELEMENT METHODOLOGY FOR NONLINEAR FREE AND
HARMONIC FORCED VIBRATIONS OF BEAM AND PLATE STRUCTURES

by

Kamolphan Decha-Umphai
B.S. March 1979, Khon Kaen University
M.E. December 1981, Old Dominion University

A Dissertation Submitted to the Faculty of
Old Dominion University in Partial Fulfillment of the
Requirements for the Degree of

DOCTOR OF PHILOSOPHY

ENGINEERING MECHANICS

OLD DOMINION UNIVERSITY
May, 1987

Approved by:

Chuh Mei (Director)

Earl A. Thornton

Stephen G. Cupschalk

Jean W. Hou

J. M. Dorrepaal

ABSTRACT

FINITE ELEMENT METHODOLOGY FOR NONLINEAR FREE AND
HARMONIC FORCED VIBRATIONS OF BEAM AND PLATE STRUCTURES

Kamolphan Decha-Umphai
Old Dominion University, 1987
Director: Dr. Chuh Mei

The literature and experiments have shown that nonlinear vibrations produce significant effects in structural analysis, especially the frequency-amplitude-force relation and the analysis of strain. An analysis was developed to predict both the frequency-amplitude-force relation and strains of beam and plate structures. The analysis was based on the use of finite element methodology for beam and plate structures. Two finite element methods were developed, namely, the iterative single-mode method (method I) and the multiple-mode method (method II). The harmonic force matrix was developed to analyze nonlinear forced vibrations. Nonlinear free vibration was a special case of the general forced vibration by setting the harmonic force matrix equal to zero. The harmonic force matrix represents the external applied force in matrix form, instead of a vector form, so that the analysis of nonlinear force vibrations can be performed as an eigenvalue problem. By solving an eigenvalue problem, the analysis can be performed efficiently to get a converged solution. The analysis was also based on the linearized nonlinear stiffness matrix and the

iterative procedures. Both inplane (longitudinal) displacement and lateral deflection are included in the formulation.

The study showed that the effect of midplane stretching due to large deflection is to increase the nonlinearity. However, the effects of inplane displacements and inertia (IDI) are to reduce nonlinearity. The concentrated force case yields a more severe response than the uniform distributed force case. For beams and plates with end supports restrained from axial movement (immovable case) only the hardening type nonlinearity is observed. For beams with large slenderness ratio (L/R<100) with movable end supports, the increase in nonlinearity due to large deflection is partially compensated by a reduction in nonlinearity due to inplane displacement and inertia. This leads to a negligible hardening type nonlinearity, therefore, the small deflection linear solution can be employed. However, for beams with a small slenderness ratio (L/R = 20) and movable end supports, the softening type nonlinearity is found. The effect of the higher modes is more pronounced for the clamped supported beam than the simply supported one. The beam without inplane displacement and inertia (IDI) yields more effect of the higher modes than the one with inplane displacement and inertia. For beams, the iterative single-mode method (method I) and the multiple-mode method (method II) converge into a true deflection shape, provided the number of modes for the multiple-mode method (method II) is high enough. Similarly, both the iterative single-mode method (method I) and the multiple-mode method (method II) yield accurate strains provided the number of modes for the multiple-mode method (method II) is high enough.

ACKNOWLEDGEMENTS

The author is grateful to Professor Chuh Mei, Chairman of his Advisory Committee, for his many suggestions, encouragement and moral support throughout this effort. He also wishes to thank Professor Earl A. Thornton and all members of the Advisory Committee for their many helpful suggestions.

The author wishes to acknowledge the generous support of the National Aeronautics and Space Administration, Langley Research Center, and the permission to use material obtained from research at the Langley Research Center, in this dissertation. Thanks are due many people at the Langley Research Center who made this effort possible. In particular, the supports of Dr. J. M. Housner and Mr. J. Walz throughout the program are appreciated.

Finally, the attainment of any worthwhile goal cannot be achieved without patience, understanding and love. The sacrifices made by my parents, Mr. and Mrs. Kasem Decha-Umphai, and my wife, Jiraprapa, cannot be repaid. This dissertation is dedicated to them.

ii

TABLE OF CONTENTS

LIST OF TABLES

vi

vii

viii

LIST OF FIGURES

x

LIST OF SYMBOLS

a	length of rectangular plate
$\bar{a}$	length of rectangular plate element
$\{a\}$	generalized coordinates in Eq. (4.59)
A	amplitude (maximum deflection)
A_i	amplitude of the i-th linear mode shape
$\bar{A}$	beam cross-sectional area
$\bar{A}_0$	dimensionless amplitude for plate $= w_{max}/h$
$\{A_0\}$	amplitude normal coordinate vector in Eq. (3.22)
b	width of rectangular plate
$\bar{b}$	width of rectangular plate element
c	constant in Eqs. (4.107) and (5.67)
$cn\ (\lambda t, \eta)$	Jacobian elliptic cosine function
$[C_0]$	extension material stiffness matrix
d	length of the loaded plate element
$[D_0]$	bending material stiffness matrix
$\{e\}$	membrane strain
E	Young's modulus
f	linearizing function for beam in Eq. (4.67)
$\{f\}$	linearizing function vector in Eq. (5.31)
$f_1,\ f_2$	linearizing functions for plate in Eq. (5.30)
$F(t)$	uniform distributed periodic lateral load
F_0	force intensity (force per unit length for beam; force per unit area for plate)

$g(t)$	modal amplitude in Eq. (4.3)
$[\bar{G}]$	matrix relating generalized coordinates and membrane strains in Eq. (5.48)
h	thickness of beam (or plate)
$[h]$	element harmonic force matrix
$[H]$	system harmonic force matrix
$[\bar{H}]$	matrix relating generalized coordinates and curvatures in Eq. (5.29)
I	area moment of inertia of beam
k	linear stiffness term in Eq. (4.8)
$\bar{k}$	nonlinear stiffness term in Eq. (4.8)
$\bar{k}_{ijrs}$	multiple-mode nonlinear stiffness term in Eq. (4.38)
$[k_L]$	element linear stiffness matrix
$[k_{Lb}]$	beam element linear stiffness matrix relating to lateral deflection in Eq. (4.78)
$[k_{Ls}]$	beam element linear stiffness matrix relating to inplane displacement in Eq. (4.77)
$[k_{NL}]$	element nonlinear stiffness matrix
$[k_{NLb}]$	beam element nonlinear bending stiffness matrix in Eq. (4.83)
$[k_{NLbs}],[k_{NLsb}]$	beam element nonlinear stiffness matrices coupling between bending and stretching in Eqs. (4.84) and (4.85)
$[k_s]$	plate element linear membrane stiffness matrix in Eq. (5.51)
$[\bar{k}_b]$	plate element nonlinear bending stiffness matrix in Eq. (5.52)
$[\bar{k}_{bs}],[\bar{k}_{sb}]$	plate element nonlinear stiffness matrices coupling between bending and membrane stretching in Eqs. (5.53) and (5.54)
$[K_L]$	system linear stiffness matrix
$[K_{Lb}]$	system linear bending stiffness matrix
$[K_{Ls}]$	system linear inplane stiffness matrix

$[K_{NL}]$	system nonlinear stiffness matrix
$[K_{NLb}]$	system nonlinear bending stiffness matrix
$[K_{NLbs}],[K_{NLsb}]$	system nonlinear stiffness matrices coupling between bending and stretching
ℓ	length of a beam element
ℓ_o	length of the loaded beam element
L	length of beam
m	mass term in Eq. (4.8)
$[m]$	element mass matrix
$[m_b]$	element bending mass matrix
$[m_s]$	element inplane mass matrix
$\{M_o\}$	bending and twisting moments
$[M]$	system mass matrix
$[M_b]$	system bending mass matrix
$[M_s]$	system inplane mass matrix
N	inplane force in Eq. (4.7)
$\{N_o\}$	membrane or inplane resultant forces in Eq. (5.5)
P_o^*	nondimensional forcing parameter for plate
$[\bar{Q}]$	matrix relating generalized coordinates and linearizing functions in Eq. (5.30)
R	radius of gyration of beam cross-section
$[RK]$	reduced system stiffness matrix
$[RM]$	reduced system mass matrix
t	time
T	kinetic energy
T_b	kinetic energy due to lateral deflection
T_s	kinetic energy due to inplane displacements
$[T]$	transformation matrix in Eq. (4.61)

xiii

[TRF]	transformation matrix by using the Guyan's reduction technique in Eq. (3.17)
$[\bar{T}_b]$, $[\bar{T}_s]$	matrices relating element nodal displacements and generalized coordinates in Eqs. (5.24) and (5.25)
u, v	inplane displacements
U	strain energy
U_b	strain energy due to bending components in Eq. (5.14)
U_s	strain energy due to membrane components in Eq. (5.15)
U_L	linear strain energy
U_{NL}	nonlinear strain energy
V	potential energy due to a uniform harmonic forcing function
w	lateral deflection
x, y, z	cartesian coordinates
$\{\alpha\}$, $\{\beta\}$	generalized coordinates in Eqs. (5.19) and (5.20)
γ_{xy}	shearing strain
$\{\delta\}$	element nodal displacements
$\{\Delta\}$	eigenvector (system nodal displacements) in Eq. (3.3)
ε	total strain for a beam element in Eq. (4.47)
$\{\varepsilon\}$	total strain for a plate element in Eq. (5.2)
$\{\zeta\}$	eigenvector related to inplane displacement terms in Eq. (3.3)
η	modulus of Jacobian elliptic function
$\{\kappa\}$	curvatures in Eq. (5.4)
λ	circular frequency of Jacobian elliptic function
ν	Poisson's ratio
ρ	mass per unit length
$\bar{\rho}$	mass density

xiv

τ	nondimensional time
$\{\phi\}$	eigenvector related to lateral deflection terms in Eq. (3.3)
$\{\phi_L\}$	normalized linear mode shape
$\{\phi_{Li}\}$	i-th linear mode shape
ψ	stress function
ψ_x	beam curvatures in Eq. (4.46)
ω_L	linear frequency, radians per second
ω_{NL}	nonlinear frequency, radians per second
ω/ω_L	fundamental frequency ratio for plate
ω_{NL1}/ω_{L1}	fundamental frequency ratio for beam

Subscripts:

b	bending
L	linear
NL	nonlinear
s	inplane (membrane) stretching

Chapter 1

INTRODUCTION

1.1 Motivation

In modern engineering, with its continuous refinement of instrumen-
tation, its improved computational capabilities, and the high precision
tolerances, the theory of nonlinear vibrations is gaining more and more
practical meaning. Although it is known that linear vibrations provide
no more than a first order approximation of an actual situation, they
are sufficient for some practical and engineering purposes. However,
the linear theory is inadequate, if the vibration of an elastic body
involves amplitudes that are not very small as assumed in the linear
theory. A nonlinear vibration approach leads to completely new
phenomena which are not possible in linear systems; for example, the
dependence of frequency, or period of vibration, on amplitude which
cannot be handled by using linear analyses. In such cases, nonlinear
theory must be used to obtain more accurate results and to explain new
phenomena. Figure 1 shows the experimental result[1] of a square clamped
panel subjected to normal incidence acoustic impingement. In this
figure, the fundamental mode frequency shifts from about 175 Hz to
somewhere between 230 and 290 Hz. The increase of the fundamental and
higher modal frequencies clearly indicates the presence of inplane
forces in the panel due to large deflections. This type of behavior was
also observed experimentally by Holehouse[2] and White[3].

1

Strain Spectrum for a Clamped Square (10"x10"x.063") Aluminum Plate 7075—T6

NONLINEAR RESPONSE   PANEL 1.063   SG. *10*
REC 14 (130 DB), 2S (142 DB), 41 (160 DB)
                                                          RMS .4616
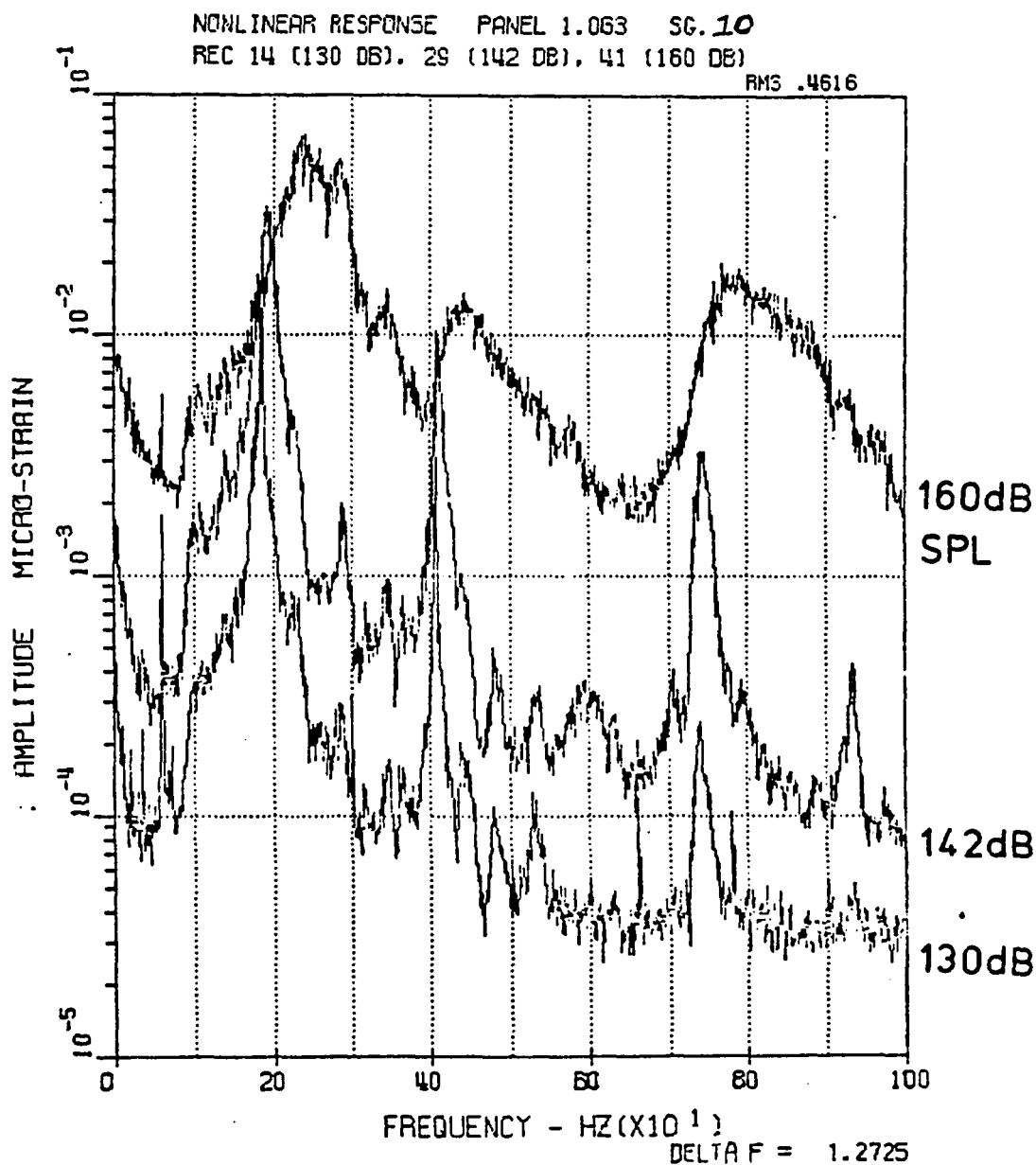
Fig. 1 Strain spectral density functions of a
        square aluminum panel [Ref. 1].

The steadily increasing demand for more realistic models of structural response has resulted in research for solution techniques to deal with nonlinear structural problems. Apart from some very few exceptions, it is generally not possible to provide analytical closed-form solutions for the differential equations occurring in nonlinear vibrations of structures. Naturally, a numerical solution may be obtained when the motion corresponding to certain initial and boundary conditions is to be determined. Because of advances in electronics, modern digital computers have been of great value in solving nonlinear problems.

In general, nonlinearities in structural mechanics problems can arise in several ways. When material behavior is nonlinear, a generalized Hooke's law is no longer valid. This type of nonlinearity is called "material" or "physical" nonlinearity. Alternatively, material behavior can be assumed to be linear, but structural deformation can become large and cause nonlinear strain-displacement relations. Deformation of a structural member can also reach a magnitude that does not overstrain the material; in such a case, curvature of the deformed median line can no longer be expressed by a linear equation. Problems involving large structural deformation are called "geometrically" nonlinear problems. Combination of material nonlinearity and geometric nonlinearity is also possible.

1.2 Literature Review

Any large-amplitude deflection of a beam which is restrained axially at its two ends results in some midplane stretching. This stretching must be considered in the formulation which can be

accomplished by using a nonlinear strain-displacement relationship (geometric nonlinearity). The nonlinear equation of motion describing this situation has been the basis of a number of investigations. Most of these works are based on a single-mode approach. Woinowsky-Krieger[4] considered the effect of an axial force on the vibration of hinged bars. The vibration of an extensible bar, carrying no transverse load and having the ends fixed at the supports, caused an axial tensile force with a period equal to the half-period of the transverse vibration of the bar. The Jacobian elliptic function was used to produce the relation of frequency and amplitude of vibration. Eringen[5] studied the nonlinear free vibrations of elastic bars having immovable hinged ends. The solution was accomplished by the use of a perturbation method. The ratio of a nonlinear period over a linear period of vibration and axial stress was shown against initial deflection. Only the hardening type nonlinearity was found. Burgreen[6] studied the nonlinear free vibrations of a pin-ended column whose ends were pinned to points fixed in space. This imposed the condition of a constant end distance instead of the usual theoretical assumption that the axial load in the column remained constant along the beam length. The exact solution was obtained by using the Jacobian elliptic function. He also found thaa the frequency was dependent upon the amplitude of vibration, the effect of the amplitude of vibration becoming more pronounced as the Euler load was approached in which the classical linear theory yielded the frequency of vibration as zero. Woodall[7] considered the nonlinear free vibrations of a thin elastic beam. In his formulation, a fixed inertial reference frame and a Lagrangian description of the motion were employed. By assuming the motion to be inextensional and, at the same

time, admitting the existence of a resultant normal force acting on each cross-section of the beam, a system of governing equations was obtained. The solutions of the simply-supported beam were obtained by using three methods: the finite difference method, a perturbation technique and the Galerkin weighted residual method. For the particular example considered in his paper, the finite difference solution appeared to be stable, even for oscillations involving angular rotations at the ends of the beam which reached the order of magnitude of 80°. Furthermore, he found that the Galerkin approximate solution was in closer agreement with the finite difference solution than the perturbation solution. Raju et al.[8] studied free flexural vibrations of a simply-supported beam when a compatible longitudinal or inplane mode was coupled with the fundamental flexural mode. The Rayleigh-Ritz method was employed. The results showed that the effects of longitudinal displacement and inertia were to reduce the nonlinearity in the flexural frequency-amplitude relationship. Tseng and Dugundji[9] investigated a straight beam with fixed ends excited by a periodic motion at its supporting base in a direction normal to the beam span. By using Galerkin's method, the governing partial differential equation was reduced to the well-known Duffing equation. The harmonic balance method was applied to solve the Duffing equation. Pandalai[10] investigated the case of straight beams, irrespective of the boundary conditions, the nonlinearity was found to be of the hardening type. He further concluded that only the hardening type existed. Later, Atluri[11] showed that there were some cases for which the softening type nonlinearity is possible. He investigated the large amplitude transverse vibration of a hinged bar with one end of the beam free to

move longitudinally. The equation was solved by the perturbation procedure of multiple-time scales. The calculated results showed that the predominant nonlinear effect was due to longitudinal inertia which was of the softening Duffing type. This result was in contrast to the earlier analyses where a hardening nonlinearity had been predicted when the only nonlinearity considered was the effect of average midplane stretching due to the out-of-plane deflection.

Through the foregoing studies, the general features of the nonlinear response of beams under harmonic excitation seem to have been clarified. However, most of the actual calculations are based on a one-term approximation for the spatial function while the interactions between the modes with amplitude are not addressed. Corresponding to this phenomena, the effect of multiple modes on the beam response is needed. Because of the complexity in the formulation, there are very few investigations on multiple-mode analysis in the literature.

McDonald[12] apparently was the first to consider modal interactions. The considered investigation was the vibration of a uniform beam with hinged ends which were restrained. The beam was subjected to a concentrated lateral force at the mid-span and then released from rest at the deflected position. The nonlinear effect in this investigation was produced by the axial stretching of the beam. By assuming a multiple-mode expansion corresponding to the deflected position, the elliptic function procedure was performed to evaluate the coefficients related to the participation of each mode. Bennett and Eisley[13] investigated the steady-state free and forced responses and stability for large amplitude nonlinear vibration of a beam with clamped ends. The general equations for response and stability were derived.

By applying Galerkin's method, a set of nonlinear ordinary differential equations was obtained. The solution of forced vibration was evaluated by the method of harmonic balance. Later, Bennett[14] considered the problem involving the ultraharmonic response of a simply supported beam. Tseng and Dugundji[15] also used a multiple-mode expansion in considering the forced response of a clamped beam about its buckled configuration. The buckled beam was excited by the harmonic motion at its supporting base. By using Galerkin's method, the governing partial differential equation was reduced to a modified Duffing equation which was solved by the harmonic balance method. Srinivasan[16] solved free and forced responses of beams undergoing moderately large amplitude steady-state oscillations by the averaging method of Ritz. The application of Ritz's method to solve the governing nonlinear partial differential equation yielded nonlinear algebraic equations instead of nonlinear ordinary differential equations. To solve these nonlinear algebraic equations, the Newton's method or bigradient matrix method had to be employed. The method was shown by assuming the first two symmetric modes of the linear system for the deflection of beam. It was clear that the method yielded as many simultaneous nonlinear algebraic equations as the number of modes included. Nayfeh et al.[17] proposed a numerical-perturbation method for the determination of nonlinear forced response of beams. The deflection curve of the beam was represented with a multiple-mode expansion in terms of the linear modes. Then the temporal problem was solved by the method of multiple scales, and internal resonances were also considered. Van Dooren and Bouc[18] considered the nonlinear transverse vibrations of a uniform beam with ends restrained and forced transversely by a two-mode function which was

harmonic in time. A simply supported beam was considered by the two-mode approach. Approximate solutions were found by using Urabe's numerical method applied to Galerkin's procedure and by an analytical harmonic balance-perturbation method. The existence of a sub-harmonic response of the order 1/3 and a harmonic response in the sub-harmonic region of the forcing function was proved. Takahashi[19] analyzed the inextensible clamped-free and free-free beams by using Galerkin's method and the harmonic balance method. Yamaki and Mori[20] investigated nonlinear forced vibrations of a clamped beam under uniformly distributed periodic lateral loading with the effects of both initial deflection and initial axial displacement taken into consideration. The problem was first reduced to that of a finite degree-of-freedom system with the Galerkin procedure, the steady-state solutions of which were obtained by applying the harmonic balance method. Actual calculation was carried out for the three degree-of-freedom system with symmetric modes. Yamaki et al.[21] also performed experiments to compare to the analytic results. The test results were reported in the root-mean-square of deflection instead of the actual deflection of beam.

Generally, the classical approach to solve nonlinear vibrations of a beam is to start with the so-called assumed mode shape. By employing the Galerkin's method, the governing nonlinear partial differential equation of motion is reduced to a system of nonlinear ordinary differential equations. The elliptic function, perturbation method or numerical methods can then be employed to solve the problem.

Following von Karman's large deflection plate theory, the basic governing equations for the nonlinear vibration of plates were established by Herrmann.[22,23] Nonlinear forced vibrations of circular

and rectangular plates with various boundary conditions had also been investigated by using the Galerkin or Ritz method[16,24-28], the Kantorovich averaging method[29,30], various perturbation methods[31-34], and an incremental harmonic balance method.[35] Studies based on the simplified Berger's hypotheses[36] had also been investigated by using the Galerkin method.[37,38]

In practice, many optimum or minimum-weight designed structures are complex. Because of the versatility of the finite element method, it is more suitable to use this method to analyze complex structures. Mei[39] investigated nonlinear vibration of beams by a matrix displacement method. Nonlinear free vibrations of various boundary conditions were investigated and good agreements were obtained between the finite element method and other numerical methods. Rao et al.[40] studied the large amplitude free oscillations of beams and orthotropic circular plates. Their finite element formulation was based on an appropriate linearization of the nonlinear strain-displacement relations. Simply supported and clamped beams were investigated. Comparison of their results with the earlier work confirmed the reliability and effectiveness of the linearization of the strain-displacement relations. Reddy and Singh[41] investigated the large-deflection analysis of thin elastic curved beams by conventional and mixed finite element methods. The conventional finite element method was based on the total potential energy expression, whereas the mixed method was based on a Reissner-type variational statement and involved the bending moments and deflections as primary dependent variables. From their result, it appeared that, in general, the mixed method yielded more accurate results. Recently, Mei and Decha-Umphai[42-44] developed the harmonic

force matrix for solving nonlinear forced vibrations of beams and plates by the finite element method. By employing the linearizing method[45] and so-called "single-mode" approach, the frequency-amplitude-force relations were obtained. There are very few attempts to solve nonlinear vibrations of beam using the finite element method with multiple-mode expansion. Busby and Weingarten[46] investigated beams of simply supported and clamped boundary conditions. Their finite element technique was performed only to obtain the nonlinear differential equations of the straight beam and the method of averaging was then used to obtain an approximate solution. Cheung and Lau[47] investigated the two-mode nonlinear vibration of beams. The essence of their method could be regarded as an incremental harmonic balance method associated with a finite strip procedure in the time-space domain. Unfortunately, the works reported in Refs. 46 and 47 could not be exactly classified as finite element method.

The accuracy of the theoretical predictions would not be completed unless the experimental studies had been compared. Bennett and Eisley[13] performed the experiment of a clamped beam to compare with their theoretical results. Tseng and Dugundji[9] conducted the experiment of a straight beam with fixed ends which was excited by the periodic motion of its supporting base in a direction normal to the beam span. These two experiments were found to compare favorably with the corresponding theoretical predictions. However, these experiments were carried out with special kinds of excitations, e.g. supporting base excitation. Yamaki et al.[21] performed the experimental studies of a clamped beam under a uniformly distributed periodic load. Besides the reasonable agreement with the theoretical predictions,[20] their experimental results

seem to provide effective data facilitating further theoretical analyses.

Applications of the finite element method to large amplitude free vibration of rectangular plates was first presented by Mei.[48] The inplane tensile force induced by the transverse deflection alone was assumed to be constant for each individual plate element. Nonlinear frequencies of rectangular plates with various boundary conditions agreed well with the approximate continuum solutions of Chu and Herrmann[23], and Yamaki[25]. Rao et al.[40] proposed a novel scheme of linearizing the nonlinear strain-displacement relations in formulating the nonlinear stiffness matrix. They studied nonlinear free vibrations of circular plates[49] and rectangular plates.[50,51] Shear deformation and rotary inertia were also included in the formulation.[52,53] Reddy and Stricklin[54] presented a linear and a quadratic isoparametric rectangular element using the linearized Reissner-type variational formulation to study large amplitude free plate vibrations. Inplane displacements were considered in their formulation. Two triangular elements have also been developed for nonlinear free vibrations of plates of arbitrary shape. The first one[55] is consistent with the higher-order bending element TRPLT1[56] in NASTRAN, and the second one[57] is consistent with the high-precision plate element of Cowper et al.[58] The solutions obtained for numerical examples include rectangular, circular, rhombic and isosceles triangular plates. Reddy and Chao[59,60] extended the earlier isoparametric rectangular elements to include transverse shear and laminated composite materials. Mei et al.[61] also extended the earlier triangular element to include laminated composite materials.

Bhashyan and Prathap[62] and Sarma and Varadan[63,64] also presented a Galerkin and a Lagrange-type finite element formulation for nonlinear free vibrations of beams with ends restrained from longitudinal movement. They obtained frequency values at the instant of maximum amplitude which was based on a new criterion for defining nonlinear frequency presented in Refs. 65 and 66. However, the results (Refs. 62 to 65) do not agree with those classic continuum solutions (Refs. 4 and 67). What they actually solved is a linear beam vibration problem subjected to an initial axial tensile force as commented on in reference 68.

It is clear that a substantial amount of literature exists on nonlinear vibrations of beams and plates. Eisley[69] published a review on nonlinear analyses of beams concerning the classical methods. Sathyamoorthy[70,71] published two excellent survey articles on nonlinear analyses of beams, one of which dealt with literature concerning classical nonlinear methods and another one dealt with the finite element method. Chia[72] and Sathyamoorthy[73] had presented their comprehensive reviews on free and forced nonlinear vibrations of plates.

1.3 Scope of Dissertation

Through the foregoing studies, the general features of the nonlinear free and forced vibrations of beams and plates have been largely clarified. However, modern structures are complex and the more accurate theoretical predictions are preferred, therefore, the multiple-mode approach has to be considered in the formulation of nonlinear vibration problems. Since the evolution of digital computers, the finite element method has become widely used to solve many types of

complex structures. It is the purpose of this research to present the finite element methodology using single and multiple-mode approaches for analysis of nonlinear vibrations of structures.

In this dissertation, the finite element methodology for nonlinear free and harmonic force vibrations of beam and plate structures are studied. Both out-of-plane deflection and inplane displacements are included in the formulation. The concepts of the finite element method for nonlinear free vibrations and the methodology for solving the harmonic forced nonlinear vibrations are provided in Chap. 2. In Chap. 3, the solution procedures for the iterative single-mode method (method I) and the multiple-mode approach (method II) are presented. In Chap. 4, the classical method is provided to review the concepts of nonlinear forced vibrations of beams. By using the concepts of the classical method, the derivation of the harmonic force matrix is given in this chapter. Also, the finite element formulation for nonlinear forced vibration of beam, and the nonlinear stiffness matrices using the linearizing method[45] are derived in this chapter. In Chap. 5, the finite element formulation for nonlinear forced vibration of plates is presented. In Chap. 6, beams and plates with various out-of-plane and inplane boundary conditions are investigated. The definition of the inplane boundary condition is also explained. The relations of frequency and amplitude for various boundary conditions and loads are tabulated and plotted. Results are also compared to other classical or experimental results whenever available. The convergence criteria are also studied. Chapter 7 gives the concluding remarks.

Chapter 2

FINITE ELEMENT METHOD

2.1 Basic Concepts

The finite element method is a numerical analysis technique for obtaining approximate solutions to problems by idealizing the continuum model as a finite number of discrete regions called elements. These elements are connected at points called nodes where normally the dependent variables such as displacements and mode shapes are determined. Numerical computations for each individual element generate element matrices which are then assembled to form system matrices to represent the entire problem. In the case of nonlinear vibration, these system matrices are the set of characteristic equations. Generally, the more elements used, the greater the accuracy of the results. Accuracy, however, can be affected by factors such as the type of element selected to represent the continuum, and the sophistication of element interpolation functions.

2.2 Finite Element Nonlinear Vibration Analysis

Once the type of elements and their interpolation functions (polynomial expansions) have been selected, the matrix equations of the individual element (element matrices) are evaluated. In nonlinear vibration analysis, the conservation of energy is employed to evaluate the element matrices.

14

In general, the kinetic energy T for an element can be represented in a quadratic form as

$$T = \frac{1}{2} \{\dot{\delta}\}^T [m] \{\dot{\delta}\} \tag{2.1}$$

where $[m]$ denotes an element mass matrix and $\{\delta\}$ denotes an element nodal displacements vector. A dot denotes differentiation with respect to time.

The strain energy U for an element can be separated into two parts as

$$U = U_L + U_{NL} \tag{2.2}$$

where U_L denotes the linear strain energy and U_{NL} denotes the nonlinear strain energy. The linear strain energy U_L can be represented into a quadratic form as

$$U_L = \frac{1}{2} \{\delta\}^T [k_L] \{\delta\} \tag{2.3}$$

where $[k_L]$ is an element linear stiffness matrix. Similarly, the nonlinear strain energy U_{NL} using the linearizing method[45] can be represented into a quadratic form as

$$U_{NL} = \frac{1}{2} \{\delta\}^T [k_{NL}] \{\delta\} \tag{2.4}$$

where $[K_{NL}]$ is an element nonlinear stiffness matrix.

The application of Lagrange's equation to the kinetic energy T and the strain energy U leads to the element nonlinear free vibration equation of motion as

$$[m]\{\ddot{\delta}\} + [[k_L] + [k_{NL}]]\{\delta\} = 0. \tag{2.5}$$

For the nonlinear forced vibration, the methodology is to relate the force to the potential energy. This potential energy, V, due to a uniform harmonic forcing function can be represented as

$$V = \frac{1}{2} \{\delta\}^T [h]\{\delta\} \tag{2.6}$$

where [h] denotes an element harmonic force matrix. The derivation of Eq. (2.6) is presented in detail in Chap. 4.

The application of Lagrange's equation to the kinetic energy T, the strain energy U and the potential energy V leads to the element nonlinear force vibration equation of motion as

$$[m]\{\ddot{\delta}\} + [[k_L] + [k_{NL}] - [h]]\{\delta\} = 0. \tag{2.7}$$

The essence of this methodology is to solve the nonlinear forced vibration problem in the same way as solving the nonlinear free vibration problem. The frequency-amplitude-force relationships can be solved from Eq. (2.7) as an eigenvalue problem. The expressions of the element mass matrix [m], the linear stiffness matrix $[k_L]$ and the nonlinear stiffness matrix $[k_{NL}]$ for beam and plate structures are shown in Chaps. 4 and 5, respectively.

Chapter 3

SOLUTION PROCEDURES

In this chapter, the solution procedures of the finite element methodology are explained in detail. There are two methods, namely, the iterative single-mode method (method I) which is the iterative process of a single mode, and the multiple-mode method (method II) which is the combination of the linear mode shapes. Each method employs the iterative process to get a converged solution. The solution procedures for each method are divided into two major parts, namely, the small deflection part which is the linear solution, and the large amplitude part which is the nonlinear solution. Each part consists of minor steps which evaluate the element and system matrices. The iterative process for the large amplitude part is also explained. The convergence criteria are provided and convergence characteristics are shown in figures. Finally, the computer flow-charts of the solution procedures for both methods are provided.

3.1 Method I: Iterative Single-Mode Method

3.1.1 Small Deflection Linear Solution

A linear solution is performed to evaluate the linear eigenvalues (frequencies) and linear eigenvectors (mode shapes).

17

The application of Lagrange's equation to the kinetic energy, Eq. (2.1), and the linear strain energy, Eq. (2.3), leads to the element equation of motion for linear free vibrations as

$$[m]\{\ddot{\delta}\} + [k_L]\{\delta\} = 0 \qquad (3.1)$$

where $[m]$ and $[k_L]$ are the element mass and linear stiffness matrices, respectively. These matrices are shown in Chaps. 4 and 5 for the beam and plate elements, respectively. After all element mass and stiffness matrices of a given structure are computed, the equation of motion for the system can be assembled as

$$[M]\{\ddot{\Delta}\} + [K_L]\{\Delta\} = 0 \qquad (3.2)$$

where $[M]$ and $[K_L]$ denote the system mass and linear stiffness matrices, respectively, $\{\Delta\}$ is the eigenvector which consists of contributions from the lateral deflection terms and the inplane displacement terms. This eigenvector $\{\Delta\}$ can be expressed as

$$\{\Delta\} = \begin{Bmatrix} \{\phi\} \\ \{\zeta\} \end{Bmatrix} \qquad (3.3)$$

where $\{\phi\}$ is the eigenvector related to the lateral deflection terms which are w and $w_{,x}$ for a beam structure, and w, $w_{,x}$, $w_{,y}$ and $w_{,xy}$ for a plate structure. The eigenvector $\{\zeta\}$ is related to the inplane displacement terms which are u and $u_{,x}$ for a beam structure, and u and v for a plate structure.

The equation of motion for the system, Eq. (3.2), can be rewritten as

$$\begin{bmatrix} M_b & 0 \\ 0 & M_s \end{bmatrix} \begin{Bmatrix} \{\ddot{\phi}\} \\ \{\ddot{\zeta}\} \end{Bmatrix} + \begin{bmatrix} K_{Lb} & 0 \\ 0 & K_{Ls} \end{bmatrix} \begin{Bmatrix} \{\phi\} \\ \{\zeta\} \end{Bmatrix} = 0 \qquad (3.4)$$

where $[M_b]$, $[M_s]$, $[K_{Lb}]$ and $[K_{Ls}]$ are the bending system mass matrix, the inplane system mass matrix, the linear bending system stiffness

matrix and the linear inplane system stiffness matrix, respectively. In the linear system, the bending and inplane parts are uncoupled. By using the bending part of Eq. (3.4), the system equation of motion for bending only can be expressed as

$$[M_b]\{\ddot{\phi}\} + [K_{Lb}]\{\phi\} = 0 \ . \tag{3.5}$$

Equation (3.5) can be rewritten in the eigenvalue problem as

$$\omega_L^2 \ [M_b]\{\phi_L\} = [K_{Lb}]\{\phi_L\} \tag{3.6}$$

where ω_L is the linear frequency (eigenvalue) and $\{\phi_L\}$ is the corresponding linear mode shape. The linear mode shape $\{\phi_L\}$ is normalized with the transverse deflection at the middle of beam (or center of plate) to be unity.

3.1.2 Large Amplitude Nonlinear Solution

In this section, the nonlinear free and forced vibrations are presented. The iterative procedure for nonlinear solution is explained.

After the linear mode shape has been determined (see Section 3.1.1, Small Deflection Linear Solution), the nonlinear solution can be performed. By using the corresponding normalized linear mode shape, Eq. (3.6), the deflection shape $\{\Delta\}$ for the first iteration is expressed as

$$\{\Delta\} = A \ \{\Delta\}_0 = A \begin{Bmatrix} \{\phi\}_0 \\ \{\zeta\}_0 \end{Bmatrix} \tag{3.7}$$

where A is the known amplitude (maximum deflection) and $\{\phi\}_0$ is the corresponding normalized linear mode shape. $\{\zeta\}_0$ is the zero vector. Because of the simplicity for understanding the iterative process, the

subscript o is used for the linear mode shape. It should be noted that $\{\phi\}_o$ is exactly the same as $\{\phi_L\}$ in Eq. (3.6).

By using Eq. (3.7), the deflection shape of each element $\{\delta\}$ can be found. The linearizing function, f, for each beam element ($\{f\}$ for each plate element) is determined. The linearizing function is expressed in Chaps. 4 and 5 for the beam and plate elements, respectively. After the linearizing function has been determined, the element nonlinear stiffness matrix $[k_{NL}]$ for each element can be evaluated. The expression of $[k_{NL}]$ is expressed in Chap. 4 for a beam element and Chap. 5 for a plate element. The harmonic force matrix $[h]$ can be determined as expressed in Chaps. 4 and 5 for a beam and plate element, respectively.

The application of Lagrange's equation to the kinetic energy, Eq. (2.1), the linear strain energy, Eq. (2.3), the nonlinear strain energy, Eq. (2.4), and the potential energy due to the uniform harmonic forcing function, Eq. (2.6), leads to the element equation for nonlinear forced vibrations as

$$[m]\{\ddot{\delta}\} + [[k_L] + [k_{NL}] - [h]]\{\delta\} = 0 . \tag{3.8}$$

Once the element mass, stiffness and harmonic force matrices have been determined for each element, the equations of motion for the system can be expressed as

$$[M]\{\ddot{\Delta}\} + [[K_L] + [K_{NL}] - [H]]\{\Delta\} = 0 \tag{3.9}$$

where $[K_{NL}]$ and $[H]$ are the system nonlinear stiffness and system harmonic force matrices, respectively. Equation (3.9) can be written as

$$\begin{bmatrix} M_b & 0 \\ 0 & M_s \end{bmatrix}\begin{Bmatrix} \{\ddot{\phi}\} \\ \{\ddot{\varsigma}\} \end{Bmatrix} + \begin{bmatrix} \begin{bmatrix} K_{Lb} & 0 \\ 0 & K_{LS} \end{bmatrix} + \begin{bmatrix} K_{NLb} & K_{NLbs} \\ K_{NLsb} & 0 \end{bmatrix} - \begin{bmatrix} H & 0 \\ 0 & 0 \end{bmatrix} \end{bmatrix}\begin{Bmatrix} \{\phi\} \\ \{\varsigma\} \end{Bmatrix} = 0 \qquad (3.10)$$

where $[K_{NLb}]$ is the nonlinear bending system stiffness matrix. $[K_{NLbs}]$ and $[K_{NLsb}]$ are the nonlinear system matrices which are coupled between bending and stretching. Equation (3.9) is in the form of an eigenvalue problem which can be expressed as

$$\omega^2_{NL} \; [M]\{\Delta\}_1 = [[K_L] + [K_{NL}] - [H]]\{\Delta\}_1 \qquad (3.11)$$

where ω_{NL} is the nonlinear frequency and $\{\Delta\}_1$ is the corresponding normalized mode shape of the first iteration. By using $\{\Delta\}_1$, the improved deflection shape for the second iteration can be expressed as

$$\{\Delta\} = A \; \{\Delta\}_1 \; . \qquad (3.12)$$

By using Eq. (3.12) instead of Eq. (3.7), the second iteration is performed from that point onward to obtain the improved nonlinear frequency ω_{NL} and deflection shape. This iterative process can be repeated until a convergence criterion (Section 3.3) is satisfied. Then the last converged deflection shape can be used to evaluate the maximum strain (or stress). It should be noted that the nonlinear stiffness matrix $[k_{NL}]$ and the harmonic force matrix $[h]$ are updated at each iteration. The flow-chart of this solution procedure is shown in Fig. 2.
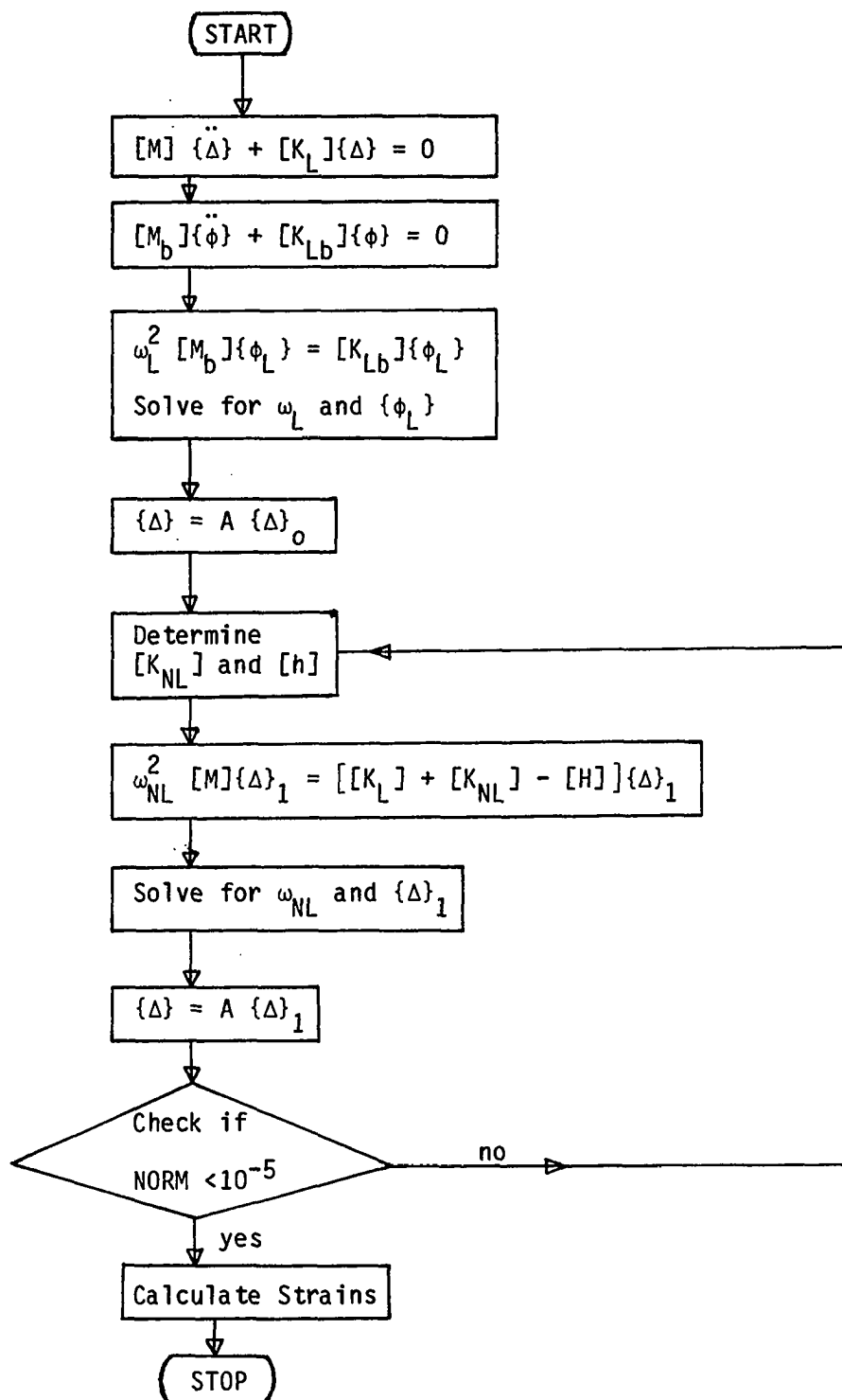
Fig. 2 Computer flow-chart (solution procedures) of
the iterative single-mode method (method I)

3.2 Method II: Multiple-Mode Method

3.2.1 Small Deflection Linear Solution

The procedure for the linear solution of the multiple-mode method is exactly the same as the one for the linear solution of the iterative single-mode method (Section 3.1.1). By performing the calculations from Eq. (3.1) to Eq. (3.6), the linear frequency (eigenvalue) and the corresponding linear mode shape normalized to unity at the middle of beam are evaluated. However, it should be pointed out that for each linear frequency, there is a corresponding linear mode shape. For example, the first linear frequency ω_{L1} corresponds to $\{\phi_{L1}\}$, ω_{L2} corresponds to $\{\phi_{L2}\}$, $\cdots$, and ω_{Ln} corresponds to $\{\phi_{Ln}\}$.

Through the foregoing procedure, the linear solution for free vibration of beam is obtained. The linear frequencies, ω_{L1}, ω_{L2}, $\cdots$, ω_{Ln} and the corresponding linear mode shapes, $\{\phi_{L1}\}$, $\{\phi_{L2}\}$, $\cdots$, $\{\phi_{Ln}\}$, have been evaluated. These linear mode shapes will be used for multiple-mode approach discussed in the next section.

3.2.2 Large Amplitude Nonlinear Solution

In this section, the multiple-mode nonlinear free and forced vibrations of a beam, determined by the finite element method, are presented. The iterative procedure is explained. The convergence criteria are discussed in Section 3.3.

After the linear mode shapes have been determined (see Section 3.2.1, Small Deflection Linear Solution), the nonlinear solution is performed as follows. By using the first linear mode shape and the

total amplitude A at the middle of the beam, the deflection shape for the first iteration is expressed as

$$\{\phi\} = A \; \{\phi_{L1}\} \; . \tag{3.13}$$

By using Eq. (3.13) the deflection shape of each element $\{\delta\}$ can be found. By using $\{\delta\}$, the linearizing function, f, for each element is determined. After the linearizing function has been determined, the element nonlinear stiffness matrix $[k_{NL}]$ for each element can be evaluated. The integration for obtaining $[k_{NL}]$ is carried out by the extended Simpson's rule with 20 intervals[74].

Next, the element harmonic force matrix [h] is determined. The expressions of the linearizing function and the element matrices are shown in Chap. 4.

The application of Lagrange's equation to the kinetic energy, Eq. (2.1), the linear strain energy, Eq. (2.3), the nonlinear strain energy, Eq. (2.4), and the potential energy due to the uniform harmonic forcing function, Eq. (2.6), leads to the element nonlinear forced vibration equation of a beam under a harmonic forcing function. This element equation of motion is expressed as

$$[m] \; \{\ddot{\delta}\} + [[k_L] + [k_{NL}] - [h]] \; \{\delta\} = 0 \; . \tag{3.14}$$

After the element mass, stiffness and harmonic force matrices have been determined for each element, the equations of motion for the system can be assembled as and expressed as

$$[M] \; \{\ddot{\Delta}\} + [[K_L] + [K_{NL}] - [H]] \; \{\Delta\} = 0 \tag{3.15}$$

where $[K_{NL}]$ and $[H]$ are the system nonlinear stiffness and system harmonic force matrices, respectively. The system equations of motion, Eq. (3.15) can be reduced into displacements containing w and $w_{,x}$. This is accomplished by using Guyan's reduction technique[75]. The definition of $\{\Delta\}$ is defined in Eq. (3.3). This reduced system equations of motion has the form

$$[RM] \{\ddot{\phi}\} + [RK] \{\phi\} = 0 \qquad (3.16)$$

where $[RM]$ denotes the reduced system mass matrix, and $[RK]$ denotes the reduced system stiffness matrix. It should be noted that $[RK]$ consists of not only the reduced system linear and nonlinear stiffness matrices but also the reduced system harmonic force matrix.

In the process of transforming Eq. (3.15) into Eq. (3.16) there exists the relation between the system deflection shape $\{\Delta\}$ and the reduced system deflection shape as [75]

$$\{\Delta\} = [TRF] \{\phi\} \qquad (3.17)$$

where $[TRF]$ is the transformation matrix.

By the definition of the multiple-mode approach, the reduced system deflection shape $\{\phi\}$ is the combination of the linear mode shapes $\{\phi_L\}$ in Eq. (3.6) and their amplitudes. This reduced system deflection shape $\{\phi\}$ can be expressed as

$$\{\phi\} = A_1 \{\phi_{L1}\} + A_2 \{\phi_{L2}\} + \cdots + A_n \{\phi_{Ln}\} \qquad (3.18)$$

where A_i is the amplitude of the i-th linear mode $\{\phi_{Li}\}$, and n is the total number of modes. Equation (3.18) can be rewritten in a matrix form as

$$\{\phi\} = [\{\phi_{L1}\} \ \{\phi_{L2}\} \ \cdots \ \{\phi_{Ln}\}] \begin{Bmatrix} A_1 \\ A_2 \\ \vdots \\ A_n \end{Bmatrix} \tag{3.19}$$

or

$$\{\phi\} = [\phi_0] \ \{A_0\} \tag{3.20}$$

where

$$[\phi_0] = [\{\phi_{L1}\} \ \{\phi_{L2}\} \ \cdots \ \{\phi_{Ln}\}] \tag{3.21}$$

$$\{A_0\} = \begin{Bmatrix} A_1 \\ A_2 \\ \vdots \\ A_n \end{Bmatrix} \ . \tag{3.22}$$

By using Eq. (3.20), Eq. (3.16) can be transformed to the normal coordinates, $\{A_0\}$, and is expressed as

or

$$[\phi_0]^T \ [RM] \ [\phi_0] \ \{\ddot{A}_0\} + [\phi_0]^T \ [RK] \ [\phi_0] \ \{A_0\} = 0 \tag{3.23}$$

$$[RM_0] \ \{\ddot{A}_0\} + [RK_0] \ \{A_0\} = 0 \tag{3.24}$$

Equation (3.24) is in the form of an eigenvalue problem which can be expressed as

$$\omega_{NL}^2 \ [RM_0] \ \{A_0\} = [RK_0] \ \{A_0\} \tag{3.25}$$

where ω_{NL} is the nonlinear frequency. By solving the eigenvalue problem, Eq. (3.25), the nonlinear frequency ω_{NL1} and the eigenvector $\{A_0\}$ can be determined. After the eigenvector $\{A_0\}$ has been obtained the amplitude ratios $\dfrac{A_i}{A_1}$; $i=1,2,\cdots$, n can be determined.

By the definition of multiple-mode approach, Eq. (3.18), the maximum deflection (amplitude) is the summation of amplitudes of all the modes. This can be expressed as

$$A = \sum_{i=1}^{n} A_i \qquad (3.26)$$

or

$$\frac{A}{A_1} = 1 + \sum_{i=2}^{n} \frac{A_i}{A_1} \qquad (3.27)$$

then A_1 can be calculated from

$$A_1 = \frac{A}{1 + \sum_{i=2}^{n} \frac{A_i}{A_1}} . \qquad (3.28)$$

The ratio $\frac{A_i}{A_1}$ is from Eq. (3.25) as mentioned earlier. The value of amplitude for i-th mode, A_i, can be solved by

$$A_i = (\frac{A_i}{A_1}) A_1; \quad i = 2,3,\cdots, n . \qquad (3.29)$$

Through the foregoing procedure, the first iteration has been completed. The next iteration starts by using

$$\{\phi\} = \sum_{i=1}^{n} A_i \{\phi_{Li}\} . \qquad (3.30)$$

By using Eq. (3.30) instead of Eq. (3.13), the next iteration is performed from that point onward to obtain the improved nonlinear frequency ω_{NL1} and i-th amplitude A_i. This iterative process can now be repeated until a convergence criterion (Section 3.3) is satisfied. It should be noted that the nonlinear stiffness matrix $[k_{NL}]$ and the harmonic matrix [h] are updated at each iteration because of the changing values of A_i. The flow-chart of this solution procedure is shown in Fig. 3.

START

$$[M]\{\ddot{\Delta}\} + [K_L]\{\Delta\} = 0$$

$$[M_b]\{\ddot{\phi}\} + [K_{Lb}]\{\phi\} = 0$$

$$\omega_L^2 [M_b]\{\phi_L\} = [K_{Lb}]\{\phi_L\}$$
Solve for ω_{Li} and $\{\phi_{Li}\}$

$$\{\phi\} = A \{\phi_{L1}\}$$

Determine $[k_{NL}]$ and $[h]$

$$[M]\{\ddot{\Delta}\} + [[K_L] + [K_{NL}] - [H]]\{\Delta\} = 0$$

Guyan's Reduction
$$[RM]\{\ddot{\phi}\} + [RK]\{\phi\} = 0$$

$$[\phi_o]^T [RM][\phi_o]\{\ddot{A}_o\} + [\phi_o]^T[RK][\phi_o]\{A\} = 0$$
or
$$[RM_o]\{\ddot{A}_o\} + [RK_o]\{A_o\} = 0$$

$$\omega_{NL}^2 [RM_o]\{A_o\} = [RK_o]\{A_o\}$$
Solve for ω_{NL1} and $\{A_o\}$

STOP

Calculate Strains

Check if NORM $< 10^{-5}$

No → Determine

Yes → Calculate Strains

$$\{\Delta\} = [TRF]\{\phi\}$$

$$\{\phi\} = \sum_{i=1}^{n} A_i \{\phi_{Li}\}$$

$$A_1 = \frac{A}{1 + \sum_{i=2}^{n} \frac{A_i}{A_1}}$$

$$A_i = \left(\frac{A_i}{A_1}\right)A_1$$

$$i = 2,3,\cdots,n$$
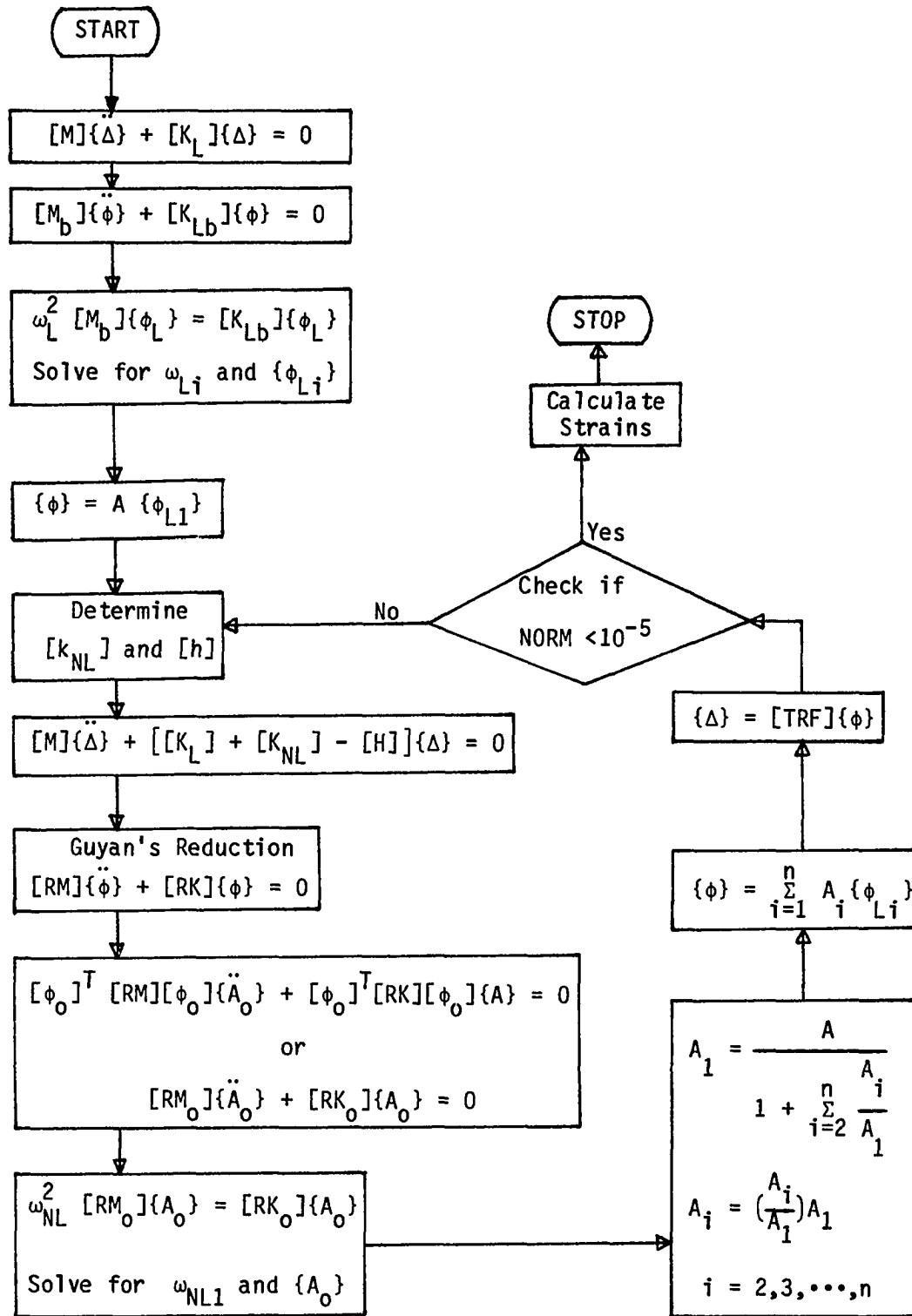
Fig. 3 Computer flow-chart (solution procedures) of
the multiple-mode method (method II)

3.3 Convergence Criteria

Three displacement convergence criteria proposed by Bergan and Clough[76] and a frequency convergence criterion are employed in the present study. The three displacement norms (criteria) are the modified absolute norm, the modified Euclidean norm and the maximum norm. The definitions of the three norms are given in the Appendix A. The frequency norm is defined as $|(\Delta\omega_{NL})_j/(\omega_{NL})_j|$, where $(\Delta\omega_{NL})_j$ is the change in nonlinear frequency during the j-th iterative cycle. Figure 4 shows a plot of the four norms versus number of iterations for a three-mode clamped beam (L/R = 1010) with inplane displacement and inertia (IDI) when both ends are immovable (u = 0 at x = 0 and L). The beam is subjected to a uniformly distributed harmonic force Fo = 0.002 N/mm at A/R = 4.0. Figure 5 shows the convergence characteristics of a simply supported square plate of length-to-thickness ratio a/h = 240 with immovable inplane edges (u=0 at x=0 and a, v=0 at y=0 and b) subjected to a uniform harmonic force of forcing parameter $P_o^* = 0.2$ at $w_{max}/h = 1.0$. For all the results presented in this dissertation, convergence is considered to be achieved whenever any one of the norms reaches a value of 10^{-5}.
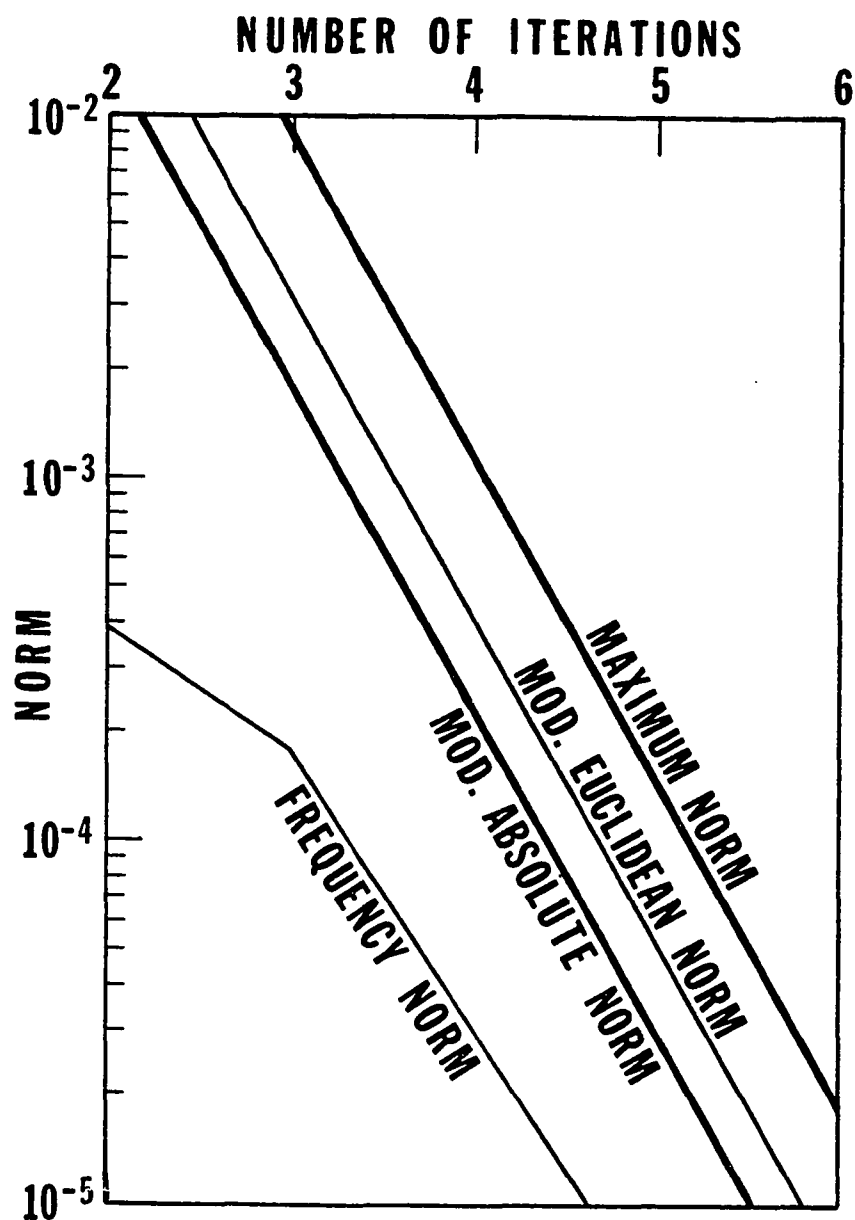
Fig. 4 Convergence characteristics of a three-mode
clamped beam (L/R = 1010) with inplane displace-
ment and inertia (IDI) subjected to a uniformly
distributed harmonic force F_0 = 0.002 N/mm at
A/R = 4.0.
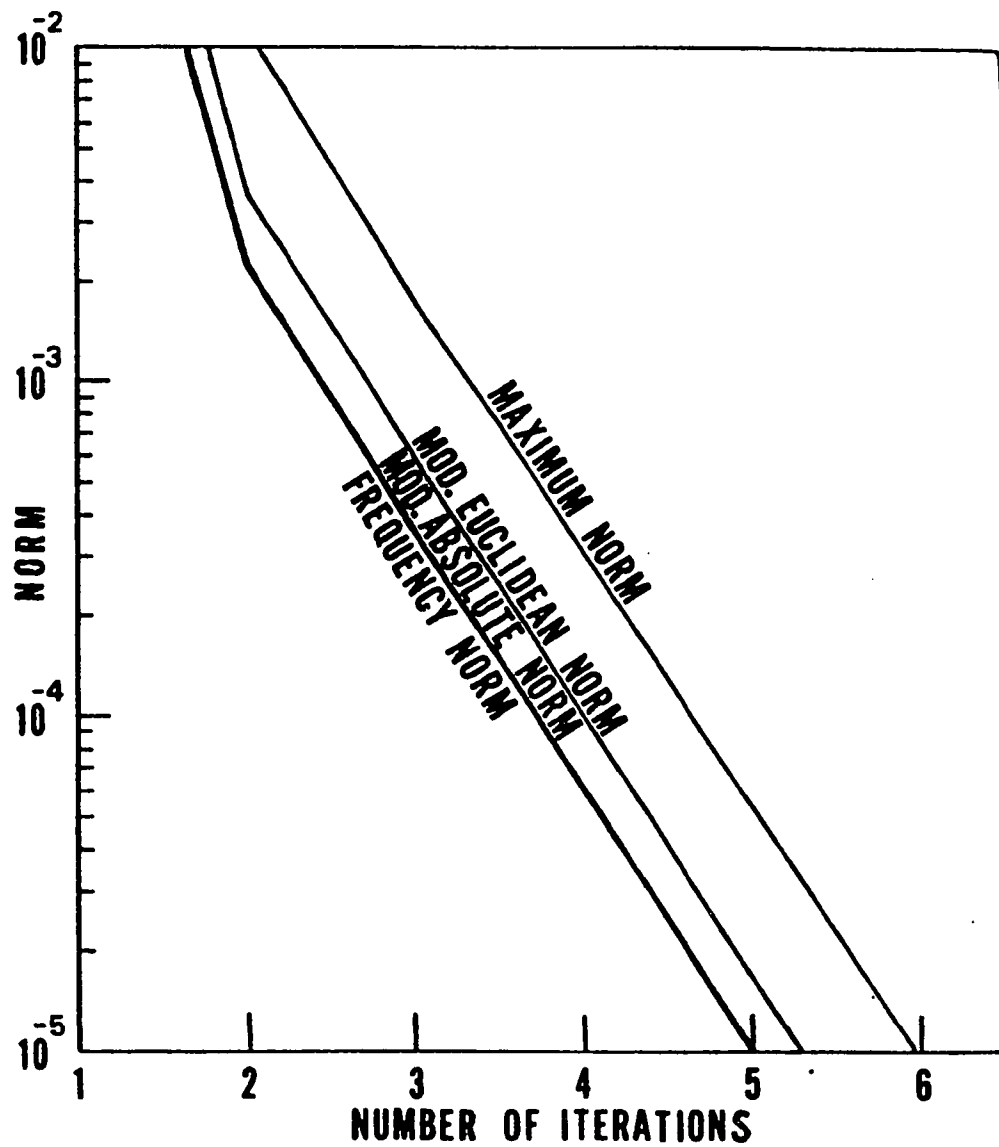
Fig. 5 Convergence characteristics of a simply
supported square plate of length-to-thickness
ratio $a/h = 240$ with immovable inplane edges
subjected to a uniform harmonic $P_o^* = 0.2$ at
$w_{max}/h = 1.0$.

Chapter 4

BEAM STRUCTURES

In this chapter, the mathematical formulations of the classical and finite element methods are presented. In the first section, the formulation of the classical method is presented. The equation of motion for an isotropic beam is given. The characteristic equations are provided using the Galerkin's method. For the single-mode approach, the frequency-amplitude-force relation is shown in a simple closed-form solution which is not possible for the multiple-mode approach. For the multiple-mode approach, the general formulation is shown to provide better understanding in the multiple-mode formulation. All of these formulations are performed in detail. The classical method provides the concept which later is utilized in the finite element method.

In the second section, the formulation of the development of the finite element method is presented. The expressions for the strain-displacement relation, kinetic energy and potential energy are provided. The linearizing function for deriving nonlinear stiffness matrices is defined. The inplane displacement and lateral deflection are expanded in the cubic order. Furthermore, the derivation of the harmonic force matrix for nonlinear forced vibration analysis is presented.

32

4.1 Classical Method

In general, the nonlinear forced vibration of a beam is solved by the assumed mode method. By employing the Galerkin's method, the assumed mode shape is substituted into the governing equation of motion, then the integration is performed over the spatial domain. The characteristic equations are then obtained. Numerical time integration or other numerical method is employed for solving the frequency-amplitude relations. Formulation for both single and multiple-mode approaches are shown.

4.1.1 Single-Mode Approach

The classical method for the single-mode approach is straight forward. The frequency-amplitude-force relation exists in a simple closed-form relation. The formulation for the single-mode approach is as follows.

Assume that a uniform beam with cross sectional area $\bar{A}$, moment of inertia I and length L is subjected to a uniformly distributed periodic lateral load F(t) as shown in Fig. 6. In this figure, a clamped beam is shown. The deflection is denoted by w(x,t). With the assumption that axial displacements at both ends are zero (immovable inplane displacement), the basic governing equation of motion for the nonlinear bending forced vibration of a beam is

$$\bar{\rho}\,\bar{A}\,\ddot{w} + EI\,w_{,xxxx} - N\,w_{,xx} - F(t) = 0 \qquad (4.1)$$
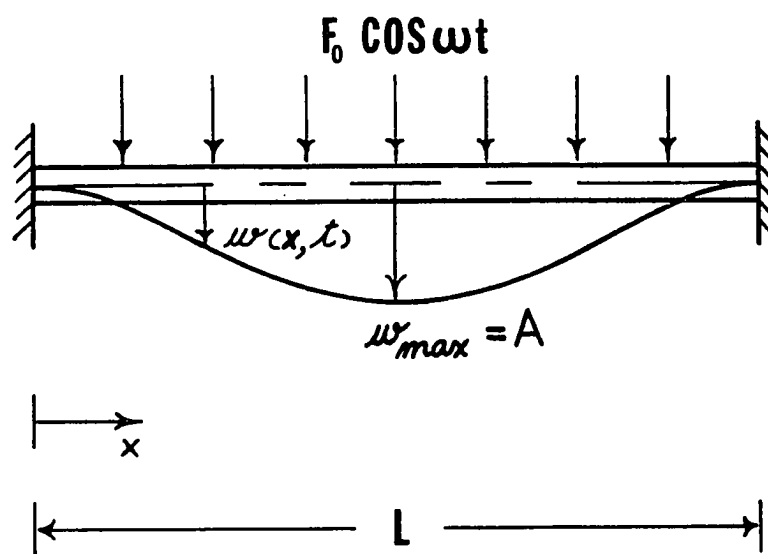
Fig. 6 Geometry of a clamped beam.

where

$$N = \frac{\bar{E}\bar{A}}{2L} \int_0^L (w,_x)^2 \, dx \tag{4.2}$$

where $\bar{\rho}$ and E are mass density and Young's modulus, respectively. The subscript x following a comma denotes differentiation with respect to x and a dot denotes differentiation with respect to time t.

For the single-mode approach, the deflection is assumed as

$$w(x,t) = \phi(x) \, g(t) \tag{4.3}$$

where $\phi(x)$ represents the normal mode of linear free vibration which satisfies the boundary conditions for the case in consideration, and the modal amplitude $g(t)$ is an unknown function of time.

Using the foregoing expression for w, the Galerkin's method can be applied to Eq. (4.1) which leads to

$$\int_0^L [\text{Eq. (4.1)}] \, \phi(x) \, dx = \text{Residual} \, \tilde{=} \, 0 \tag{4.4}$$

Equation (4.4) can be expressed as

$$[\bar{\rho} \, \bar{A} \int_0^L \phi^2 \, dx] \, \ddot{g} + [EI \int_0^L \phi,_{xxxx} \, \phi \, dx] \, g$$

$$- [N \int_0^L \phi,_{xx} \, \phi \, dx] \, g - F(t) \int_0^L \phi \, dx = 0 \tag{4.5}$$

Equation (4.5) can be rewritten in the form as

$$\bar{\rho} \, \bar{A} \, \ddot{g} + [EI \int_0^L \phi,_{xxxx} \, \phi \, dx] \, g / \int_0^L \phi^2 \, dx$$

$$- [N \int_0^L \phi,_{xx} \, \phi \, dx] \, g / \int_0^L \phi^2 \, dx - F(t) \int_0^L \phi \, dx / \int_0^L \phi^2 \, dx = 0 \, . \tag{4.6}$$

By substituting Eq. (4.3) with Eq. (4.2), the inplane force N can be expressed as

$$N = [\frac{\bar{EA}}{2L} \int_0^L (\phi,_x)^2 \, dx] \, g^2 \, . \tag{4.7}$$

By using this value of N, Eq. (4.7), in conjunction with Eq. (4.6), the characteristic equation is obtained in the form as

$$m \, \ddot{g} + kg + \bar{k} \, g^3 - c \, F(t) = 0 \tag{4.8}$$

where m, k and $\bar{k}$ are the mass, linear stiffness and nonlinear stiffness terms, respectively. The values of m, k and $\bar{k}$ can be expressed as

$$m = \bar{\rho} \, \bar{A} \tag{4.9}$$

$$k = EI \int_0^L \phi,_{xxxx} \, \phi \, dx / \int_0^L \phi^2 \, dx \tag{4.10}$$

$$\bar{k} = \frac{\bar{EA}}{2L} \int_0^L (\phi,_x)^2 \, dx \int_0^L \phi,_{xx} \, \phi \, dx / \int_0^L \phi^2 \, dx \, . \tag{4.11}$$

The value of the constant c is expressed as

$$c = \int_0^L \phi \, dx / \int_0^L \phi^2 \, dx \tag{4.12}$$

The characteristic equation, Eq. (4.8), can be written as

$$m \, \ddot{g} + kg + \bar{k} \, g^3 - P(t) = 0 \tag{4.13}$$

where P(t) is the force term which is expressed as

$$P(t) = c \, F(t) \, . \tag{4.14}$$

For harmonic loading, the force term, P(t), is written as

$$P(t) = P_0 \cos(\omega t) \qquad (4.15)$$

and by Eq. (4.14),

$$P_0 = c \, F_0 \qquad (4.16)$$

and

$$F(t) = F_0 \cos(\omega t) \qquad (4.17)$$

where F_0 is the force intensity which has the dimension of force per unit length. Equation (4.13) can be written as

$$\ddot{g} + \omega_L^2 \, g + \bar{\beta} \, g^3 = \bar{P}(t) \qquad (4.18)$$

and

$$\omega_L^2 = k/m \qquad (4.19)$$

$$\bar{\beta} = \bar{k}/m \qquad (4.20)$$

$$\bar{P}(t) = \bar{P}_0 \cos(\omega t) = \frac{P_0}{m} \cos(\omega t) \qquad (4.21)$$

where ω_L is the linear frequency which has the dimension of radians per second.

The characteristic equation, Eq. (4.18), can be solved for the frequency-amplitude-force relation in a closed-form solution by various approximate methods. It should be pointed out that many of these approximate methods yield the same closed-form solution which can be classified as a standard form. Because of the simplicity of the following method, the derivation of the closed-form solution will be shown in detail. This method is based on omitting the higher harmonic term.

To obtain the frequency-amplitude-force relation in closed-form solution, Eq. (4.15) is rewritten as

$$\ddot{g} = - \omega_L^2 g - \bar{\beta}g^3 + \bar{P}_0 \cos(\omega t) \ . \qquad (4.22)$$

By adding $\omega^2 g$ to the left and right sides of Eq. (4.22), the characteristic equation is written as

$$\ddot{g} + \omega^2 g = (\omega^2 - \omega_L^2) \ g - \bar{\beta} \ g^3 + \bar{P}_0 \cos(\omega t) \ . \qquad (4.23)$$

By assuming, $\omega \approx \omega_L$, $\bar{\beta} \ll 1$, and $\bar{P}_0 \ll 1$, then Eq. (4.23) is approximated as

$$\ddot{g} + \omega^2 g \approx 0 \ . \qquad (4.24)$$

The solution of Eq. (4.24) is

$$g(t) \approx A \cos(\omega t) \ . \qquad (4.25)$$

By using Eq. (4.25), $g^3(t)$ is expressed as

$$g^3(t) = A^3 \cos^3(\omega t)$$

$$= A^3 \ [\frac{3}{4} \cos(\omega t) + \frac{1}{4} \cos(3\omega t)] \ . \qquad (4.26)$$

Since $A \cos(\omega t)$ is an approximate solution to Eq. (4.23), the estimation of the right-hand side of Eq. (4.23) can be evaluated by substituting Eqs. (4.25) and (4.26) with Eq. (4.23) as,

$$\ddot{g} + \omega^2 g = \{(\omega^2 - \omega_L^2) \ A \cos(\omega t) - \bar{\beta} \ A^3 \ [\frac{3}{4} \cos(\omega t) + \frac{1}{4} \cos(3\omega t)]$$

$$+ \bar{P}_0 \cos(\omega t)\}$$

$$= [(\omega^2 - \omega_L^2) \ A - \frac{3}{4} \bar{\beta} \ A^3 + \bar{P}_0] \cos(\omega t)$$

$$- \frac{1}{4} \bar{\beta} \ A^3 \cos(3\omega t) \ . \qquad (4.27)$$

To obtain a periodic solution, the coefficient of $\cos(\omega t)$ must equal zero as

$$(\omega^2 - \omega_L^2) A - \frac{3}{4} \bar{\beta} A^3 + \bar{P}_0 = 0$$

$$\omega^2 = \omega_L^2 + \frac{3}{4} \bar{\beta} A^2 - \frac{\bar{P}_0}{A} . \tag{4.28}$$

Equation (4.28) is the standard closed-form relation between frequency, amplitude and force. It should be noted that Eq. (4.27) is then expressed as,

$$\ddot{g} + \omega^2 g \approx -\frac{1}{4} \bar{\beta} A^3 \cos(3\omega t) \tag{4.29}$$

which yields the solution as

$$g(t) = \bar{A}_1 \cos(\omega t) + \frac{1}{32} \bar{\beta} \frac{A^3}{\omega^2} \cos(3\omega t) \tag{4.30}$$

where $\bar{A}_1$ is arbitrary.

4.1.2 Multiple-Mode Approach

The classical multiple-mode approach follows the same path as the single-mode approach. But the multiple-mode approach cannot give a simple closed-form frequency-amplitude-force relation, thus, a numerical integration or other approximate method is employed.

The general formulation of the multiple-mode approach is as follows,

$$w(x,t) = \sum_{i=1}^{n} \phi_i(x) g_i(t) \tag{4.31}$$

where $\phi_i(x)$ is the i-th normalized linear mode shape with a maximum of unity at the center of the beam, and $g_i(t)$ is the time function. Only symmetrical modes are considered in Eq. (4.31) due to the fact that the loading is uniform. The total number of modes in consideration is n.

The time function $g_i(t)$ can be expressed as

$$g_i(t) = A_i \cos(\omega t) \tag{4.32}$$

where A_i is the amplitude of i-th mode shape. By using the assumed expression of w, Eq. (4.31), the Galerkin's method is applied to Eq. (4.1) as follows:

$$\int_0^L [\text{Eq. (4.1)}] \, \phi_i(x) \, dx = \text{Residual} \cong 0 \tag{4.33}$$
$$i = 1,2..., n .$$

By substituting Eq. (4.31) with Eq. (4.2), the axial force N is expressed as

$$N = \frac{E\bar{A}}{2L} \int_0^L [\sum_{i=1}^n \phi_{i,x} \, g_i]^2 \, dx . \tag{4.34}$$

By substituting Eq. (4.34) with Eq. (4.33), the following set of nonlinear ordinary differential equations are obtained:

$$m_i \ddot{g}_i + k_i \, g_i + \sum_{j=1}^n \sum_{r=1}^n \sum_{s=1}^n \bar{k}_{ijrs} \, g_j g_r g_s$$

where
$$= P_i(t) \qquad i = 1,2,\cdots, n \tag{4.35}$$

$$m_i = \bar{\rho} \, \bar{A} \tag{4.36}$$

$$k_i = EI \int_0^L \phi_{i,xxxx} \phi_i \, dx / \int_0^L \phi_i^2 \, dx \qquad (4.37)$$

$$\bar{k}_{ijrs} = - \frac{\bar{EA}}{2L} \frac{\int_0^L \phi_{j,x} \phi_{r,x} \, dx \int_0^L \phi_{s,xx} \phi_i \, dx}{\int_0^L \phi_i^2 \, dx} \qquad (4.38)$$

$$P_i(t) = \int_0^L F(x,t) \phi_i \, dx / \int_0^L \phi_i^2 \, dx \; . \qquad (4.39)$$

The set of nonlinear ordinary differential equations shown by Eq. (4.35) is the set of characteristic equations for nonlinear forced vibrations. In general, the number of characteristic equations is the same as the number of mode shapes included in the assumed deflection shape, Eq. (4.31). These characteristic equations are highly nonlinear and coupled, thus, it is very tedious to solve for the steady-state solution. One way to obtain the frequency-amplitude-force relation is by performing numerical integration, e.g., the Runge-Kutta method.

To clarify the method, a two-mode approach is performed as follows:

$$w(x,t) = \sum_{i=1}^{2} \phi_i(x) g_i(t) \; . \qquad (4.40)$$

The deflection shape $w(x,t)$ is assumed as the combination of two modes. In this case, n is equal two. The value of N, Eq. (4.34), can be expressed as

$$N = \frac{\bar{EA}}{2L} [(\int_0^L \phi_{1,x}^2 \, dx) g_1^2 + (\int_0^L \phi_{2,x}^2 \, dx) g_2^2$$

$$+ (2 \int_0^L \phi_{1,x} \phi_{2,x} \, dx) g_1 g_2] \; . \qquad (4.41)$$

By using Eqs. (4.40) and (4.41), the set of characteristic equations, Eq. (4.35), is expanded as

$$m_1 \ddot{g}_1 + k_1 g_1 + \bar{k}_{1111} g_1^3 + (\bar{k}_{1112} + \bar{k}_{1121} + \bar{k}_{1211}) g_1^2 g_2$$

$$+ (\bar{k}_{1122} + \bar{k}_{1212} + \bar{k}_{1221}) g_1 g_2^2 + \bar{k}_{1222} g_2^3 = P_1(t) \quad (4.42)$$

$$m_2 \ddot{g}_2 + k_2 g_2 + \bar{k}_{2111} g_1^3 + (\bar{k}_{2112} + \bar{k}_{2121} + \bar{k}_{2211}) g_1^2 g_2$$

$$+ (\bar{k}_{2122} + \bar{k}_{2212} + \bar{k}_{2221}) g_1 g_2^2 + \bar{k}_{2222} g_2^3 = P_2(t) \quad (4.43)$$

where

$$m_1 = \bar{\rho} \bar{A}$$

$$k_1 = EI \int_0^L \phi_{1,xxxx} \, \phi_1 \, dx / \int_0^L \phi_1^2 \, dx$$

$$\bar{k}_{1111} = - \frac{E\bar{A}}{2L} \int_0^L \phi_{1,x}^2 \, dx \int_0^L \phi_{1,xx} \, \phi_1 \, dx / \int_0^L \phi_1^2 \, dx$$

$$\bar{k}_{1112} = - \frac{E\bar{A}}{2L} \int_0^L \phi_{1,x}^2 \, dx \int_0^L \phi_{2,xx} \, \phi_1 \, dx / \int_0^L \phi_1^2 \, dx$$

$$\bar{k}_{1121} = - \frac{E\bar{A}}{2L} \int_0^L \phi_{1,x} \, \phi_{2,x} \, dx \int_0^L \phi_{1,xx} \, \phi_1 \, dx / \int_0^L \phi_1^2 \, dx$$

$$\bar{k}_{1122} = - \frac{E\bar{A}}{2L} \int_0^L \phi_{1,x} \, \phi_{2,x} \, dx \int_0^L \phi_{2,xx} \, \phi_1 \, dx / \int_0^L \phi_1^2 \, dx$$

$$\bar{k}_{1211} = -\frac{E\bar{A}}{2L} \int_0^L \phi_{2,x}\, \phi_{1,x}\, dx \int_0^L \phi_{1,xx}\, \phi_1\, dx \Big/ \int_0^L \phi_1^2\, dx$$

$$\bar{k}_{1212} = -\frac{E\bar{A}}{2L} \int_0^L \phi_{2,x}\, \phi_{1,x}\, dx \int_0^L \phi_{2,xx}\, \phi_1\, dx \Big/ \int_0^L \phi_1^2\, dx$$

$$\bar{k}_{1221} = -\frac{E\bar{A}}{2L} \int_0^L \phi_{2,x}^2\, dx \int_0^L \phi_{1,xx}\, \phi_1 dx \Big/ \int_0^L \phi_1^2\, dx$$

$$\bar{k}_{1222} = -\frac{E\bar{A}}{2L} \int_0^L \phi_{2,x}^2\, dx \int_0^L \phi_{2,xx}\, \phi_1\, dx \Big/ \int_0^L \phi_1^2\, dx$$

$$P_1(t) = \int_0^L F(x,t)\, \phi_1\, dx \Big/ \int_0^L \phi_1^2\, dx$$

$$m_2 = \bar{\rho}\, \bar{A}$$

$$k_2 = EI \int_0^L \phi_{2,xxxx}\, \phi_2\, dx \Big/ \int_0^L \phi_2^2\, dx$$

$$\bar{k}_{2111} = -\frac{E\bar{A}}{2L} \int_0^L \phi_{1,x}^2\, dx \int_0^L \phi_{1,xx}\, \phi_2\, dx \Big/ \int_0^L \phi_2^2\, dx$$

$$\bar{k}_{2112} = -\frac{E\bar{A}}{2L} \int_0^L \phi_{1,x}^2\, dx \int_0^L \phi_{2,xx}\, \phi_2\, dx \Big/ \int_0^L \phi_2^2\, dx$$

$$\bar{k}_{2121} = - \frac{E\bar{A}}{2L} \int_0^L \phi_{1,x} \, \phi_{2,x} \, dx \int_0^L \phi_{1,xx} \, \phi_2 \, dx / \int_0^L \phi_2{}^2 \, dx$$

$$\bar{k}_{2122} = - \frac{E\bar{A}}{2L} \int_0^L \phi_{1,x} \, \phi_{2,x} \, dx \int_0^L \phi_{2,xx} \, \phi_2 \, dx / \int_0^L \phi_2{}^2 \, dx$$

$$\bar{k}_{2211} = - \frac{E\bar{A}}{2L} \int_0^L \phi_{2,x} \, \phi_{1,x} \, dx \int_0^L \phi_{1,xx} \, \phi_2 \, dx / \int_0^L \phi_2{}^2 \, dx$$

$$\bar{k}_{2212} = - \frac{E\bar{A}}{2L} \int_0^L \phi_{2,x} \, \phi_{1,x} \, dx \int_0^L \phi_{2,xx} \, \phi_2 \, dx / \int_0^L \phi_2{}^2 \, dx$$

$$\bar{k}_{2221} = - \frac{E\bar{A}}{2L} \int_0^L \phi_{2,x}{}^2 \, dx \int_0^L \phi_{1,xx} \, \phi_2 \, dx / \int_0^L \phi_2{}^2 \, dx$$

$$\bar{k}_{2222} = - \frac{E\bar{A}}{2L} \int_0^L \phi_{2,x}{}^2 \, dx \int_0^L \phi_{2,xx} \, \phi_2 \, dx / \int_0^L \phi_2{}^2 \, dx$$

$$P_2(t) = \int_0^L F(x,t) \, \phi_2 \, dx / \int_0^L \phi_2{}^2 \, dx \ . \tag{4.44}$$

The steady-state response for a two-mode nonlinear vibration problem can be obtained by employing Runge-Kutta numerical integration for solving the nonlinear coupled characteristic equations, Eqs. (4.42) and (4.43). Results are obtained for comparison with the finite element solutions shown in Chap. 6.

4.2 Finite Element Formulation

In this section, the formulation of the finite element method for a beam element is developed. The expressions for the strain-displacement relation, kinetic energy and potential energy are provided. The linearizing function for deriving nonlinear stiffness matrices is defined. The inplane displacement and lateral deflection are expanded in the cubic order polynomials. Furthermore, the derivation of the harmonic force matrix is presented.

4.2.1 Strain-and Curvature-Displacement Relations

The strain-displacement relation for a beam under large deflection is given by

$$\varepsilon_x = u,_x + \frac{1}{2} w,_x^2 \tag{4.45}$$

where ε_x is the strain in the x-direction of the beam, u is the inplane displacement and w is the lateral deflection. The curvature-displacement relation is defined as

$$\psi_x = w,_{xx} \tag{4.46}$$

where ψ_x is the curvature. The total strain, ε, is

$$\varepsilon = u,_x + \frac{1}{2} w,_x^2 - z \, w,_{xx} . \tag{4.47}$$

4.2.2 Kinetic and Strain Energies

The kinetic energy of a beam element shown in Fig. 7 is given by

$$T = \frac{1}{2} \rho \int_o^\ell (\dot{u}^2 + \dot{w}^2) \, dx \tag{4.48}$$

$$F_o \ COS \ \omega t$$
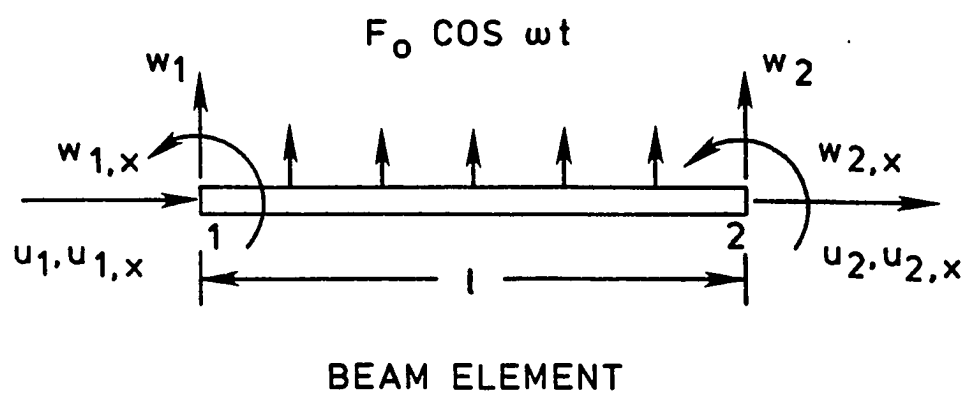
BEAM ELEMENT

Fig. 7   Beam finite element.

where ρ is the mass per unit length, and ℓ is the element length. The kinetic energy can be separated into two parts as

$$T = T_s + T_b .$$ (4.49)

The kinetic energy due to mid-plane displacement T_s is defined as

$$T_s = \frac{1}{2} \rho \int_0^\ell \dot{u}^2 \, dx$$ (4.50)

and the kinetic energy due to lateral deflection T_b is defined as

$$T_b = \frac{1}{2} \rho \int_0^\ell \dot{w}^2 \, dx .$$ (4.51)

The total strain energy of a beam element is given by

$$U = \frac{1}{2} \int_0^\ell (E \bar{A} \epsilon_x^2 + E I \psi_x^2) \, dx$$ (4.52)

where E is Young's modulus, $\bar{A}$ is the cross-sectional area of the beam, and I is the moment of inertia. By substituting Eqs. (4.45) and (4.46) with Eq. (4.52) the strain energy in terms of the displacements can be written as

$$U = \frac{1}{2} \int_0^\ell E \bar{A} [u,_x^2 + 2u,_x (\frac{1}{2} w,_x^2) + (\frac{1}{2} w,_x^2)^2] \, dx$$

$$+ \frac{1}{2} \int_0^\ell E I w,_{xx}^2 \, dx .$$ (4.53)

The strain energy U can be separated into two parts, namely, linear strain energy U_L and nonlinear strain energy U_{NL}, so that

$$U = U_L + U_{NL} .$$ (4.54)

The linear strain energy for Eq. (4.54) is expressed as

$$U_L = \frac{1}{2} \int_0^{\ell} E \bar{A} u_{,x}^2 \, dx + \frac{1}{2} \int_0^{\ell} E I w_{,xx}^2 \, dx \ . \tag{4.55}$$

Similarly, the nonlinear strain energy for Eq. (4.54) is expressed as

$$U_{NL} = \frac{1}{2} \int_0^{\ell} E \bar{A} [2 u_{,x} (\frac{1}{2} w_{,x}^2) + (\frac{1}{2} w_{,x}^2)^2] \, dx \ . \tag{4.56}$$

4.2.3 Displacement Functions

The displacement functions are chosen to be the cubic-order polynomials as follows:

$$w = a_1 + a_2 x + a_3 x^2 + a_4 x^3 \tag{4.57}$$

and

$$u = a_5 + a_6 x + a_7 x^2 + a_8 x^3 \ . \tag{4.58}$$

The generalized coordinates a_1, $\cdots\cdots$, a_8 can be written in vector form as

$$\{a\}^T = [a_1 \ a_2 \ a_3 \ a_4 \ a_5 \ a_6 \ a_7 \ a_8] \tag{4.59}$$

and the element nodal displacements, Fig. 6, are defined as

$$\{\delta\}^T = [w_1 \ \theta_1 \ w_2 \ \theta_2 \ u_1 \ \alpha_1 \ u_2 \ \alpha_2] \tag{4.60}$$

where θ_i and α_i are the differentiation with respect to x of w_i and u_i at node i, respectively. The generalized coordinates in Eq. (4.59) can be written as

$$\{a\} = [T] \{\delta\} \tag{4.61}$$

where [T] is a transformation matrix which is given in Appendix B.

The displacements u and w, including their derivatives, can be expressed in terms of the element nodal displacements as

$$u = [0 \ 0 \ 0 \ 0 \ 1 \ x \ x^2 \ x^3] \ \{a\}$$

$$= [B] \ [T] \ \{\delta\} \tag{4.62}$$

$$u,_x = [0 \ 0 \ 0 \ 0 \ 0 \ 1 \ 2x \ 3x^2] \ \{a\}$$

$$= [C] \ [T] \ \{\delta\} \tag{4.63}$$

$$w = [1 \ x \ x^2 \ x^3 \ 0 \ 0 \ 0 \ 0] \ \{a\}$$

$$= [D] \ [T] \ \{\delta\} \tag{4.64}$$

$$w,_x = [0 \ 1 \ 2x \ 3x^2 \ 0 \ 0 \ 0 \ 0] \ \{a\}$$

$$= [E] \ [T] \ \{\delta\} \tag{4.65}$$

$$w,_{xx} = [0 \ 0 \ 2 \ 6x \ 0 \ 0 \ 0 \ 0] \ \{a\}$$

$$= [G] \ [T] \ \{\delta\} \tag{4.66}$$

4.2.4 Linearizing Function

A linearizing function is defined as[8,45]

$$f = \frac{1}{2} \ w,_x \ . \tag{4.67}$$

By substituting Eq. (4.65) with (4.67), the linearizing function can be expressed as

$$f = \frac{1}{2} \ [E] \ [T] \ \{\delta\} \ . \tag{4.68}$$

This linearizing function f is assumed to be constant for each element. The main advantage of using a linearizing function is shown in the following sections.

4.2.5 Element Equations of Motion for Nonlinear Free Vibration

The nonlinear free vibration is the backbone of the investigation of steady-state response. The equations of motion can be derived by applying Lagrange's equations as follows.

From Eqs. (4.50) and (4.62), the expression of kinetic energy due to inplane motion mid-plane stretching T_s can be written in matrix form as

$$T_s = \frac{1}{2} \{\dot{\delta}\}^T [T]^T \int_o^\ell \rho [B]^T [B] \, dx \, [T] \{\dot{\delta}\}$$

$$= \frac{1}{2} \{\dot{\delta}\}^T [m_s] \{\dot{\delta}\} \tag{4.69}$$

where $[m_s]$ is the element mass matrix due to inplane displacement and expressed as

$$[m_s] = [T]^T \int_o^\ell \rho [B]^T [B] \, dx \, [T] . \tag{4.70}$$

Similarly, from Eqs. (4.51) and (4.64), the expression of kinetic energy due to bending T_b can be written as

$$T_b = \frac{1}{2} \{\dot{\delta}\}^T [m_b] \{\dot{\delta}\} \tag{4.71}$$

where $[m_b]$ is the element mass matrix due to bending and expressed as

$$[m_b] = [T]^T \int_o^\ell \rho [D]^T [D] \, dx \, [T] . \tag{4.72}$$

The kinetic energy T, Eq. (4.49) can be expressed in matrix form as

$$T = \frac{1}{2} \{\dot{\delta}\}^T [m] \{\dot{\delta}\} \tag{4.73}$$

where [m] is the element mass matrix and expressed as

$$[m] = [m_s] + [m_b] . \tag{4.74}$$

The linear strain energy U_L, Eq. (4.55), can be expressed in matrix form as

$$U_L = \frac{1}{2} \{\delta\}^T [k_L] \{\delta\} \tag{4.75}$$

where $[k_L]$ is the element linear stiffness matrix. The element linear stiffness matrix $[k_L]$ can be separated into u-part $[k_{Ls}]$ and w-part $[k_{Lb}]$ as

$$[k_L] = [k_{Ls}] + [k_{Lb}] \tag{4.76}$$

where

$$[k_{Ls}] = [T]^T \int_o^{\ell} E \bar{A} [C]^T [C] \, dx \, [T] \tag{4.77}$$

$$[k_{Lb}] = [T]^T \int_o^{\ell} EI [G]^T [G] \, dx \, [T] . \tag{4.78}$$

The nonlinear strain energy U_{NL}, Eq. (4.56), can be written by using the linearizing function f, Eq. (4.67), as

$$U_{NL} = \frac{1}{2} \int_o^{\ell} E \bar{A} [2f \, u,_x \, w,_x + f^2 \, w,_x^2] \, dx . \tag{4.79}$$

By substituting Eqs. (4.63) and (4.65) with Eq. (4.79), the nonlinear strain energy can be expressed in matrix form as

$$U_{NL} = \frac{1}{2} \{\delta\}^T [k_{NL}] \{\delta\} \tag{4.80}$$

where $[k_{NL}]$ is the element nonlinear stiffness matrix and expressed as

$$[k_{NL}] = [T]^T \int_0^{\ell} \{E \bar{A} f [[C]^T [E] + [E]^T [C]] .$$

$$+ E \bar{A} f^2 [E]^T [E]\} dx [T] . \tag{4.81}$$

The element nonlinear stiffness matrix can be expressed as

$$[k_{NL}] = [k_{NLb}] + [k_{NLsb}] + [k_{NLbs}] \tag{4.82}$$

where

$$[k_{NLb}] = [T]^T \int_0^{\ell} E \bar{A} f^2 [E]^T[E] dx [T] \tag{4.83}$$

$$[k_{NLbs}] = [T]^T \int_0^{\ell} E \bar{A} f [C]^T[E] dx [T] \tag{4.84}$$

$$[k_{NLsb}] = [T]^T \int_0^{\ell} E \bar{A} f [E]^T[C] dx [T] . \tag{4.85}$$

The linearizing function f which is constant for each element linearized the nonlinear strain energy U_{NL} as quadratic in the nodal displacements as shown in Eq. (4.80). The strain energy U, Eq. (4.54), can be written as

$$U = \frac{1}{2} \{\delta\}^T [k] \{\delta\} \tag{4.86}$$

where [k] is the element stiffness matrix and is expressed as

$$[k] = [k_L] + [k_{NL}] \tag{4.87}$$

The application of Lagrange's equation to the kinetic energy T, Eq. (4.73), and the strain energy, Eq. (4.86), leads to the element nonlinear free vibration equation of motion as

$$[m] \{\ddot{\delta}\} + [[k_L] + [k_{NL}]] \{\delta\} = 0 \tag{4.88}$$

which can be rewritten as

$$\begin{bmatrix} [m_b] & 0 \\ 0 & [m_s] \end{bmatrix} \{\ddot{\delta}\} + \left[\begin{bmatrix} [k_{Lb}] & 0 \\ 0 & [k_{Ls}] \end{bmatrix} + \begin{bmatrix} [k_{NLb}] & [k_{NLbs}] \\ [k_{NLsb}] & 0 \end{bmatrix} \right] \{\delta\} = 0 \tag{4.89}$$

4.2.6 Element Harmonic Force Matrix

In Section 4.1.1, the equation of motion for nonlinear forced vibration in the classical approach is expressed in Eq. (4.13) as

$$m \ddot{g} + kg + \bar{k} g^3 = P(t) , \tag{4.90}$$

and Eq. (4.90) is rewritten in Eq. (4.15) as

$$\ddot{g} + \omega_L^2 g + \bar{\beta} g^3 = \bar{P}(t) , \tag{4.91}$$

when the forcing function P(t) is a simple harmonic P_o cos (ωt). An approximate solution of Eq.(4.90) is in the form of Eq. (4.28) as

$$\omega^2 = \omega_L^2 + \frac{3}{4} \bar{\beta} A^2 - \bar{P}_o/A \tag{4.92}$$

and $\bar{P}_o$ is expressed in Eq. (4.18) as

$$\bar{P}_o = P_o/m . \tag{4.93}$$

When the forcing function P(t) is a simple elliptic function and expressed as

$$P(t) = B^* A cn (\lambda t, \eta)$$

$$= B^* g \qquad (4.94)$$

where g is the Jacobian elliptic function and expressed as

$$g = A cn (\lambda t, \eta) \qquad (4.95)$$

and

$$\lambda = (\omega_L^2 + \bar{\beta} A^2)^{1/2} \qquad (4.96)$$

$$\eta = [\bar{\beta} A^2/2 (\omega_L^2 + \bar{\beta} A^2)]^{1/2} \qquad (4.97)$$

where B^* is forcing amplitude factor, λ is circular frequency of the Jacobian elliptic function and η is modulus of the Jacobian elliptic function.

By expanding the elliptic forcing function into Fourier series and comparing the order of the magnitude of the various components, Hsu[77] concluded that the harmonic forcing function $P_0 \cos (\omega t)$ is the first order approximation of the elliptic forcing function $B^* A cn (\lambda t, \eta)$. Further, the first order approximation of the elliptic response of Eq. (4.90) yields the same frequency-amplitude-force relation of Eq. (4.92) which is the perturbation solution (standard form, Eq. (4.28)). To obtain the exact elliptic response of Eq. (4.90), the forcing function P(t) in Eq. (4.94) is treated as a linear spring in the Duffing equation, Eq. (4.90). This is expressed as

$$m\ddot{g} + kg + \bar{k}\,g^3 = B^*\,g$$

$$m\ddot{g} + (k - B^*)\,g + \bar{k}\,g^3 = 0 \ . \tag{4.98}$$

This linear spring force B^*g possesses a potential energy as $B^*\,g^2/2$. Similarly, the potential energy of a beam due to the uniform harmonic forcing function F_0 cos ωt can thus be approximated by

$$V = \Sigma\,\frac{B^*}{2}\int_0^{\ell} w^2 \ dx \tag{4.99}$$

where the summation denotes the sum of all elements.

To relate the value of B^*, to the actual force applied to the beam F_0, the conclusion by Hsu[77] is employed (Eq. (4.94)) as follows:

$$P(t) = B^*\,g$$

$$= B^*\,A\ cn\ (\lambda t, \eta) \tag{4.100}$$

so,

$$P_0\ cos(\omega t) \stackrel{\sim}{=} B^*A\ cn\ (\lambda t, \eta)\ . \tag{4.101}$$

By using Hsu's conclusion, the harmonic function cos (ωt) is the first order approximation of the elliptic function cn $(\lambda t, \eta)$, thus,

$$cos\ (\omega t) \stackrel{\sim}{=} cn\ (\lambda t, \eta) \tag{4.102}$$

when η^2 is small in comparison with unity. When $1-\lambda^2$ is restricted to the order of η^2, the first harmonic in Eq. (4.100) will be the order of η^2 which yields the relation in Eq. (4.101). Hsu[77] further proved that the approximation relation in Eqs. (4.101) and (4.102) yielded the same frequency-amplitude-force relation, Eq. (4.92), as the perturbation

solution. By using the relation of Eq. (4.102), the value of B^* in Eq. (4.101) can be expressed as

$$B^* = P_0/A .$$ (4.103)

From Eq. (4.16), the relation of P_0 is expressed as follows

$$P_0 = c F_0$$ (4.104)

where the constant c is expressed in Eq. (4.12). The constant c is equal to the ratio of the area under mode shape and square of mode shape. And the nonlinear mode shape in a multiple-mode approach is assumed to be the sum of the linear modes, thus, the deflection $w(x,t)$ can be written as

$$w(x,t) = \phi^*(x) \, g^*(t)$$ (4.105)

where $\phi^*(x)$ is the normalized nonlinear mode and $g^*(t)$ is the time function, thus,

$$\phi^*(x) = \frac{1}{A} \sum_{i=1}^{n} A_i \, \phi_i(x)$$ (4.106)

where A_i and $\phi_i(x)$ are the amplitude of i-th mode shape and the i-th normalized linear mode shape, respectively. By using Eq. (4.106), and the definition of c in Eq. (4.12), the expression of c for simple harmonic loading is expressed as

$$c = \frac{\int^{(Load\ elements)} \phi^* \, dx}{\int_0^L (\phi^*)^2 \, dx} .$$ (4.107)

The term "Load elements" is defined as those elements subjected to distributed harmonic force. Thus, for the uniformly distributed force over the entire beam, the value of c is expressed as

$$c = \frac{\int_o^L \phi^* \, dx}{\int_o^L (\phi^*)^2 \, dx} \, . \qquad (4.108)$$

In the finite element method, the concentrated force can be simulated by a distributed force over a very small length, thus, the value of c for the concentrated force case can be expressed as

$$c = \frac{\int_{a_o}^{b_o} \phi^* \, dx}{\int_o^L (\phi^*)^2 \, dx} \qquad (4.109)$$

where a_0 and b_0 are coordinates of a beam under that distributed force. It should be noted that the nonlinear mode shape in the single-mode approach is defined as $\phi(x)$, thus, the deflection $w(x,t)$ can be written as

$$w(x,t) = \phi(x) \, g^*(t) \, . \qquad (4.110)$$

Thus, the values of the constant c for the uniformly distributed force over the entire beam and the concentrated force case can be evaluated by substituting $\phi(x)$ for $\phi^*(x)$ in Eqs. (4.108) and (4.109), respectively.

By using the Eq. (4.99), the element harmonic force matrix can be derived from

$$V = \frac{B^*}{2} \int_o^\ell w^2 \, dx \qquad (4.111)$$

where B^* is expressed in Eq. (4.103). By substituting Eq. (3.64) with (4.111), the potential energy due to the uniform harmonic force can be expressed as

$$V = \frac{B^*}{2} \{\delta\}^T [T]^T \int_0^{\ell} [D]^T [D] \, dx \, [T] \, \{\delta\}$$

$$= \frac{1}{2} \{\delta\}^T [h] \{\delta\} \tag{4.112}$$

where $[h]$ is the element harmonic force matrix and expressed as

$$[h] = B^* [T]^T \int_0^{\ell} [D]^T [D] \, dx \, [T] \; . \tag{4.113}$$

By comparing Eq. (4.113) with Eq. (4.72) and using the expression of B^* and P_0, Eqs. (4.103) and (4.104), the harmonic force matrix can be written as

$$[h] = \frac{c \, F_0}{A \, \rho} [m_b] \tag{4.114}$$

where c is a constant expressed in Eqs. (4.107), (4.108) or (4.109).

4.2.7 Element Equations of Motion for Nonlinear Forced Vibration

The application of Lagrange's equation to the kinetic energy T, the strain energy U and the potential energy V, due to the uniform harmonic forcing function, leads to the equations of motion for nonlinear forced vibration of a beam element. By using Eqs. (4.73), (4.86) and (4.112), the equation of motion is expressed as

$$[m] \{\ddot{\delta}\} + [[k_L] + [k_{NL}] - [h]] \{\delta\} = 0 \tag{4.115}$$

where $[m]$ is the element mass matrix in Eq. (4.74), $[k_L]$ is the element linear stiffness matrix in Eq. (4.76), $[k_{NL}]$ is the element nonlinear stiffness matrix in Eq. (4.81), and $[h]$ is the element harmonic force matrix in Eq. (4.114). It should be noted that all these matrices are symmetric. Therefore, Eq. (4.115) can be rewritten as

$$
\begin{bmatrix} [m_b] & 0 \\ 0 & [m_s] \end{bmatrix} \{\ddot{\delta}\} + \left[\begin{bmatrix} [k_{Lb}] & 0 \\ 0 & [k_{Ls}] \end{bmatrix} + \begin{bmatrix} [k_{NLb}] & [k_{NLbs}] \\ [k_{NLsb}] & 0 \end{bmatrix} - \begin{bmatrix} [h] & 0 \\ 0 & 0 \end{bmatrix} \right] \{\delta\} = 0
$$

$$(4.116)$$

where $[m_b]$, $[m_s]$, $[k_{Lb}]$, $[k_{Ls}]$, $[k_{NLb}]$, $[k_{NLsb}]$, $[k_{NLbs}]$ and $[h]$ are expressed in Eqs. (4.72), (4.70), (4.78), (4.77), (4.83), (4.85), (4.84) and (4.114), respectively.

Chapter 5

FINITE ELEMENT FORMULATION FOR PLATE STRUCTURES

In this chapter, the mathematical formulation of the development of the finite element method is presented. The classical equations of motion and the characteristic equations are also provided using the Galerkin's method. This brief derivation of the classical method provides the concept which later is utilized in the finite method. The formulation of the finite element method for nonlinear free and harmonic forced vibrations is presented. The expressions for the strain-displacement relations, kinetic energy and potential energy are provided. The linearizing functions for deriving nonlinear stiffness matrices are defined. The inplane displacements and lateral deflection are included in the formulation. Furthermore, the derivation of the harmonic force matrix for nonlinear forced vibration analysis is presented.

5.1 Strain and Curvature - Displacement Relations

Following von Karman's large deflection plate theory[22], the nonlinear strain displacement relations are defined as

$$\{\varepsilon\} = \{e\} + z\{\kappa\} . \tag{5.1}$$

The total strain vector $\{\varepsilon\}$, the membrane or midsurface strains $\{e\}$, and curvatures $\{\kappa\}$ are given by

60

$$\{\varepsilon\} = \begin{Bmatrix} \varepsilon_x \\ \varepsilon_y \\ \gamma_{xy} \end{Bmatrix} \tag{5.2}$$

$$\{e\} = \begin{Bmatrix} \dfrac{\partial u}{\partial x} + \dfrac{1}{2}\left(\dfrac{\partial w}{\partial x}\right)^2 \\ \dfrac{\partial v}{\partial y} + \dfrac{1}{2}\left(\dfrac{\partial w}{\partial y}\right)^2 \\ \dfrac{\partial u}{\partial y} + \dfrac{\partial v}{\partial x} + \dfrac{\partial w}{\partial x}\dfrac{\partial w}{\partial y} \end{Bmatrix} \tag{5.3}$$

$$\{\kappa\} = \begin{Bmatrix} -\dfrac{\partial^2 w}{\partial x^2} \\ -\dfrac{\partial^2 w}{\partial y^2} \\ -2\dfrac{\partial^2 w}{\partial x \partial y} \end{Bmatrix} \tag{5.4}$$

where ε_x and ε_y are the normal strains in x and y directions, respectively, and γ_{xy} is the shearing strain. The displacements of the plate midsurface in the x, y, z - directions are u, v and w, respectively.

The membrane or inplane resultant forces $\{N_0\}$, and bending and twisting moments $\{M_0\}$ are related to the strains and curvatures by

$$\{N_0\} = \begin{Bmatrix} N_x \\ N_y \\ N_{xy} \end{Bmatrix} = [C_0]\{e\} \tag{5.5}$$

$$\{M_0\} = \begin{Bmatrix} M_x \\ M_y \\ M_{xy} \end{Bmatrix} = [D_0]\{\kappa\} \tag{5.6}$$

where $[C_0]$ and $[D_0]$ are the extensional and bending material stiffness matrices, respectively. For plates of isotropic material and a uniform thickness h, the material stiffness matrices are

$$[C_0] = \frac{Eh}{1-\nu^2} \begin{bmatrix} 1 & \nu & 0 \\ \nu & 1 & 0 \\ 0 & 0 & \frac{1-\nu}{2} \end{bmatrix} \quad (5.7)$$

$$[D_0] = \frac{Eh^3}{12(1-\nu^2)} \begin{bmatrix} 1 & \nu & 0 \\ \nu & 1 & 0 \\ 0 & 0 & \frac{1-\nu}{2} \end{bmatrix} \quad (5.8)$$

where E and ν are the Young's modulus and Poisson's ratio, respectively.

5.2 Kinetic and Strain Energies

The kinetic energy of a plate element executing harmonic oscillations is

$$T = \frac{1}{2}\bar{\rho}h \int_0^{\bar{b}} \int_0^{\bar{a}} (\dot{u}^2 + \dot{v}^2 + \dot{w}^2) \, dx \, dy \quad (5.9)$$

where $\bar{\rho}$ and h are the mass density and the plate thickness, respectively. The length and width of a plate element shown in Fig. 8 are $\bar{a}$ and $\bar{b}$, respectively. A dot denotes differentiation with respect to time t. The kinetic energy can be separated into two parts as

$$T = T_s + T_b . \quad (5.10)$$

The kinetic energy due to membrane (inplane) stretching T_s is defined as

$$T_s = \frac{1}{2}\bar{\rho}h \int_0^{\bar{b}} \int_0^{\bar{a}} (\dot{u}^2 + \dot{v}^2) \, dx , \quad (5.11)$$

and the kinetic energy due to bending T_b is defined as

$$T_b = \frac{1}{2} \bar{\rho} h \int_0^{\bar{b}} \int_0^{\bar{a}} \dot{w}^2 \, dx \, .$$

(5.12)

The strain energy U for a plate element is given by

$$U = U_b + U_s$$

(5.13)

and

$$U_b = \frac{1}{2} \int_0^{\bar{b}} \int_0^{\bar{a}} \{M_o\}^T \{\kappa\} \, dx \, dy$$

$$= \frac{1}{2} \int_0^{\bar{b}} \int_0^{\bar{a}} \{\kappa\}^T [D_o] \{\kappa\} \, dx \, dy$$

(5.14)

$$U_s = \frac{1}{2} \int_0^{\bar{b}} \int_0^{\bar{a}} \{N_o\}^T \{e\} \, dx \, dy$$

$$= \frac{1}{2} \int_0^{\bar{b}} \int_0^{\bar{a}} \{e\}^T [C_o] \{e\} \, dx \, dy$$

(5.15)

where U_b and U_s denote the strain energies due to the bending and membrane components, respectively.

5.3   Displacement Functions

The displacement functions of the conforming rectangular plate with 24 degrees-of-freedom[78] shown in Fig. 8 is expanded as

$$w = \alpha_1 + \alpha_2 x + \alpha_3 y + \alpha_4 x^2 + \alpha_5 xy + \alpha_6 y^2$$

$$+ \alpha_7 x^3 + \alpha_8 x^2 y + \alpha_9 xy^2 + \alpha_{10} y^3$$

PLATE ELEMENT TO UNIFORM HARMONIC LOADING
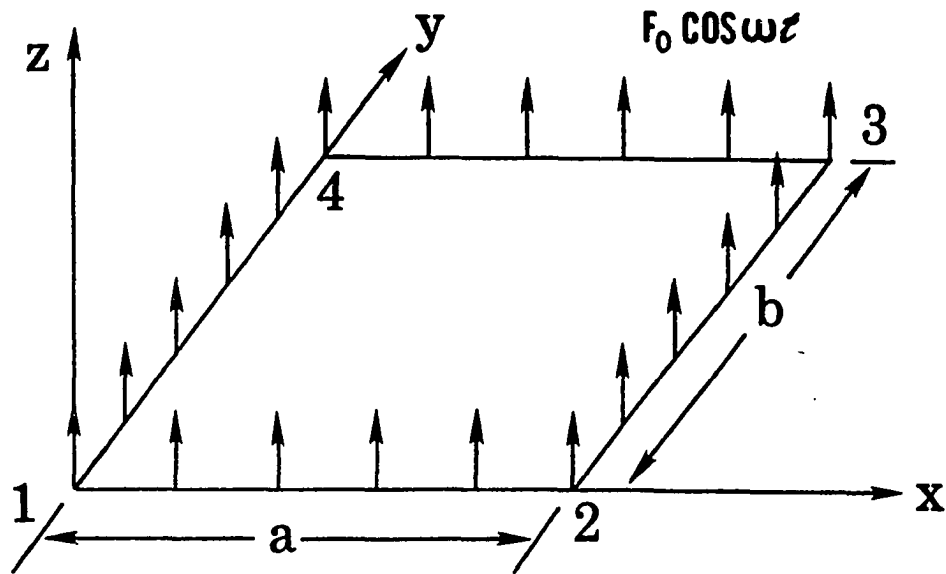
Fig. 8 Rectangular plate finite element.

$$+ \alpha_{11}x^3y + \alpha_{12}x^2y^2 + \alpha_{13}xy^3$$

$$+ \alpha_{14}x^3y^2 + \alpha_{15}x^2y^3 + \alpha_{16}x^3y^3 \qquad (5.16)$$

$$u = \beta_1 + \beta_2 x + \beta_3 y + \beta_4 xy \qquad (5.17)$$

$$v = \beta_5 + \beta_6 x + \beta_7 y + \beta_8 xy . \qquad (5.18)$$

The twenty four generalized coordinates $\alpha_1, \cdots, \alpha_{16}, \beta_1, \cdots, \beta_8$ can be written in vector form as

$$\{\alpha\}^T = [\alpha_1, \alpha_2, \cdots, \alpha_{16}] \qquad (5.19)$$

$$\{\beta\}^T = [\beta_1, \beta_2, \cdots, \beta_8] \qquad (5.20)$$

and the element nodal displacements are defined as

$$\{\delta\}^T = [\{\delta_b\}^T, \{\delta_s\}^T] \qquad (5.21)$$

where

$$\{\delta_b\}^T = [W_1, W_2, W_3, W_4, W_{x1}, \cdots,$$

$$W_{y1}, \cdots, W_{xy1}, \cdots, W_{xy4}] \qquad (5.22)$$

$$\{\delta_s\}^T = [U_1, U_2, U_3, U_4, V_1, V_2, V_3, V_4] . \qquad (5.23)$$

The relationship between the generalized coordinates and the element nodal displacements can be written as

$$\{\alpha\} = [\bar{T}_b] \{\delta_b\} \tag{5.24}$$

$$\{\beta\} = [\bar{T}_s] \{\delta_s\} . \tag{5.25}$$

The transformation matrices $[\bar{T}_b]$ and $[\bar{T}_s]$ are given in Appendix C.

By performing the differentiations to Eq. (5.16), the curvatures can be expressed as

$$- \frac{\partial^2 w}{\partial x^2} = - (2\alpha_4 + 6x\alpha_7 + 2y\alpha_8 + 6 xy\alpha_{11} + 2y^2\alpha_{12}$$

$$+ 6xy^2\alpha_{14} + 2y^3\alpha_{15} + 6xy^3\alpha_{16}) \tag{5.26}$$

$$- \frac{\partial^2 w}{\partial y^2} = - (2\alpha_6 + 2x\alpha_9 + 6y\alpha_{10} + 2x^2\alpha_{12}$$

$$+ 6xy\alpha_{13} + 2x^3\alpha_{14} + 6x^2 y\alpha_{15} + 6x^3 y\alpha_{16}) \tag{5.27}$$

$$- 2 \frac{\partial^2 w}{\partial x \, \partial y} = - 2(\alpha_5 + 2x\alpha_8 + 2y\alpha_9 + 3x^2\alpha_{11}$$

$$+ 4xy\alpha_{12} + 3y^2\alpha_{13} + 6x^2 y\alpha_{14}$$

$$+ 6xy^2\alpha_{15} + 9x^2 y^2\alpha_{16}) . \tag{5.28}$$

By using Eqs. (5.4), (5.26), (5.27), (5.28) and (5.24), the curvatures can be expressed in a matrix form as

$$\{\kappa\} = [\bar{H}] \{\alpha\} \tag{5.29}$$

Matrix $[\bar{H}]$ is given in Appendix C.

5.4 Linearizing Functions

The linearizing functions are defined in a vector form as

$$\{f\} = \left\{ \begin{array}{c} f_1 \\ f_2 \end{array} \right\} = \frac{1}{2} \left\{ \begin{array}{c} \frac{\partial w}{\partial x} \\ \frac{\partial w}{\partial y} \end{array} \right\} . \tag{5.30}$$

By performing the differentiation to Eq. (5.16), the linearizing functions can be expressed as

$$\{f\} = \frac{1}{2} [\bar{Q}]\{\alpha\} . \tag{5.31}$$

Matrix $[\bar{Q}]$ is given in Appendix C.

By substituting Eq. (5.24) into Eq. (5.31), the linearizing functions can be expressed as

$$\{f\} = \frac{1}{2} [\bar{Q}] [\bar{T}_b]\{\delta_b\} . \tag{5.32}$$

The linearizing functions are assumed to be constant in each element.

5.5 Element Equations of Motion for Nonlinear Free Vibration

The displacements u, v and w from Eqs. (5.16), (5.17) and (5.18) can be expressed in matrix forms as

$$u = [1 \ x \ y \ xy \ 0 \ 0 \ 0 \ 0] \ \{\beta\}$$
$$= [\bar{B}]\{\beta\} \tag{5.33}$$

$$v = [0 \ 0 \ 0 \ 0 \ 1 \ x \ y \ xy] \ \{\beta\}$$
$$= [\bar{C}] \ \{\beta\} \tag{5.34}$$

$$w = [1 \ x \ y \ x^2 \ xy \ y^2 \ x^3 \ x^2y \ xy^2 \ y^3$$

$$x^3y \ x^2y^2 \ xy^3 \ x^3y^2 \ x^2y^3 \ x^3y^3] \ \{\alpha\}$$

$$= [\bar{D}] \ \{\alpha\} \ . \tag{5.35}$$

By substituting Eq. (5.25) with Eqs. (5.33) and (5.34), and Eq. (5.24) with Eq. (5.35), the displacements can be expressed as

$$u = [\bar{B}][\bar{T}_s]\{\delta_s\} \tag{5.36}$$

$$v = [\bar{C}][\bar{T}_s]\{\delta_s\} \tag{5.37}$$

$$w = [\bar{D}][\bar{T}_b]\{\delta_b\} \ . \tag{5.38}$$

From Eqs. (5.11), (5.36) and (5.37), the expression of the kinetic energy due to membrane (inplane) stretching T_s can be written as

$$T_s = \frac{1}{2} \{\dot{\delta}_s\}^T [\bar{T}_s] \int_0^{\bar{b}} \int_0^{\bar{a}} \bar{\rho}h[[\bar{B}] + [\bar{C}]]^T [[\bar{B}] + [\bar{C}]]dx \ dy \ [\bar{T}_s]\{\dot{\delta}_s\}$$

$$= \frac{1}{2} \{\dot{\delta}_s\}^T [m_s]\{\dot{\delta}_s\} \tag{5.39}$$

where $[m_s]$ is the element mass matrix due to membrane (inplane) displacements and expressed as

$$[m_s] = [\bar{T}_s]^T \int_0^{\bar{b}} \int_0^{\bar{a}} \bar{\rho}h \ [\bar{E}]^T \ [\bar{E}] \ dx \ dy \ [\bar{T}_s] \tag{5.40}$$

where

$$[\bar{E}] = [\bar{B}] + [\bar{C}] \ . \tag{5.41}$$

Similarly, the expression of kinetic energy due to bending T_b can be derived from Eqs. (5.12) and (5.38) as

$$T_b = \frac{1}{2} \{\dot{\delta}_b\}^T [m_b]\{\dot{\delta}_b\} \tag{5.42}$$

where $[m_b]$ is the element mass matrix due to bending and expressed as

$$[m_b] = [\bar{T}_b]^T \int_o^{\bar{b}} \int_o^{\bar{a}} \bar{\rho} h \, [\bar{D}]^T \, [\bar{D}] \, dx \, dy \, [\bar{T}_b] \; . \tag{5.43}$$

The kinetic energy T, Eq. (5.10), can be expressed as

$$T = \frac{1}{2} \, \{\dot{\delta}\}^T \, [m]\{\dot{\delta}\} \tag{5.44}$$

where $[m]$ is the element mass matrix and expressed as

$$[m] = [m_b] + [m_s] \; . \tag{5.45}$$

By substituting Eq. (5.29) with Eq. (5.14), the bending strain energy U_b is expressed as

$$U_b = \frac{1}{2} \, \{\delta_b\}^T [k_b]\{\delta_b\} \tag{5.46}$$

where $[k_b]$ is the element linear bending stiffness matrix and expressed as

$$[k_b] = [\bar{T}_b]^T \int_o^{\bar{b}} \int_o^{\bar{a}} [\bar{H}]^T [D_o][\bar{H}] \, dx \, dy \, [\bar{T}_b] \; . \tag{5.47}$$

By using the linearizing functions, Eqs. (5.30), (5.31) and (5.32), Eq. (5.3) can be expressed as

$$\{e\} = [\bar{F}] \left\{ \begin{array}{c} \dfrac{\partial w}{\partial x} \\[2mm] \dfrac{\partial w}{\partial y} \end{array} \right\} + \left\{ \begin{array}{c} \dfrac{\partial u}{\partial x} \\[2mm] \dfrac{\partial v}{\partial y} \\[2mm] \dfrac{\partial u}{\partial y} + \dfrac{\partial v}{\partial x} \end{array} \right\}$$

$$= [\bar{F}][\bar{Q}] \, \{\alpha\} + [\bar{G}] \, \{\beta\}$$

$$= [[\bar{F}][\bar{Q}] \quad [\bar{G}]] \left\{ \begin{array}{c} \{\alpha\} \\ \{\beta\} \end{array} \right\} \tag{5.48}$$

and $[\bar{F}]$ is expressed as

$$[\bar{F}] = \begin{bmatrix} f_1 & 0 \\ 0 & f_2 \\ f_2 & f_1 \end{bmatrix} \tag{5.49}$$

and matrix $[\bar{G}]$ is given in Appendix C.

By substituting Eq. (5.48) with Eq. (5.15), the linearized membrane strain energy U_s can be expressed as

$$U_s = \frac{1}{2} [\{\delta_b\}^T \ \{\delta_s\}^T] \left[\begin{bmatrix} [\bar{k}_b] & [\bar{k}_{bs}] \\ [\bar{k}_{sb}] & 0 \end{bmatrix} \right.$$

$$\left. + \begin{bmatrix} 0 & 0 \\ 0 & [k_s] \end{bmatrix} \right] \begin{Bmatrix} \{\delta_b\} \\ \{\delta_s\} \end{Bmatrix} \tag{5.50}$$

where $[k_s]$ is the element linear membrane stiffness matrix, and $[\bar{k}_b]$, $[\bar{k}_{bs}]$ and $[\bar{k}_{sb}]$ are the nonlinear stiffness matrices due to bending and coupling between bending and membrane stretching, respectively. These matrices are expressed as

$$[k_s] = [\bar{T}_s]^T \int_0^{\bar{b}} \int_0^{\bar{a}} [\bar{G}]^T [C_0][\bar{G}] \ dx \ dy \ [\bar{T}_s] \tag{5.51}$$

$$[\bar{k}_b] = [\bar{T}_b]^T \int_0^{\bar{b}} \int_0^{\bar{a}} [\bar{Q}]^T [\bar{F}]^T [C_0] [\bar{F}] [\bar{Q}] \ dx \ dy \ [\bar{T}_b] \tag{5.52}$$

$$[\bar{k}_{bs}] = [\bar{T}_b]^T \int_0^{\bar{b}} \int_0^{\bar{a}} [\bar{Q}]^T [\bar{F}]^T [C_0] [\bar{G}] \ dx \ dy \ [\bar{T}_s] \tag{5.53}$$

$$[\bar{k}_{sb}] = [\bar{k}_{bs}]^T . \tag{5.54}$$

The application of Lagrange's equation to the kinetic energy T and the strain energy U leads to the element nonlinear free vibration equation of motion as

$$
\begin{bmatrix} [m_b] & 0 \\ 0 & [m_s] \end{bmatrix} \{\ddot{\delta}\} + \left[\begin{bmatrix} [k_b] & 0 \\ 0 & [k_s] \end{bmatrix} + \begin{bmatrix} [\bar{k}_b] & [\bar{k}_{bs}] \\ [\bar{k}_{sb}] & 0 \end{bmatrix} \right] \{\delta\} = 0. \tag{5.55}
$$

5.6 Element Harmonic Force Matrix

In the classic continuum approach, the dynamic von Karman plate equations of motion are given by

$$
\nabla^4 \psi = E (w,_{xy}^2 - w,_{xx} w,_{yy}) \tag{5.56}
$$

$$
\bar{L} (w,\psi) = \bar{\rho}h\, w,_{tt} + D\nabla^4 w - h (\psi,_{yy} w,_{xx}
$$

$$
+ \psi,_{xx} w,_{yy} - 2\psi,_{xy} w,_{xy}) - F^*(t) = 0 . \tag{5.57}
$$

For the single mode approximate solutions, the deflection function is assumed in the form

$$
w = h\, q(t)\, \phi(x,y) \tag{5.58}
$$

where mode shape ϕ satisfies the related boundary conditions. Substitution of Eq. (5.58) with Eq. (5.56) yields a solution to the stress function $\psi(x,y)$ from the compatibility equation (5.56). Application of the Galerkin's method $\iint \bar{L} (w,\psi) \phi(x,y)\, dx\, dy = 0$ yields a modal equation in the Duffing form[16, 24-27] as

$$
mq,_{tt} + kq + \bar{k}\, q^3 = F^*(t) , \tag{5.59}
$$

or in nondimensional time τ [77]

$$q_{,\tau\tau} + q + \beta_o q^3 = F^*(\tau) \tag{5.60}$$

where $\tau = t \, (k/m)^{1/2}$, $\beta_o = \bar{k}/k$ and $F^*(\tau) = F^*(t)/m$. When forcing function $F^*(\tau)$ is a simple harmonic $P_o^* \cos \omega\tau$, an approximate solution of Eq. (5.60), using the perturbation method, is the well-known result[24-25,77]

$$\left(\frac{\omega}{\omega_L}\right)^2 = 1 + \frac{3}{4} \beta_o A_o^2 - \frac{P_o^*}{A_o} . \tag{5.61}$$

With a simple elliptic forcing function $F^*(\tau) = B \, A_o \, cn \, (\lambda_o\tau, \, \eta_o) = B_o q$ as the external excitation to the Duffing system, an elliptic response[16,24-27,77]

$$q = \bar{A}_o \, cn \, (\lambda_o\tau, \, \eta_o) \tag{5.62}$$

where

$$\lambda_o = (1 + \beta_o \, \bar{A}_o^2)^{1/2}$$

$$\eta_o = [\beta_o \, \bar{A}_o^2 /2 \, (1 + \beta_o\bar{A}_o^2)]^{1/2} \tag{5.62a}$$

is obtained as an exact solution of Eq. (5.60), where B_o is the nondimensional forcing amplitude factor, λ_o and η_o are the circular frequency and the modulus of the Jacobian elliptic function, and $\bar{A}_o = w_{max}/h$ is the amplitude. By expanding the elliptic forcing function into Fourier series and comparing the orders of magnitude of the various harmonic components, Hsu[77] showed that the single harmonic forcing function $P_o^* \cos \omega\tau$ is the first order approximate of the elliptic forcing function $B_o \, \bar{A}_o \, cn \, (\lambda_o\tau, \eta_o)$. Also, the first order approximation of the elliptic response of Eq. (5.60) yields the same

frequency-amplitude relations of Eq. (5.61) as the perturbation solution. In obtaining the exact elliptic response of Eq. (5.60), the excitation force $F(\tau) = B_0 q$ is treated as a linear spring in the Duffing equation

$$q,_{\tau\tau} + (1-B_0) q + \beta_0 q^3 = 0 \tag{5.63}$$

This linear spring force $\beta_0 q$ possesses a potential energy of $V = B_0 q^2/2$. The potential energy of a plate element subjected to a uniform harmonic forcing function can thus be approximated by

$$V = \frac{B_0}{2} \int_0^{\bar{b}} \int_0^{\bar{a}} w^2 \, dx \, dy \; . \tag{5.64}$$

An examination of Eqs. (5.12), (5.42) and (5.64) indicates that the harmonic force matrix [h] for a plate element under uniform loading F_0 cos (ωt) is

$$[h] = \frac{C \, F_0}{\bar{A}_0 \bar{\rho} \, h^2} [m_b] \; . \tag{5.65}$$

The actual applied distributed force intensity F_0 (N/m^2 or psi) is related to the dimensionless forcing parameter P_0^* and the dimensionless forcing amplitude factor B_0 by

$$B_0 = \frac{P_0^*}{\bar{A}_0} = \frac{c \, F_0}{\bar{A}_0 \bar{\rho} \, h^2 \, \omega_L^2} \tag{5.66}$$

where

$$c = \frac{\displaystyle\iint^{\text{(Load elements)}} \phi \; dx \; dy}{\displaystyle\int_0^{\bar{b}} \int_0^{\bar{a}} \phi^2 \qquad dx \; dy} \; . \tag{5.67}$$

For plates under uniformly distributed force over an entire plate

$$c = \frac{\int_0^{\bar{b}} \int_0^{\bar{a}} \phi \ dx \ dy}{\int_0^{\bar{b}} \int_0^{\bar{a}} \phi^2 \ dx \ dy} \ . \tag{5.68}$$

The constant c for plates is simply the ratio of volumes under a plate mode shape and the square of a mode shape. The harmonic force matrix of Eq. (5.65) depends on the plate amplitude $\bar{A}_0 = w_{max}/h$ and P_0^* (or F_0).

It should be noted that the derivation of the harmonic force matrix for plates is the same as for beams. The only difference is that the nondimensional form is employed to derive the harmonic force matrix for plates.

5.7 Element Equations of Motion for Nonlinear Forced Vibration

The application of the Lagrange's equation to the kinetic energy, the strain energy and the potential energy due to a uniformly distributed force, Eqs. (5.9), (5.13) and (5.64), leads to the equations of motion for the present rectangular plate under the influences of inertia, elastic, large deflection and uniform harmonic excitation force as

$$\begin{bmatrix} [m_b] & 0 \\ 0 & [m_s] \end{bmatrix} \{\ddot{\delta}\} + \left\{ \begin{bmatrix} [k_b] & 0 \\ 0 & [k_s] \end{bmatrix} \right.$$

$$+ \begin{bmatrix} [\bar{k}_b] & [\bar{k}_{bs}] \\ [\bar{k}_{sb}] & 0 \end{bmatrix} - \left. \begin{bmatrix} [h] & 0 \\ 0 & 0 \end{bmatrix} \right\} \{\delta\} = 0 \tag{5.69}$$

and Eq. (5.69) can be rewritten as

$$[m] \{\ddot{\delta}\} + [[k_L] + [k_{NL}] - [h]] \{\delta\} = 0 . \qquad (5.70)$$

It should be noted that the equations of motion for a plate element is exactly the same form as for a beam element.

Chapter 6

RESULTS AND DISCUSSION

The fundamental frequency ratio of nonlinear free and forced vibrations at various amplitudes for simply supported and clamped supported conditions are reported in this chapter. The fundamental frequency ratio is defined as the ratio between the first nonlinear frequency and the first linear frequency. The fundamental frequency ratio of beams is specified by ω_{NL1}/ω_{L1}. Similarly, the fundamental frequency ratio of plates is ω/ω_L. Both immovable and movable inplane edges conditions are considered. Finite element results with and without inplane displacement and inertia (IDI) are given. The meaning of "without inplane displacement and inertia" is to neglect inplane displacements, completely from the formulations. For beams, the harmonic balance solution[20], Runge-Kutta solution and experimental results[21] are also given for comparison with the finite element results. The iterative single-mode method (method I) and the multiple-mode method (method II) are performed. Because of symmetry, only a half of a beam divided into twenty elements is considered herein. For plates, the elliptic function solution[24], the perturbation solution[77], and the Rayleigh-Ritz solution[8] are also given for comparison with the finite element results. The study of gridwork refinement is investigated. The iterative single-mode method (method I) is performed.

76

6.1 Boundary Conditions

The transverse deflection boundary condition for a simply supported condition is defined by letting the deflection equal zero at the boundary. For a clamped supported condition, the transverse deflection boundary conditions are the deflection and its associated slope equal to zero at the boundary. The inplane boundary conditions are divided into two categories, namely, immovable and movable inplane edge. The definition of an immovable inplane edge is defined as the inplane displacements u and v at the boundary equal to zero. For a movable inplane edge, the inplane displacements u and v are set free at the boundary.

6.2 Beams

Most of the finite element results are calculated by the multiple-mode method (method II) unless otherwise specified. The multiple-mode method (method II) and the iterative single-mode method (method I) are explained in Chap. 3.

6.2.1 Material Properties

All the beam results presented here are based on the following material (steel) properties:

mass density	$\bar{\rho} = 26.6832 \text{ E-10 N} - \sec^2/\text{mm}^4$
thickness	$h = 0.514 \quad \text{mm}$
width	$B = 26.0 \quad \text{mm}$
Young's modulus	$E = 6.98 \text{ E+04 N/mm}^2$
radius of gyration	$R = 0.148379 \text{ mm}$.

For nonlinear vibrations, the effect of the slenderness ratio (L/R) has some influence in the solutions. In this dissertation, there are many slenderness ratios in use as shown in Table 1. These slenderness ratios are calculated by changing the beam length and keeping the radius of gyration constant. Most of the results reported herein, are based on a 150 mm beam length (L/R = 1010) unless otherwise specified. This 150 mm long beam (L/R = 1010) has the same dimensions as the beam for which Yamaki et al.[21] performed the experiment.

6.2.2 Improved Nonlinear Free Vibration

The fundamental frequency ratios $(\omega_{NL1}/\omega_{L1})$ of free vibration at various amplitudes (A/R) without inplane displacement and inertia (IDI) for clamped and simply supported beams (L/R = 1010) are shown in Table 2 for the cases of single, two and three-mode method, respectively. The amplitude ratio for these beams are also provided in Table 3. Table 2 shows that the more numbers of modes are used in the analysis the less the frequency ratio will be, e.g., at A/R = 5.0, the three-mode solution yields a smaller frequency ratio than the two-mode solution. Table 3 shows the influence of the amplitudes of the higher modes, especially the amplitude of the second mode. Table 4 shows the comparison of a two-mode response between the finite element method and Runge-Kutta method for clamped and simply supported beams (L/R = 1010) without inplane displacement and inertia (IDI). This clearly demonstrates the remarkable agreement between the finite element and Runge-Kutta solutions. These results are also shown in Figs. 9 and 10 for the clamped and simply supported cases, respectively.

Table 1   Relations Between Slenderness
Ratio (L/R) and Beam Length

Slenderness Ratio L/R	Beam Length L (mm)
1010	150.000
100	14.840
50	7.420
20	2.968

Table 2 Frequency Ratios for Nonlinear Free Vibration of
Clamped and Simply Supported Beams (L/R = 1010)
without Inplane Displacement and Inertia (IDI)

A/R	Frequency Ratio, ω_{NL1}/ω_{L1}			
	1 mode		2 modes	3 modes
	Finite Element	Elliptic Solution	Finite Element	Finite Element
Clamped Beam				
1.0	1.0218	1.0222	1.0218 (2)[a]	1.0217 (3)
2.0	1.0845	1.0857	1.0844 (3)	1.0831 (4)
3.0	1.1817	1.1831	1.1814 (5)	1.1757 (4)
4.0	1.3056	1.3064	1.3051 (6)	1.2900 (6)
5.0	1.4495	1.4488	1.4490 (8)	1.4188 (9)
Simply Supported Beam				
1.0	1.0897	1.0892	1.0888 (3)	1.0888 (3)
2.0	1.3229	1.3178	1.3120 (5)	1.3119 (5)
3.0	1.6394	1.6257	1.6030 (7)	1.6022 (7)
4.0	2.0000	1.9760	1.9248 (11)	1.9218 (11)
5.0	2.3848	2.3501	2.2624 (17)	2.2549 (18)

[a.] Number in brackets denotes the number of iterations to get a
converged solution 10^{-5}.

Table 3   Amplitude Ratios for Nonlinear Free Vibration of Clamped
and Simply Supported Beams (L/R = 1010) without Inplane
Displacement and Inertia (IDI)

A/R	Amplitude Ratio		
	2 modes	3 modes	
	A_1/A_2	A_1/A_2	A_1/A_3
Clamped Beam			
1.0	- 1054	- 1056	2164
2.0	- 280	- 282	559
3.0	- 137	- 139	261
4.0	- 87	- 89	157
5.0	- 64	- 66	109
Simply Supported Beam			
1.0	446	446	*
2.0	125	125	7652
3.0	66	66	1972
4.0	45	44	848
5.0	35	34	480

* Number is larger than $\left|10^4\right|$.

Table 4   Comparison Between Runge-Kutta Method and Finite
Element Method for Two-Mode Nonlinear Free Vibration
of Clamped and Simply Supported Beams (L/R = 1010)
without Inplane Displacement and Inertia (IDI).

A/R	Frequency Ratio, ω_{NL1}/ω_{L1}		% Difference[†]
	Finite Element	Runge-Kutta	
Clamped Beam			
1.0	1.0218	1.0222	0.04
2.0	1.0845	1.0852	0.07
3.0	1.1817	1.1810	0.03
4.0	1.3056	1.3009	0.32
5.0	1.4495	1.4373	0.81
Simply Supported Beam			
1.0	1.0888	1.0888	0.00
2.0	1.3120	1.3135	0.11
3.0	1.6030	1.6115	0.53
4.0	1.9248	1.9467	1.13
5.0	2.2624	2.3023	1.73

[†] % Difference $= \left| \dfrac{(\text{Runge-Kutta}) - (\text{Finite Element})}{(\text{Runge-Kutta})} \right| \times 100$ %.
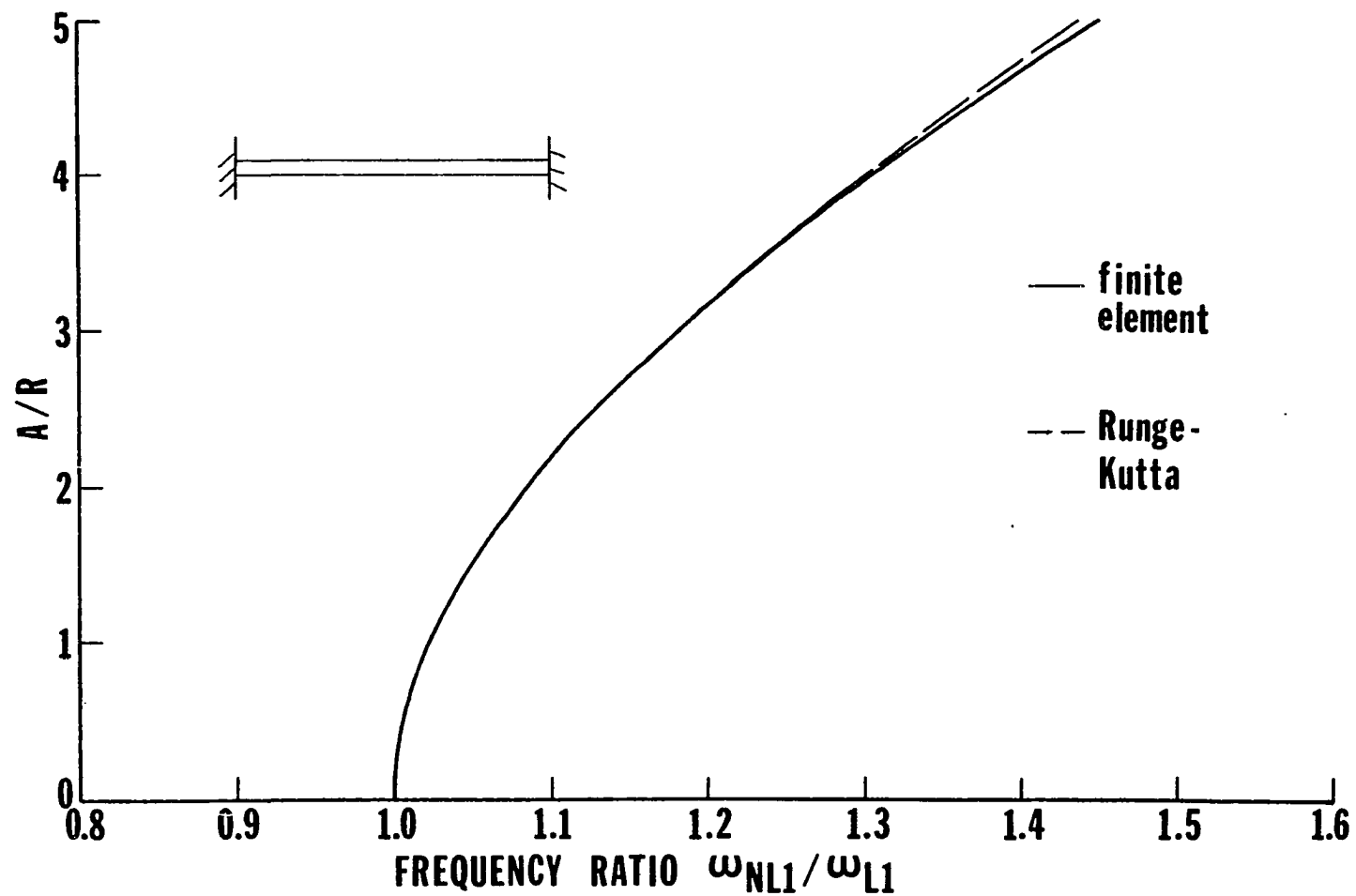
Fig. 9   Comparison between the finite element method (method II) and Runge-Kutta method for a two-mode clamped beam (L/R = 1010).
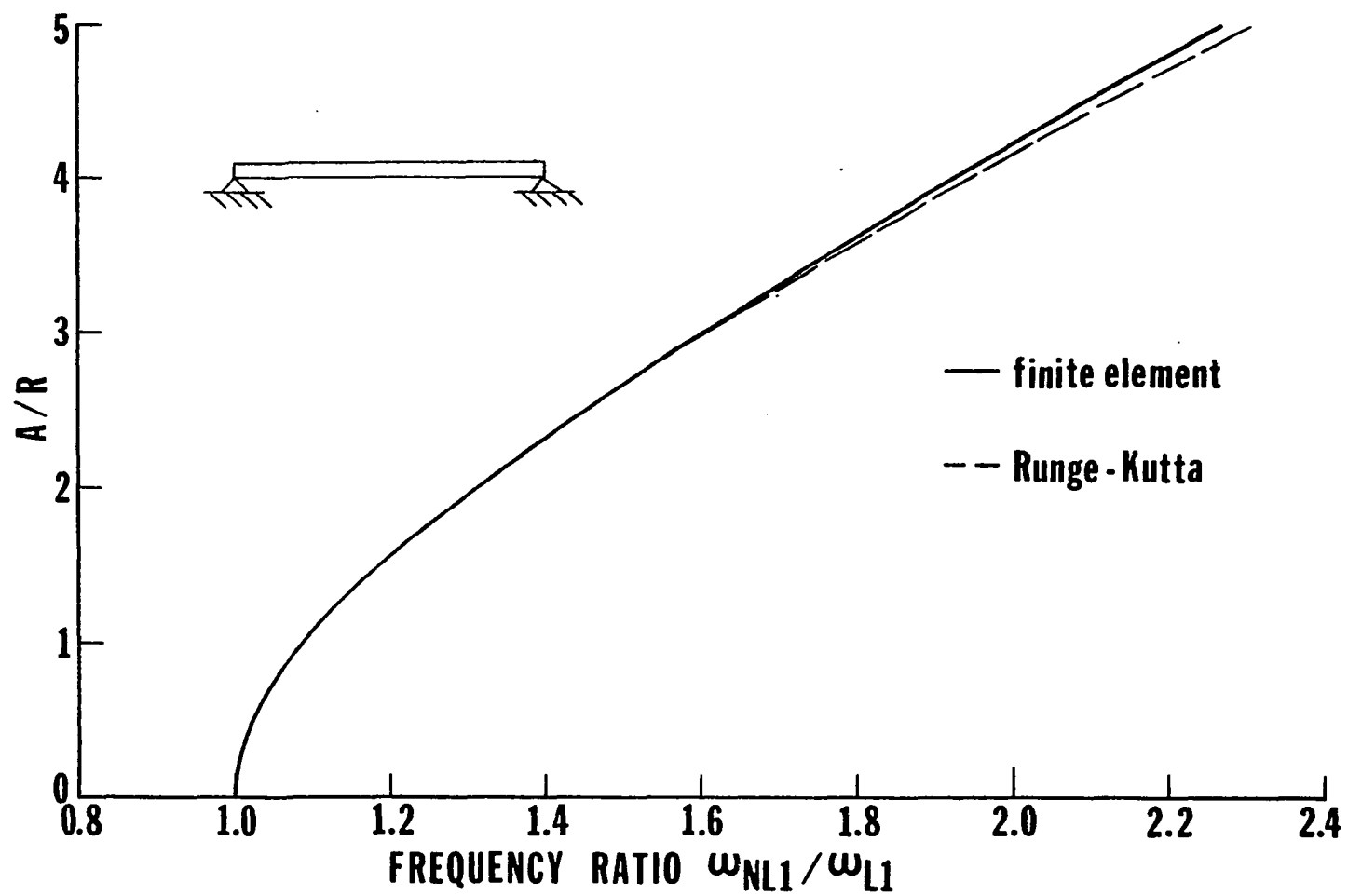
Fig. 10 Comparison between the finite element method (method II) and Runge-Kutta method for a two-mode simply supported beam (L/R = 1010).

The clamped and simply supported free vibration results (L/R = 1010) with inplane displacement and inertia (IDI) for both ends restrained from longitudinal movement (immovable case) are shown in Table 5, and the amplitude ratios for this clamped beam are also shown in Table 6. Table 5 shows the good agreement between the results using the iterative single-mode method (method I) and the results of three-mode responses using the multiple-mode method (method II). It can be interpreted that the iterative single-mode method (method I) and the multiple-mode method (method II) will yield the same beam deflection provided a large number of modes is used for the multiple-mode method (method II). The evidence of this effect can also be seen in Section 6.2.3 (Table 11) and Section 6.2.5 (Table 17). The frequency-amplitude relationships for three-mode responses of these clamped and simply supported beams are also shown in Fig. 11. This figure clearly shows that the simply supported beam yields the higher nonlinearity than the clamped beam.

The responses for both ends free to move longitudinally (movable case) are shown in Tables 7 and 8. Table 7 shows the frequency-amplitude relations for a three-mode solution of clamped and simply supported beams with inplane deformation and inertia for the slenderness ratios of 100, 50 and 20. The result for the clamped case is also shown in Fig. 12. From this figure, the high slenderness ratio beam (L/R = 100) yields almost none of nonlinearity. Conversely, the less slenderness ratio case (L/R = 20) leads to a situation that eventually exhibits a slightly softening type of nonlinearity. The softened type exists when the nonlinear frequency is less than the linear frequency ($\omega_{NL1}/\omega_{L1} < 1.0$). Atluri[11] also obtained the similar softening type in his investigation.

Table 5 Frequency Ratios for Nonlinear Free Vibration of
Clamped and Simply Supported Immovable Beams
(L/R = 1010) with Inplane Displacement and Inertia
(IDI)

A/R	Frequency Ratio, ω_{NL1}/ω_{L1}				
	1 mode			2 modes	3 modes
	Finite Element (method I)	Finite Element (method II)	Rayleigh Ritz[8]	Finite Element (method II)	Finite Element (method II)
Clamped Beam					
1.0	1.0149 (2)[a]	1.0149	-	1.0149 (2)[a]	1.0149 (2)
2.0	1.0580 (3)	1.0582	-	1.0581 (3)	1.0581 (3)
3.0	1.1259 (4)	1.1268	-	1.1264 (4)	1.1259 (4)
4.0	1.2139 (5)	1.2164	-	1.2151 (5)	1.2140 (2)
5.0	1.3174 (6)	1.3226	-	1.3202 (6)	1.3176 (6)
Simply Supported Beam					
1.0	1.0607 (2)	1.0607	1.0607[b]	1.0607 (2)	1.0607 (2)
2.0	1.2247 (2)	1.2247	1.2246	1.2247 (2)	1.2247 (2)
3.0	1.4577 (2)	1.4577	1.4573	1.4577 (2)	1.4577 (2)
4.0	1.7320 (2)	1.7320	1.7309	1.7320 (2)	1.7320 (2)
5.0	2.0310 (2)	2.0310	2.0289	2.0310 (2)	2.0310 (2)

[a.] Number in brackets denotes the number of iterations to get a converged solution 10^{-5}.

[b.] L/R = 100.

Table 6 Amplitude Ratios for Nonlinear Free Vibration of
Clamped Immovable Beams (L/R = 1010) with Inplane
Displacement and Inertia (IDI)

A/R	Amplitude Ratio		
	2 modes	3 modes	
	A_1/A_2	A_1/A_2	A_1/A_3
1.0	- 1354	- 1354	*
2.0	- 346	- 346	2690
3.0	- 159	- 159	1202
4.0	- 94	- 95	678
5.0	- 64	- 64	442

* Number is larger than $\left|10^4\right|$.
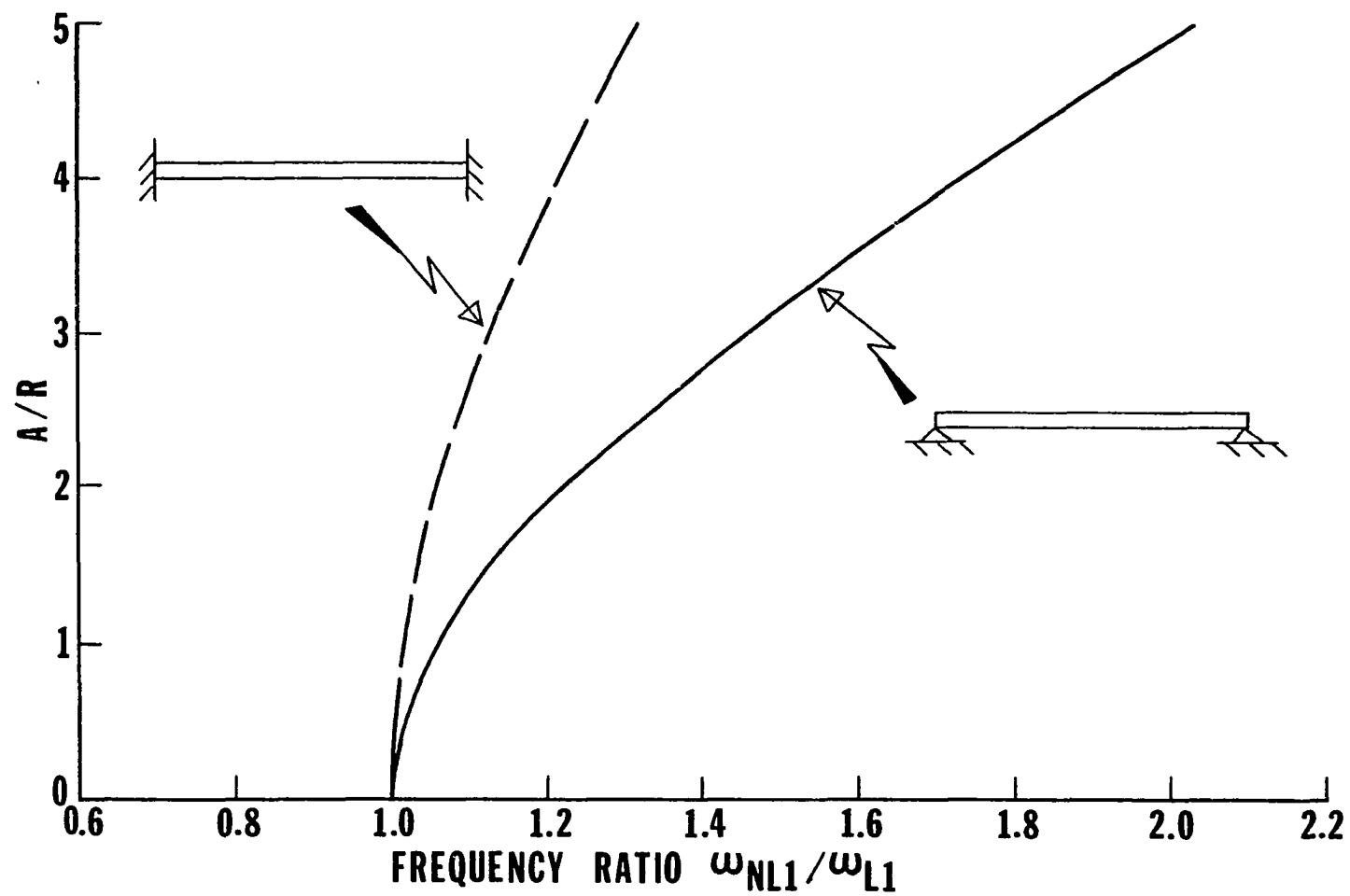
Fig. 11 Amplitude versus frequency for three-mode clamped and simply supported
beams (L/R = 1010) with immovable ends.

Table 7 Frequency Ratios (ω_{NL1}/ω_{L1}) for Three-Mode Nonlinear
Free Vibration of Clamped and Simply Supported Movable
Beams with Inplane Displacement and Inertia (IDI) for
Different Slenderness Ratio (L/R)

A/R	Slenderness Ratio, L/R		
	100	50	20
Clamped Beam			
1.0	.9999 (2)[a]	.9997 (2)	.9983 (2)
2.0	.9997 (2)	.9989 (2)	.9933 (2)
3.0	.9994 (2)	.9976 (2)	.9850 (3)
4.0	.9989 (2)	.9957 (2)	.9737 (3)
5.0	.9983 (2)	.9933 (2)	.9596 (3)
Simply Supported Beam			
1.0	1.0000 (2)	.9999 (2)	.9993 (2)
2.0	.9999 (2)	.9996 (2)	.9973 (2)
3.0	.9998 (2)	.9990 (2)	.9938 (2)
4.0	.9996 (2)	.9982 (2)	.9891 (2)
5.0	.9993 (2)	.9973 (2)	.9832 (2)

[a] Number in brackets denotes the number of iterations to get a
converged solution 10^{-5}.

Table 8 Amplitude Ratios for Three-Mode Nonlinear Free Vibration of Clamped and Simply Supported Mov able Beams (L/R = 20) with Inplane Displacement and Inertia (IDI)

A/R	Amplitude Ratio	
	A_1/A_2	A_1/A_3
Clamped beam		
1.0	6410	*
2.0	1613	*
3.0	724	- 8914
4.0	414	- 5152
5.0	270	- 3413
Simply Supported Beam		
1.0	*	*
2.0	*	*
3.0	5178	*
4.0	2936	*
5.0	1898	*

* Number is larger than $\left|10^4\right|$.
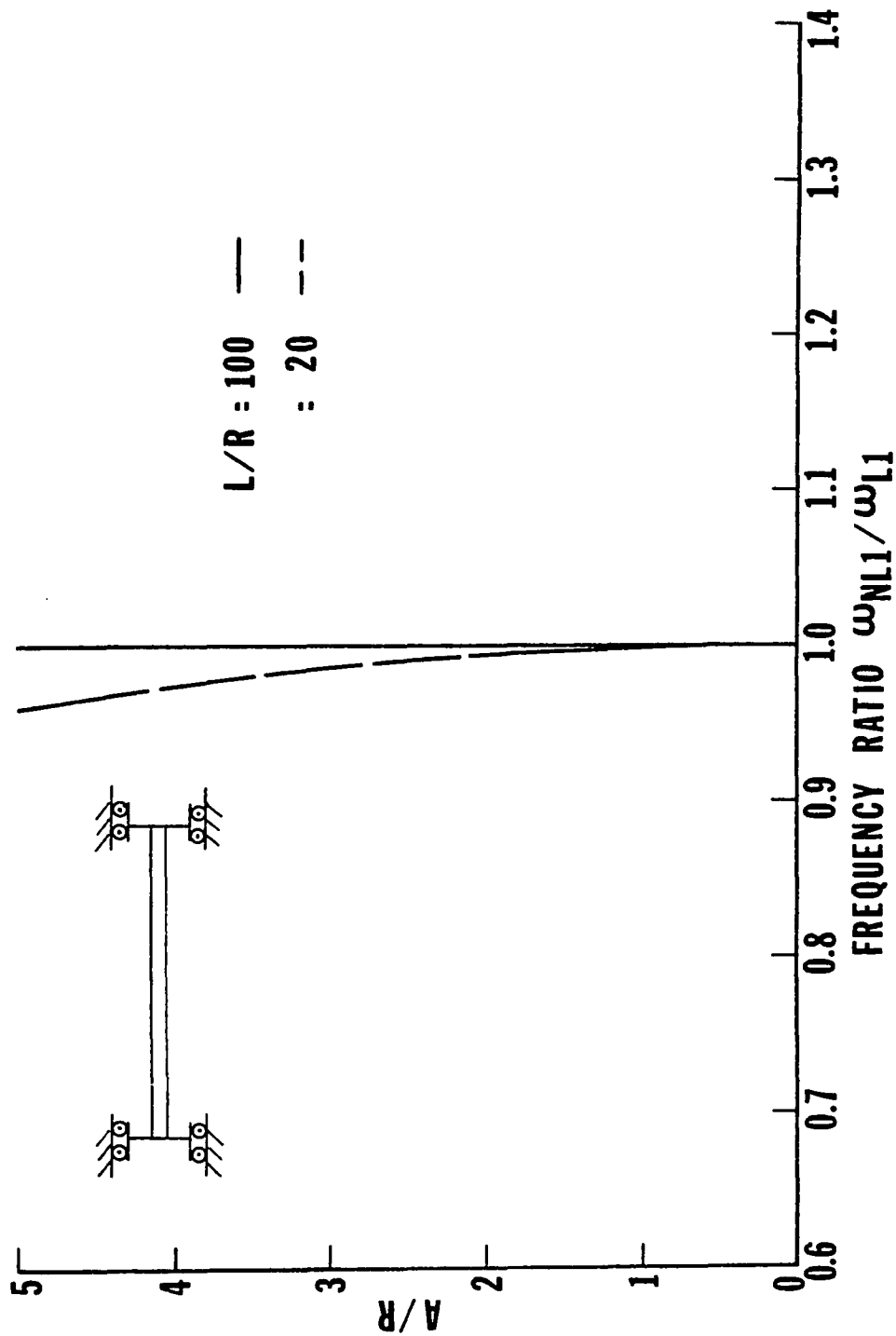
Fig. 12 Amplitude versus frequency for a three-mode clamped beam (L/R = 1010) with movable ends.

The simply supported case as shown in Table 7, exhibits less influence of the softening type than the clamped case. Table 8 shows the amplitude ratios for the three-mode solutions of clamped and simply supported movable beams (L/R = 20) with IDI. The comparison of the amplitude ratio of the movable clamped case (Table 8) to the immovable clamped case (Table 6) shows that the higher modes have more influence on the immovable case than the movable case.

6.2.3 Nonlinear Response to Distributed Harmonic Force

The responses of clamped and simply supported beams (L/R = 1010) without IDI are shown in Tables 9 and 10. Table 9 shows the frequency ratios for the cases of single, two and three-mode approaches. It should be noted that as the amplitude is increased, the more iteration is needed. The amplitude ratios for these beams are shown in Table 10. The frequency-amplitude relations for these clamped and simply supported beams with various force intensity (F_0) are also plotted in Figs. 13 and 14 for the three-mode solution, respectively.

The responses of clamped and simply supported immovable beams (L/R = 1010) with IDI are shown in Tables 11 and 12. Table 11 shows the frequency ratios for the cases of single, two and three-mode approaches (method II), and the iterative single-mode method (method I). Table 11 shows the good agreement between the results using the iterative single-mode method (method I) and the results of three-mode responses using the multiple-mode method (method II). It can be interpreted that the iterative single-mode method (method I) and the multiple-mode method (method II) will yield the same beam deflection provided a large number of modes is used for the multiple-mode method (method II). The evidence

Table 9 Frequency Ratios for Nonlinear Forced Vibration of
Clamped and Simply Supported Beams (L/R = 1010) without
Inplane Displacement and Inertia (IDI) under Uniform
Harmonic Distributed Force

A/R	Frequency Ratio, ω_{NL1}/ω_{L1}		
	1 mode	2 modes	3 modes
Clamped Beam: F_0 = 0.002 N/mm			
± 1.0	.4101	.4105 (3)[a]	.4097 (3)
	1.3856	1.3855 (3)	1.3856 (2)
± 2.0	.8592	.8595 (4)	.8573 (3)
	1.2705	1.2701 (3)	1.2694 (4)
± 3.0	1.0509	1.0511 (5)	1.0440 (5)
	1.2994	1.2987 (4)	1.2940 (4)
± 4.0	1.2189	1.2189 (6)	1.2019 (7)
	1.3869	1.3860 (6)	1.3725 (6)
± 5.0	1.3877	1.3878 (8)	1.3554 (9)
	1.5087	1.5078 (8)	1.4794 (8)
Simply Supported Beam: F_0 = 0.001 N/mm			
- 1.0	1.8328	1.8331 (3)	1.8331 (3)
± 2.0	.8150	.7937 (5)	.7934 (5)
	1.6840	1.6771 (5)	1.6771 (5)
± 3.0	1.4013	1.3560 (7)	1.3549 (7)
	1.8470	1.8168 (7)	1.8162 (7)
± 4.0	1.8593	1.7760 (11)	1.7725 (11)
	2.1314	2.0629 (11)	2.0603 (11)
± 5.0	2.2920	2.1625 (17)	2.1543 (18)
	2.4742	2.3581 (17)	2.3511 (18)

[a]. Number in brackets denotes the number of iterations to get a
converged solution 10^{-5}.

Table 10   Amplitude Ratios for Nonlinear Forced Vibration of Clamped and Simply Supported Beams (L/R = 1010) without Inplane Displacement and Inertia (IDI) under Uniform Harmonic Distributed Force

A/R	Amplitude Ratio		
	2 modes	3 modes	
	A_1/A_2	A_1/A_2	A_1/A_3
Clamped Beam: $F_0 = 0.002$ N/mm			
± 1.0	- 1054	- 1056	2164
± 2.0	- 280	- 282	559
± 3.0	- 137	- 139	261
± 4.0	- 87	- 89	157
± 5.0	- 64	- 66	109
Simply Supported Beam: $F_0 = 0.001$ N/mm			
- 1.0	446	446	*
± 2.0	125	125	7652
± 3.0	66	66	1972
± 4.0	45	44	848
± 5.0	35	34	480

* Number is larger than $\left|10^4\right|$.
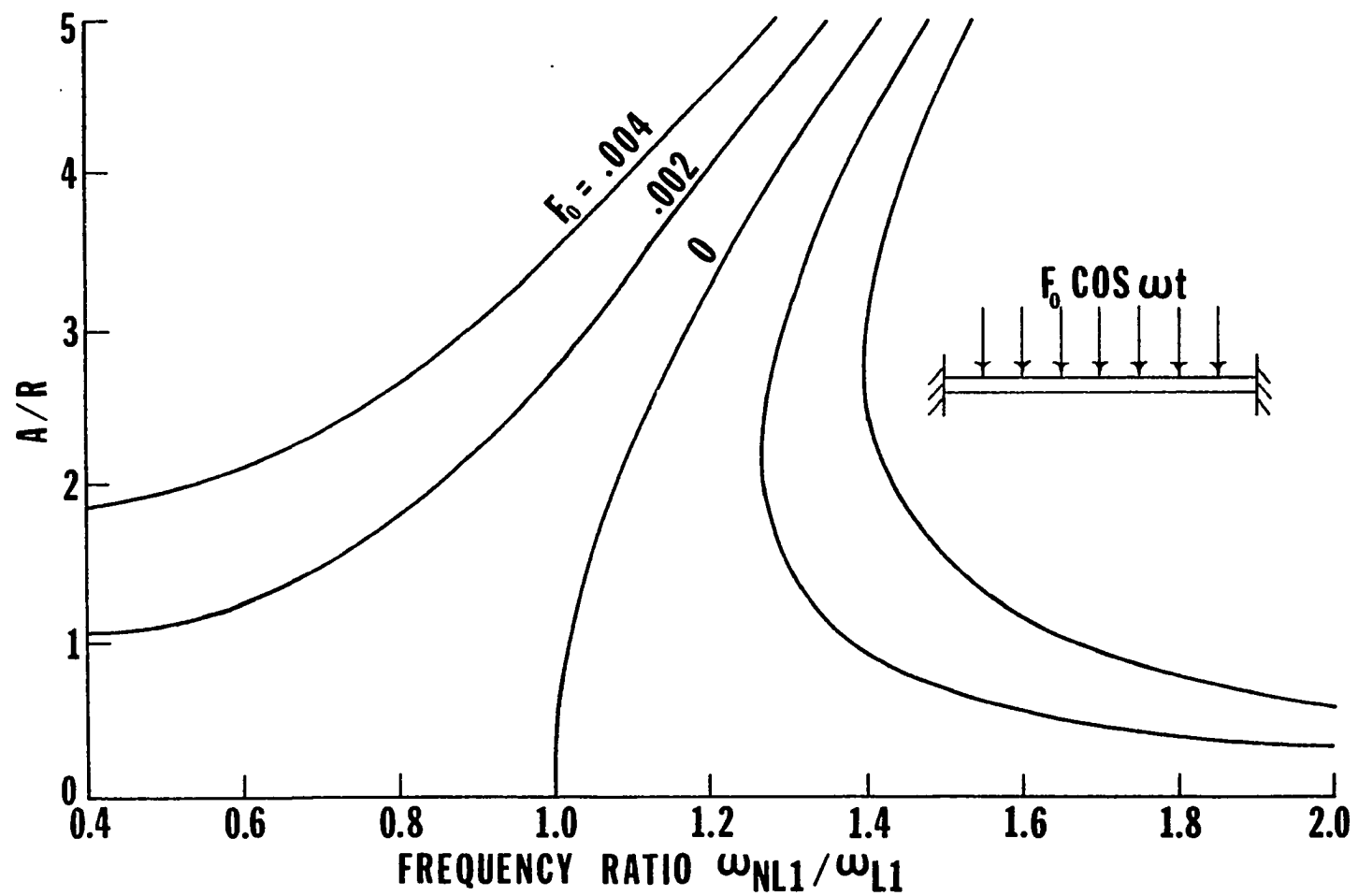
Fig. 13 Amplitude versus frequency a for three-mode simply supported beam (L/R = 1010) under uniform harmonic force intensity F_0.
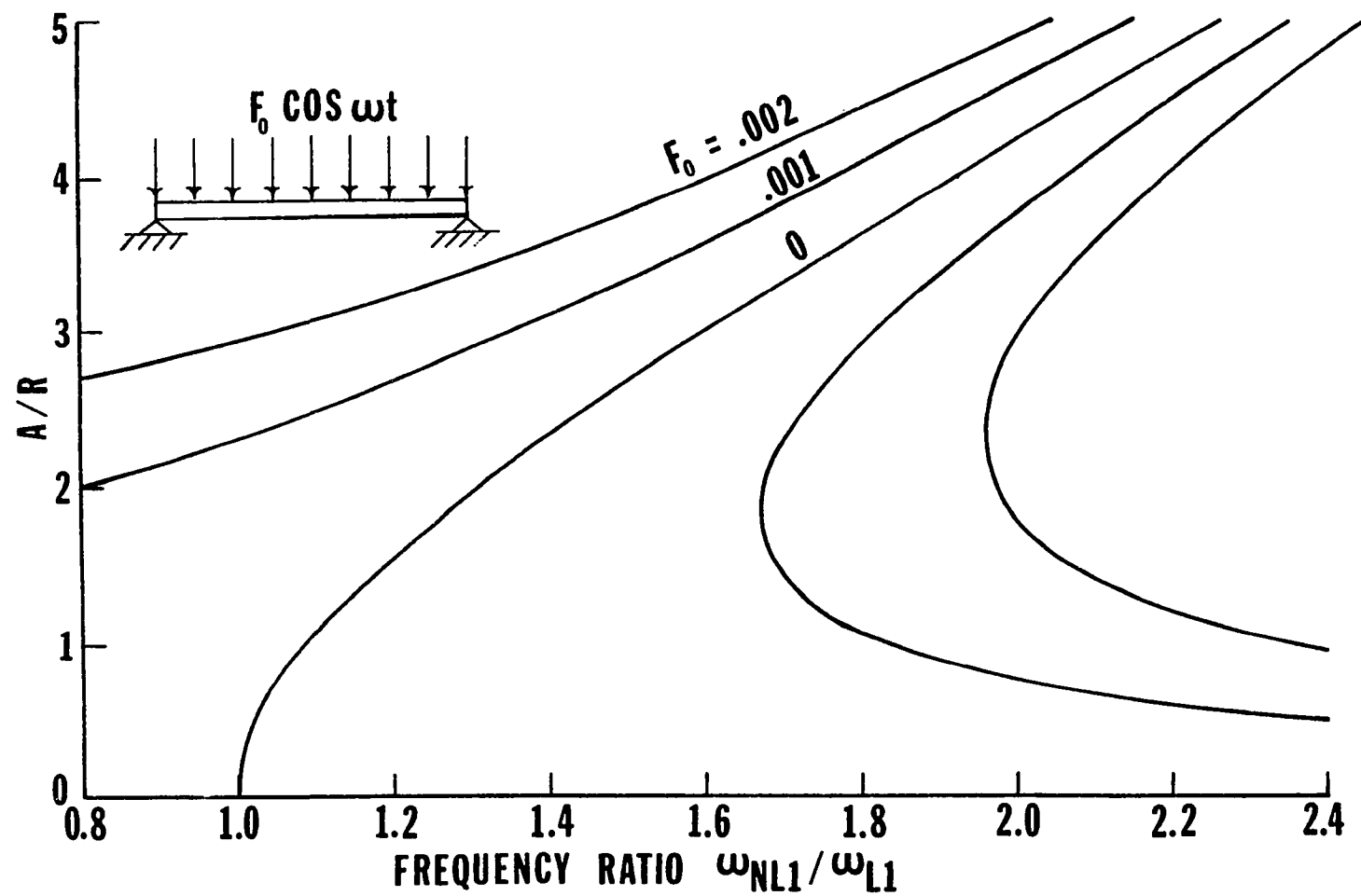
Fig. 14   Amplitude versus frequency for a three-mode simply supported beam
(L/R = 1010) under uniform harmonic force intensity F_o.

Table 11 Frequency Ratios for Nonlinear Forced Vibration
of Clamped and Simply Supported Immovable Beams
(L/R = 1010) with Inplane Displacement and Inertia
(IDI) under Uniform Harmonic Distributed Force

A/R	Frequency Ratio, ω_{NL1}/ω_{L1}			
	Iterative Single-Mode (method I)	1 mode (method II)	2 modes (method II)	3 modes (method II)
Clamped Beam: F_0 = 0.002 N/mm				
± 1.0	.3928 (3)[a]	.3925	.3929 (3)	.3928 (3)
	1.3804 (3)	1.3805	1.3804 (3)	1.3804 (3)
± 2.0	.8258 (4)	.8258	.8260 (4)	.8258 (4)
	1.2478 (3)	1.2481	1.2478 (3)	1.2478 (3)
± 3.0	.9881 (4)	.9888	.9888 (4)	.9881 (4)
	1.2486 (3)	1.2497	1.2489 (3)	1.2486 (4)
± 4.0	1.1204 (5)	1.1227	1.1220 (5)	1.1205 (5)
	1.3006 (4)	1.3033	1.3017 (4)	1.3007 (4)
± 5.0	1.2495 (6)	1.2546	1.2527 (6)	1.2497 (6)
	1.3819 (6)	1.3872	1.3845 (6)	1.3821 (6)
Simply Supported Beam F_0 = 0.001 N/mm				
- 1.0	1.8156 (2)	1.8156	1.8156 (2)	1.8156 (2)
± 2.0	.6436 (2)	.6436	.6436 (2)	.6436 (2)
	1.6080 (2)	1.6080	1.6080 (2)	1.6080 (2)
± 3.0	1.1837 (2)	1.1837	1.1837 (2)	1.1837 (2)
	1.6879 (2)	1.6879	1.6879 (2)	1.6879 (2)
± 4.0	1.5675 (2)	1.5675	1.5675 (2)	1.5675 (2)
	1.8823 (2)	1.8823	1.8823 (2)	1.8823 (2)
± 5.0	1.9211 (2)	1.9211	1.9211 (2)	1.9211 (2)
	2.1352 (2)	2.1352	2.1352 (2)	2.1352 (2)

[a]. Number in brackets denotes the number of iterations to
get a converged solution 10^{-5}.

Table 12 Amplitude Ratios for Nonlinear Forced Vibration of Clamped Immovable Beam (L/R = 1010) with Inplane Displacement and Inertia (IDI) under Uniform Harmonic Distributed Force; F_o = 0.002 N/mm.

| A/R | Amplitude Ratio | | |
| | 2 modes | 3 modes | |
	A_1/A_2	A_1/A_2	A_1/A_3
± 1.0	- 1354	- 1354	*
± 2.0	- 346	- 346	2689
± 3.0	- 159	- 159	1202
± 4.0	- 94	- 94	682
± 5.0	- 64	- 64	442

* Number is larger than $\left|10^4\right|$.

of this effect can also be seen in Section 6.2.2 (Table 5) and Section 6.2.5 (Table 17). Table 11 also shows that the higher modes are more important for the clamped beam than the simply supported beam. This can be observed by looking at one of the amplitudes, e.g., A/R = + 5.0, the frequency ratio for the clamped beam is changed for the different numbers of modes used in the formulation, but the frequency ratio for the simply supported beam apparently remains the same no matter how many modes are used in the formulation. Figure 15 shows the frequency-amplitude relation for the three-mode clamped immovable beam under the uniform harmonic force intensity of F_0 = 0 (free-vibration case), 0.002 and 0.004 N/mm. It should be noted that all curves in this figure show the hardening type nonlinearity. Figure 16 shows the comparison of the harmonic balance method[20], experiment[21] and the finite element method for a clamped immovable beam under the uniform harmonic distributed force intensity F_0 = 0.004170277 N/mm. It clearly demonstrates the remarkable agreement between the experiment and the finite element (with IDI) solution.

The responses for the movable cases are shown in Table 13 and 14. Table 13 shows the frequency ratios and amplitude ratios for a three-mode clamped movable beam with IDI under a uniform harmonic force. Similarly, the results of the simply supported beam are shown in Table 14. Figure 17 shows the frequency-amplitude relation for a three-mode clamped movable beam of slenderness ratio L/R = 20. All of the curves in this figure shows that the beam eventually exhibits slightly the softening type nonlinearity. Figure 18 shows the comparison of the immovable case to the movable case for a three-mode clamped beam (L/R = 100) with IDI under the force intensity F_0 = 20 N/mm. This

Fig. 15 Amplitude versus frequency for three-mode clamped and simply supported beams (L/R = 1010) with immovable ends under uniform harmonic force intensity F_0.
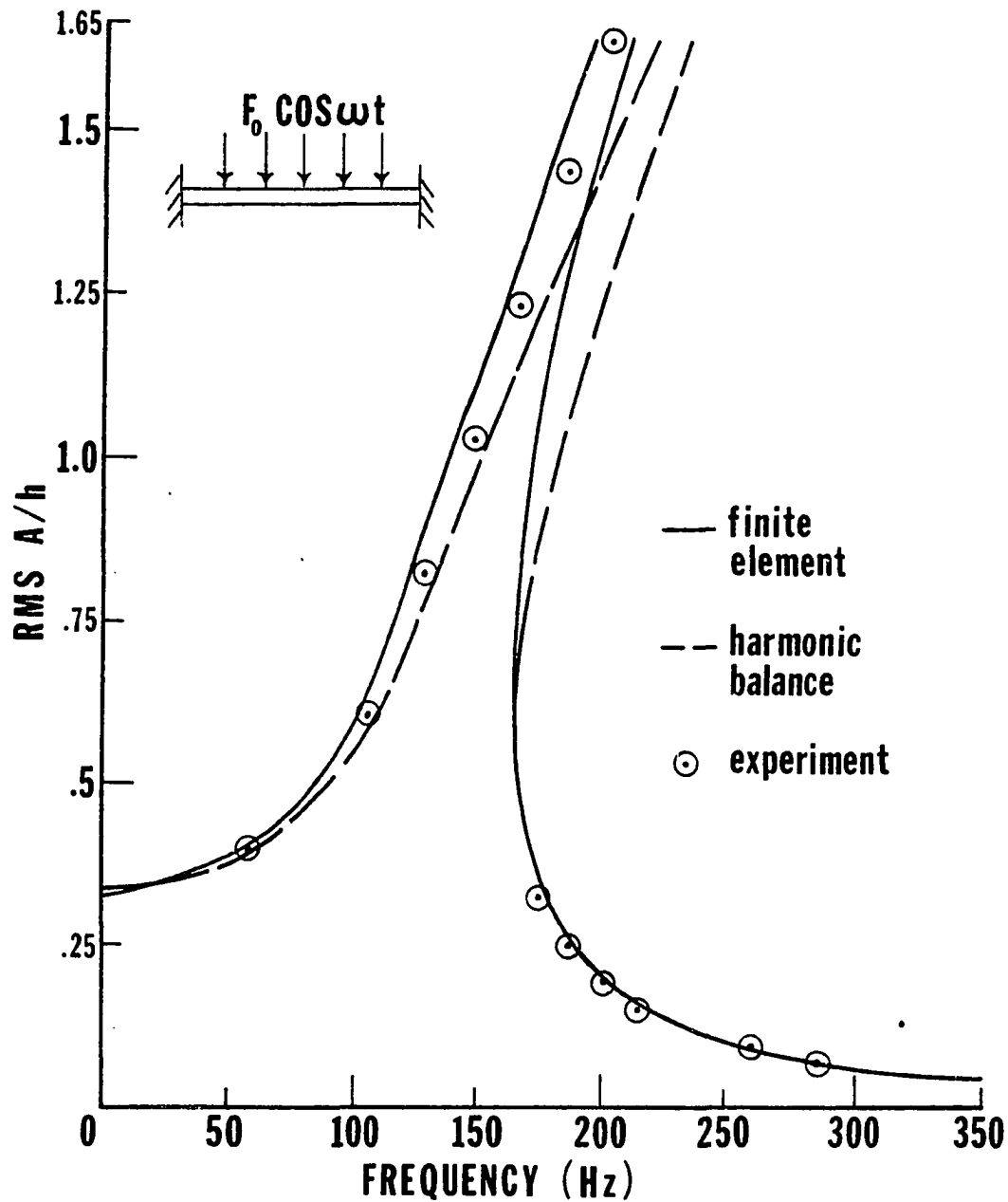
Fig. 16   Comparison of the harmonic balance method,
           experiment and the finite element method for a
           three-mode clamped beam (L/R = 1010) with
           immovable ends under a uniform distributed
           force intensity F_o = 0.004170277 N/mm.

Table 13 Frequency Ratios and Amplitude Ratios for
Three-Mode Nonlinear Forced Vibration of
Clamped Movable Beam with Inplane Displace-
ment and Inertia (IDI) under Uniform Harmonic
Distributed Force

A/R	Frequency Ratio, ω_{NL1}/ω_{L1}	Amplitude Ratio	
		A_1/A_2	A_1/A_3
L/R = 100; F_0 = 20 N/mm			
± 1.0	.4011 (2)[a]	*	*
	1.3560 (2)	*	*
± 2.0	.7617 (2)	*	*
	1.1911 (2)	*	*
± 3.0	.8482 (2)	*	*
	1.1306 (2)	*	*
± 4.0	.8880 (2)	*	*
	1.0987 (2)	8271	*
± 5.0	.9107 (2)	7704	*
	1.0788 (2)	5488	*
L/R = 20; F_0 = 5000 N/mm			
± 1.0	.8137 (3)	9653	*
	1.1538 (2)	4797	*
± 2.0	.9061 (3)	1940	*
	1.0734 (3)	1380	*
± 3.0	.9282 (3)	817	*
	1.0387 (2)	651	- 8020
± 4.0	.9319 (3)	452	- 5620
	1.0137 (3)	381	- 4757
± 5.0	.9268 (3)	290	- 3655
	.9913 (3)	252	- 3202

[a]. Number in brackets denotes the number of iterations
to get a converged solution 10^{-5}.

Table 14 Frequency Ratios and Amplitude Ratios for Three-Mode Nonlinear Forced Vibration of Simply Supported Movable Beam with Inplane Displacement and Inertia (IDI) under Uniform Harmonic Distributed Force

A/R	Frequency Ratio ω_{NL1}/ω_{L1}	Amplitude Ratio A_1/A_2	A_1/A_3
$L/R = 100$; $F_o = 3$ N/mm			
± 1.0	.6131 (2)	*	*
	1.2744 (2)	*	*
± 2.0	.8293 (2)	*	*
	1.1453 (2)	*	*
± 3.0	.8897 (2)	*	*
	1.0988 (2)	*	*
± 4.0	.9183 (2)	*	*
	1.0747 (2)	*	*
± 5.0	.9349 (2)	*	*
	1.0598 (2)	*	*
$L/R = 20$; $F_o = 1000$ N/mm			
± 1.0	.8162 (2)	*	*
	1.1537 (2)	*	*
± 2.0	.9105 (2)	*	*
	1.0770 (2)	9929	*
± 3.0	.9371 (2)	5825	*
	1.0475 (2)	4660	*
± 4.0	.9471 (3)	3203	*
	1.0295 (2)	2709	*
± 5.0	.9499 (3)	2034	*
	1.0154 (2)	1779	*

a. Number in brackets denotes the number of iterations to get a converged solution 10^{-5}.
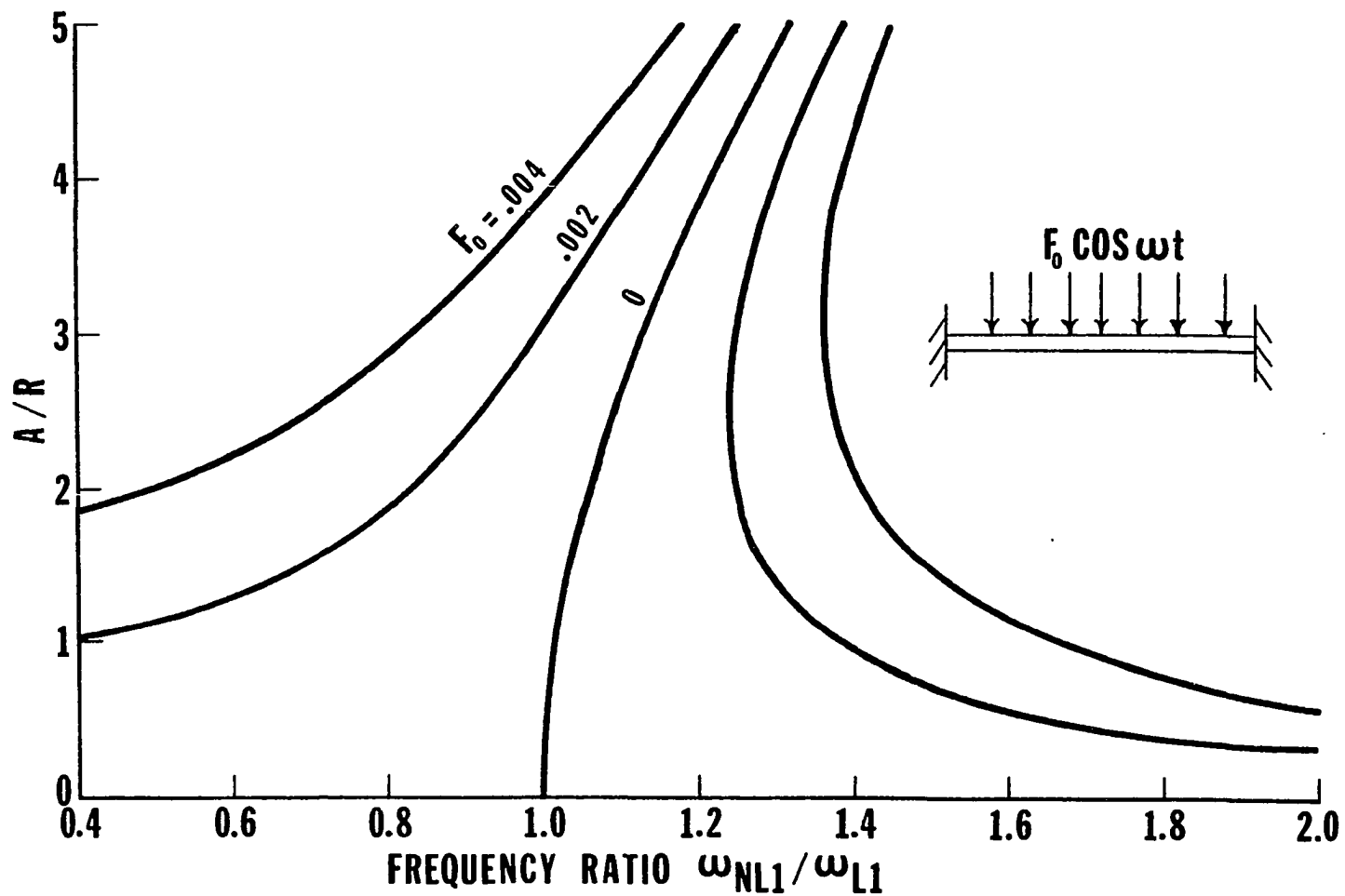
Fig. 17 Amplitude versus frequency for a three-mode clamped beam (L/R = 20) with movable ends under a uniform harmonic force intensity F_0 = 5000 N/mm.
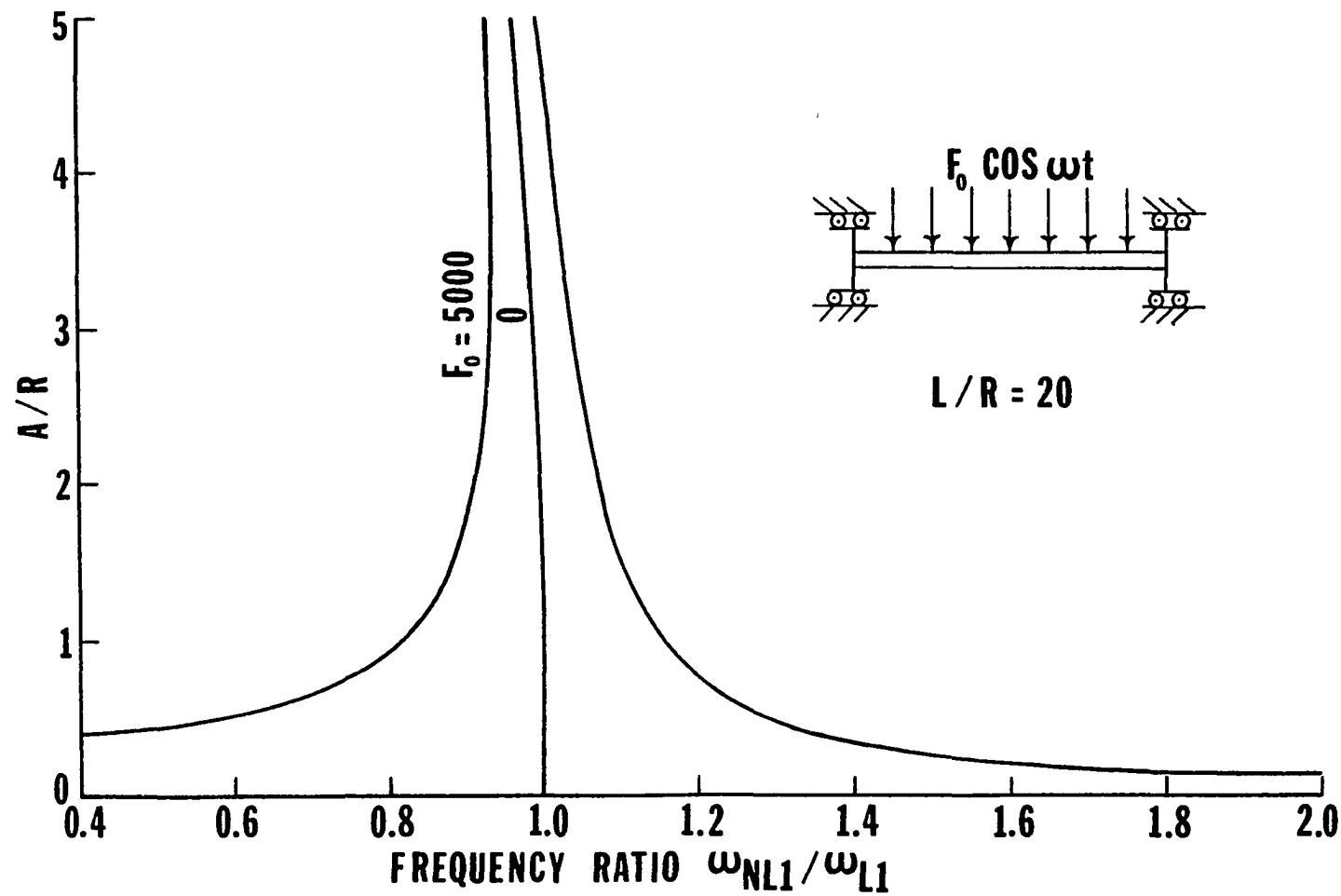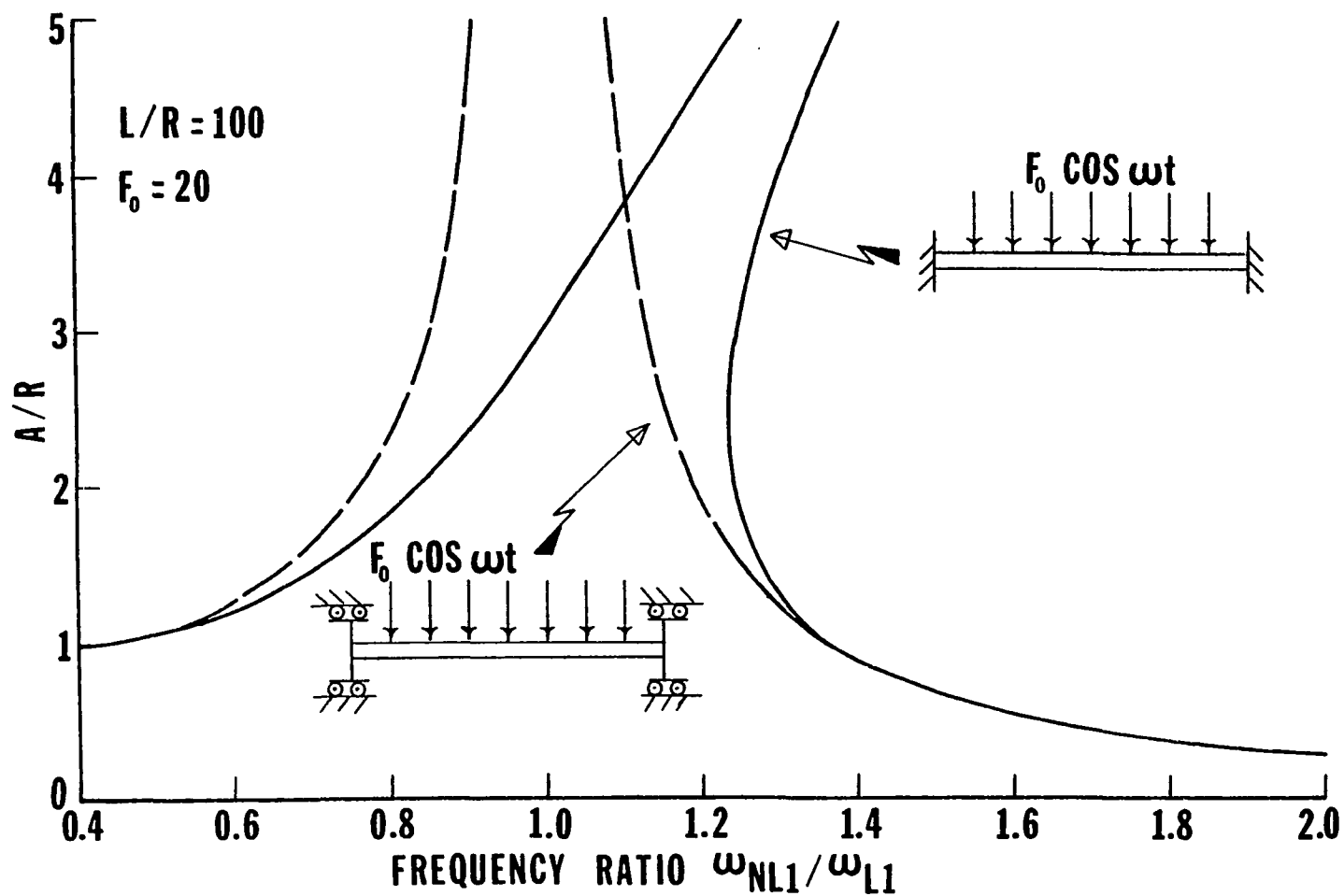
Fig. 18 Comparison between immovable and movable case for a three-mode clamped
beam (L/R = 1010) under a uniform harmonic force intensity F_0 = 20 N/mm.

clearly shows that the movable case reduces beam nonlinearity when compared to the immovable case.

6.2.4 Nonlinear Response to Concentrated Harmonic Force

The application of the finite element method to simulate the case of a concentrated force is to let the length of the loaded element become smaller and smaller. By letting ℓ_0 be the length of the loaded element from coordinate x=a to x=b, the constant c which provides the harmonic force matrix [h] can be evaluated. The effect of the length of the loaded element, ℓ_0, is studied and shown in Table 15 for a three-mode clamped immovable beam (L/R = 1010) with inplane displacement and inertia (IDI) for the total force P of 0.3 N at the middle of beam. The simulated distributed force intensity over the loaded element is calculated by $F_0 = P/\ell_0$. Similarly, the effect of ℓ_0 is shown in Table 16 for a two-mode simply supported immovable beam (L/R = 1010) with inplane displacement and inertia (IDI). The comparison of the beam under the same amount of the total force P = 0.3 N to the different kinds of loading is shown in Fig. 19. In this figure, a three-mode clamped immovable beam (L/R = 1010) with inplane displacement and inertia (IDI) under a concentrated force at the middle ($\ell_0/L=2\%$) is plotted against the similar beam under uniformly distributed force over the entire beam (F_0 = 0.002 N/mm). Similarly, the two-mode simply supported solutions for the total force P = 0.15N, F_0 = 0.001 N/mm for uniform distributed force over entire beam case, are plotted in Fig. 20. It shows that the concentrated force cases are much more severe than the uniform distributed force for the cases studied.

Table 15   Frequency Ratios for Three-Mode Forced Vibration
of Clamped Immovable Beam (L/R = 1010) with Inplane
Displacement and Inertia (IDI) under Concentrated
Harmonic Force: Total Force P = 0.3 N

	Frequency Ratio, ω_{NL1}/ω_{L1}		
	(ℓ_0/L) percent		
A/R	5	2	1
− 1.0	1.6425 (3)[a]	1.6436 (3)	1.6437 (3)
± 2.0	.5372 (4) 1.3965 (4)	.5357 (4) 1.3971 (4)	.5354 (4) 1.3972 (4)
± 3.0	.8468 (5) 1.3485 (4)	.8462 (5) 1.3489 (4)	.8461 (5) 1.3490 (4)
± 4.0	1.0314 (6) 1.3724 (5)	1.0310 (6) 1.3727 (5)	1.0310 (6) 1.3728 (5)
± 5.0	1.1879 (7) 1.4356 (5)	1.1876 (7) 1.4359 (5)	1.1876 (7) 1.4359 (5)

[a]   Number in brackets denotes the number of iterations to
get a converged solution 10^{-5}.

Table 16 Frequency Ratios for Two-Mode Nonlinear Forced
Vibration of Simply Supported Immovable Beam
(L/R = 1010) with Inplane Displacement and Inertia
(IDI) under Concentrated Harmonic Force: Total Force
P = 0.15 N

| A/R | Frequency Ratio, ω_{NL1}/ω_{L1} | | |
| | (ℓ_o/L) percent | | |
	5	2	1
- 1.0	2.1286 (2)[a]	2.1296 (2)	2.1297 (2)
- 2.0	1.7897 (2)	1.7903 (2)	1.7904 (2)
± 3.0	.9949 (2)	.9941 (2)	.9940 (2)
	1.8056 (2)	1.8060 (2)	.8061 (2)
± 4.0	1.4658 (2)	1.4654 (2)	1.4654 (2)
	1.9625 (2)	1.9628 (2)	1.9628 (2)
± 5.0	1.8558 (2)	1.8555 (2)	1.8555 (2)
	2.1923 (2)	2.1925 (2)	2.1925 (2)

[a]. Number in brackets denotes the number of iteratives to get
a converged solution 10^{-5}.
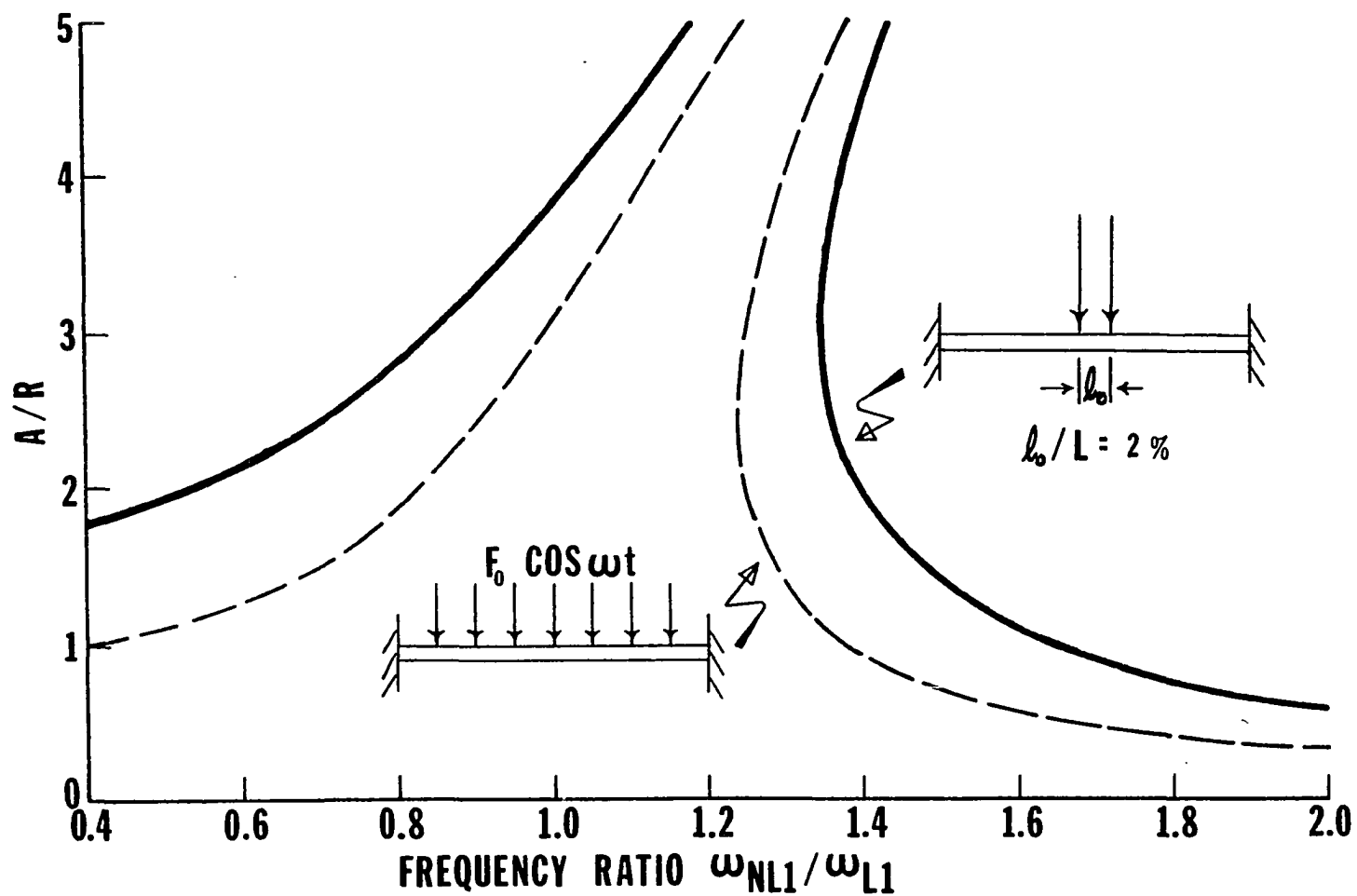
Fig. 19 Comparison of a three-mode clamped beam (L/R = 1010) with immovable ends under the same total force P = 0.3 N for concentrated and uniform distributed loading.
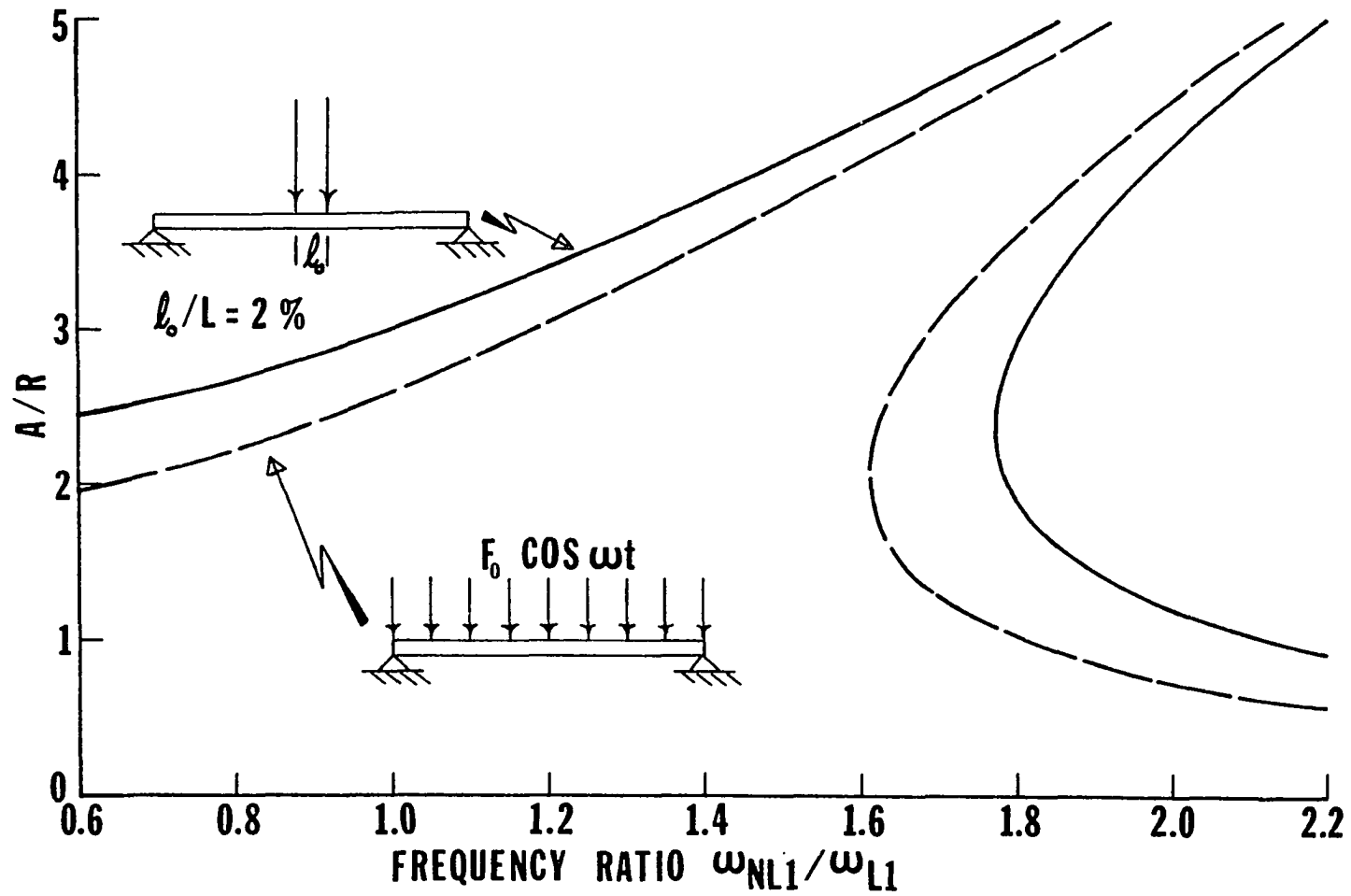
Fig. 20 Comparison of a two-mode simply-supported beam (L/R = 1010) with immovable ends under the same total force P = 0.15 N for concentrated and uniform distributed loading.

6.2.5 Strains

Table 17 shows the maximum strain-amplitude relations for a clamped immovable beam (L/R = 1010) with inplane displacement and inertia (IDI) for the cases of single, two and three-mode approaches (method II), and the iterative single-mode method (method I). It also shows the good agreement between the results using the iterative single-mode method (method I) and the results of three-mode responses using the multiple-mode method (method II). It can be interpreted that the iterative single-mode method (method I) and the multiple-mode method (method II) will yield the same beam deflection, provided a large number of modes is used for the multiple-mode method (method II). The evidence of this effect can also be seen in Section 6.2.2 (Table 5) and Section 6.2.3 (Table 11).

6.3 Plates

All of the finite element results are calculated by the iterative single mode (method I) which is explained in Chap. 3.

6.3.1 Improved Nonlinear Free Vibration

The fundamental frequency ratios ω/ω_L of free vibration at various amplitude $\bar{A}_0 = w_{max}/h$ for simply supported square (a/h = 240) and rectangular (a/b = 2 and a/h = 480) plates with immovable inplane edges (u = 0 at x = 0 and a, v = 0 at y = 0 and b) are shown in Table 18. Due to symmetry, only one quarter of the plate modelled with 9 (or 3 x 3 gridwork) elements of equal sizes is used. Both finite element results with and without inplane displacements and inertia (IDI) are given. It

Table 17 Maximum Strain for Nonlinear Vibration of
a Clamped Immovable Beam (L/R = 1010) with
Inplane Displacement and Inertia (IDI)

A/R	Strain ($\times 10^{-5}$)			
	Iterative Single-Mode (Method I)	1 mode	2 modes	3 modes
1.0	5.0527	5.0138	5.0389	5.0451
2.0	10.8118	10.5044	10.7019	10.7503
3.0	17.4908	16.4712	17.1185	17.2793
4.0	25.2769	22.9136	24.3890	24.7624
5.0	34.3251	29.8309	32.5780	33.2904

Table 18   Free Vibration Frequency Ratios ω/ω_L for a Simply
Supported Plate with Immovable Inplane Edges

$\bar{A}_0 = \dfrac{w_{max}}{h}$	Without IDI[a]	With Inplane Deformation (No Inertia)		With IDI	
	Finite Element Result	Elliptic Function Result[24,77]	Perturbation Solution	Rayleigh Ritz Result[8]	Present Finite Element Result
Square Plate (a/h = 240)					
0.2	1.0185(3)[b]	1.0195	1.0196	1.0149	1.0134(3)
0.4	1.0716(3)	1.0757	1.0761	1.0583	1.0528(3)
0.6	1.1533(4)	1.1625	1.1642	1.1270	1.1154(4)
0.8	1.2565(6)	1.2734	1.2774	1.2166	1.1979(5)
1.0	1.3752(7)	1.4024	1.4097	1.3230	1.2967(6)
Rectangular Plate (a/b = 2, a/h = 480)					
0.2	1.0238(3)	1.0241	1.0241	1.0177	1.0168(3)
0.4	1.0918(4)	1.0927	1.0933	1.0690	1.0658(4)
0.6	1.1957(6)	1.1975	1.1998	1.1493	1.1439(5)
0.8	1.3264(8)	1.3293	1.3347	1.2533	1.2467(6)
1.0	1.4762(11)	1.4808	1.4903	1.3753	1.3701(8)

[a] Inplane displacement and inertia.

[b] Number inside parenthesis denotes the number of iterations to get a converged solution.

shows that the improved finite element results by including IDI in the formulation are to reduce the nonlinearity. The elliptic function solution and perturbation solution (with inplane deformation only[77,24]) are also given to demonstrate the closeness of the earlier finite element results without IDI. Raju et al.[8] used the Rayleigh-Ritz method in their investigation of the effects of IDI on large amplitude free flexural vibration of thin plates. The linear mode shape is very close to the nonlinear mode shape for the simply supported case. Therefore, the Rayleigh-Ritz solution demonstrates a good result compared to the presently improved finite element solution.

6.3.2 Convergence with Gridwork Refinement

Table 19 shows the frequency ratios for a simply supported square plate (a/h = 240) with immovable inplane edges subjected to a uniform harmonic force of P^*_o = 0.2 with three finite element grid refinements. Only one quarter of the plate was used in the analysis due to symmetry. Examination of the results shows that the present finite element formulation exhibits excellent convergence characteristics. Therefore, a 3 x 3 (or 9 elements) in a quarter of plate was used in modelling the plates in the remainder of the nonlinear forced responses presented unless otherwise specified.

6.3.3 Nonlinear Forced Response of Plates with Immovable Inplane Edges

Table 20 shows the frequency ratios ω/ω_L for simply supported and clamped square plates (a/h = 240) subjected to a uniform harmonic force of P^*_o = 0.2. It demonstrates the closeness between the earlier finite

Table 19 Convergence of Frequency Ratio with Grid
Refinement for a Simply Supported Square Plate
(a/h = 140) with Immovable Inplane Edge
Subjected to $P_o^* = 0.2$

$\bar{A}_o = \dfrac{W_{max}}{h}$	Gridwork		
	2 x 2 (4 Elements)	3 x 3 (9 Elements)	4 x 4 (16 Elements)
± 0.2	0.1645(3)*	0.1643(3)	0.1636(3)
	1.4248(3)	1.4238(3)	1.4237(3)
± 0.4	0.7815(3)	0.7800(3)	0.7792(3)
	1.2697(3)	1.2682(3)	1.2677(3)
± 0.6	0.9576(4)	0.9544(4)	0.9530(4)
	1.2588(4)	1.2560(4)	1.2550(4)
± 0.8	1.0937(5)	1.0886(5)	1.0865(5)
	1.3026(5)	1.2981(5)	1.2963(5)
± 1.0	1.2242(5)	1.2171(6)	1.2143(5)
	1.3781(5)	1.3717(6)	1.3691(5)

* Number in parenthesis denotes the number of iterations to get a converged solution.

Table 20 Forced Vibration Frequency Ratios ω/ω_L for a Square Plate (a/h = 240) with Immovable Inplane Edges Subjected to $P_o^* = 0.2$

$\bar{A}_0 = \frac{w_{max}}{h}$	Simple Elliptic Response[24,77]	Perturbation Solution	Finite Element	
			Without IDI[a]	With IDI
Simply Supported				
± 0.2	0.1944	0.1987	0.1932(3)[b]	0.1643(3)
	1.4281	1.4281	1.4274(3)	1.4238(3)
± 0.4	0.8102	0.8111	0.8052(3)	0.7800(3)
	1.2874	1.2876	1.2839(3)	1.2682(3)
± 0.6	1.0084	1.0110	0.9984(4)	0.9544(4)
	1.2983	1.2995	1.2898(4)	1.2560(4)
± 0.8	1.1703	1.1755	1.1528(6)	1.0886(5)
	1.3686	1.3718	1.3524(6)	1.2981(5)
± 1.0	1.3283	1.3369	1.3004(7)	1.2171(6)
	1.4726	1.4789	1.4460(7)	1.3717(6)
Clamped				
± 0.2	0.1200	0.1227	0.1180(2)	0.1033(3)
	1.4195	1.4195	1.4195(2)	1.4183(3)
± 0.4	0.7483	0.7438	0.7459(3)	0.7372(4)
	1.2490	1.2491	1.2477(3)	1.2426(4)
± 0.6	0.8951	0.8956	0.8905(4)	0.8746(4)
	1.2117	1.2119	1.2083(4)	1.1966(4)
± 0.8	0.9941	0.9954	0.9863(5)	0.9617(5)
	1.2203	1.2210	1.2137(5)	1.1938(5)
± 1.0	1.0822	1.0845	1.0700(6)	1.0362(5)
	1.2540	1.2555	1.2429(6)	1.2140(5)

[a] Inplane displacement and inertia.
[b] Number inside parenthesis denotes the number of iterations to get a converged solution.

element formulation without IDI, the simple elliptic response [24,77] and the perturbation solution (with inplane deformation only). The present improved finite element results indicate clearly that the effects of IDI are to reduce the nonlinearity. The present finite element results of a square plate (a/h = 240) to uniform harmonic excitation of P^*_0 = 0, 0.1 and 0.2 are given in Figs. 21 and 22 for simply supported and clamped boundary conditions, respectively.

6.3.4 Nonlinear Forced Response of Plates with Movable Inplane Edges

The dimensionless amplitude $\bar{A}_0$ versus the fundamental frequency ratio ω/ω_L for a simply supported square plate (a/h = 240) with movable inplane edges subjected to uniform harmonic load P^*_0 = 0, 0.1 and 0.2 is shown in Fig. 23. The nonlinearity is greatly reduced with the inplane edges no longer restrained as compared to the case of immovable inplane edges in Fig. 21.

6.3.5 Concentrated Harmonic Force

Application of the present finite element to the case of a concentrated force is to let the area of the loaded element become smaller and smaller. This is demonstrated by a concentrated force at the center of a simply supported square plate (a/h = 240) with immovable inplane edges. The magnitude of the concentrated force is equal to the same plate under a uniformly distributed harmonic loading of P^*_0 = 0.1 (F_0 = 45.74 N/m^2 or 0.6634×10^{-2} psi) over the total plate area. Therefore, the uniform loading of the loaded element for the concentrated case is F_0 = 45.74 $(a/d)^2$ N/m^2 where d is the length of the loaded square element. Table 21 gives the fundamental frequency ratios

Fig. 21 Amplitude versus frequency for a simply supported square plate (a/h = 240) with immovable inplane edges at $P_o^* = 0$, 0.1 and 0.2.

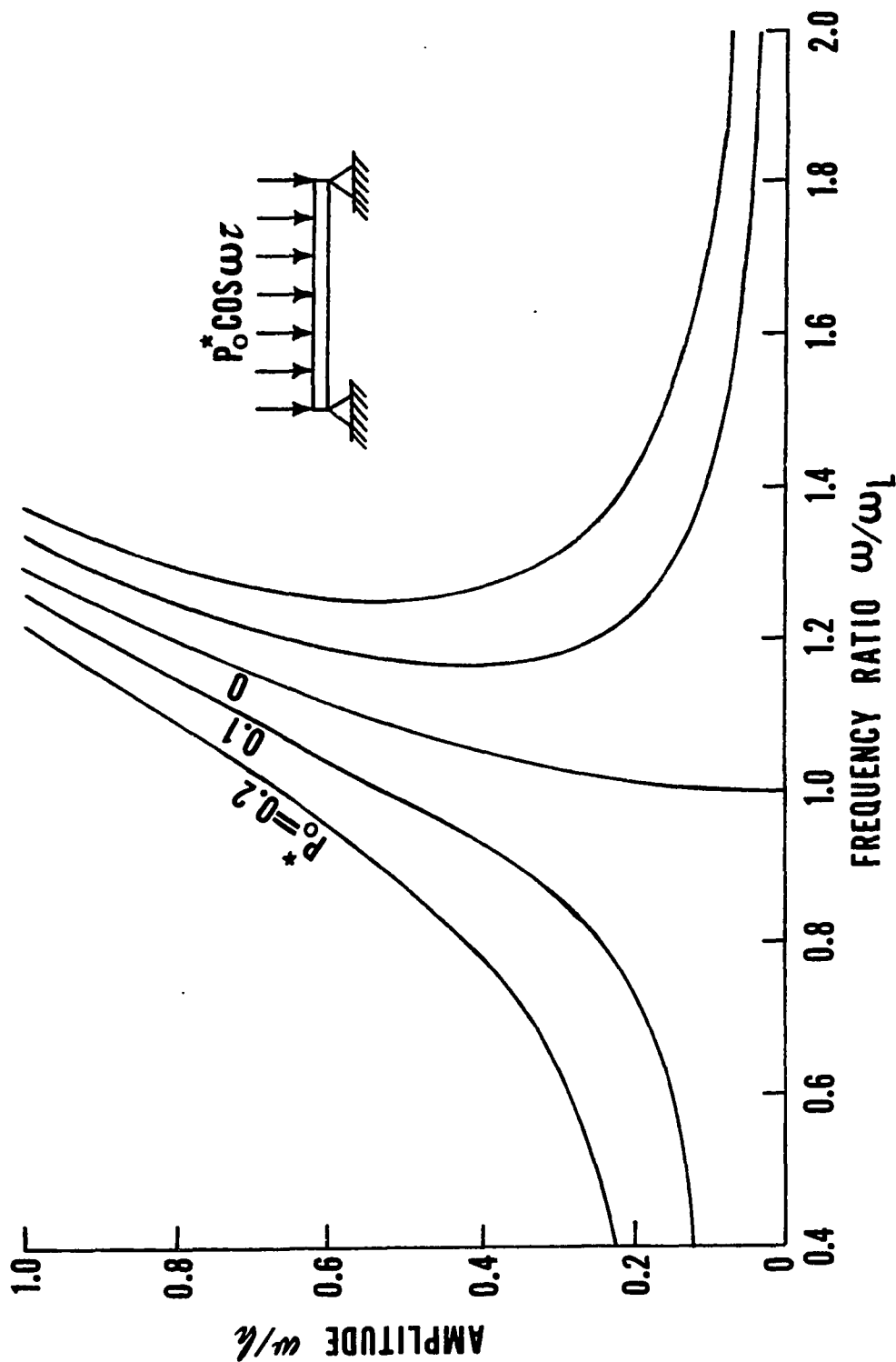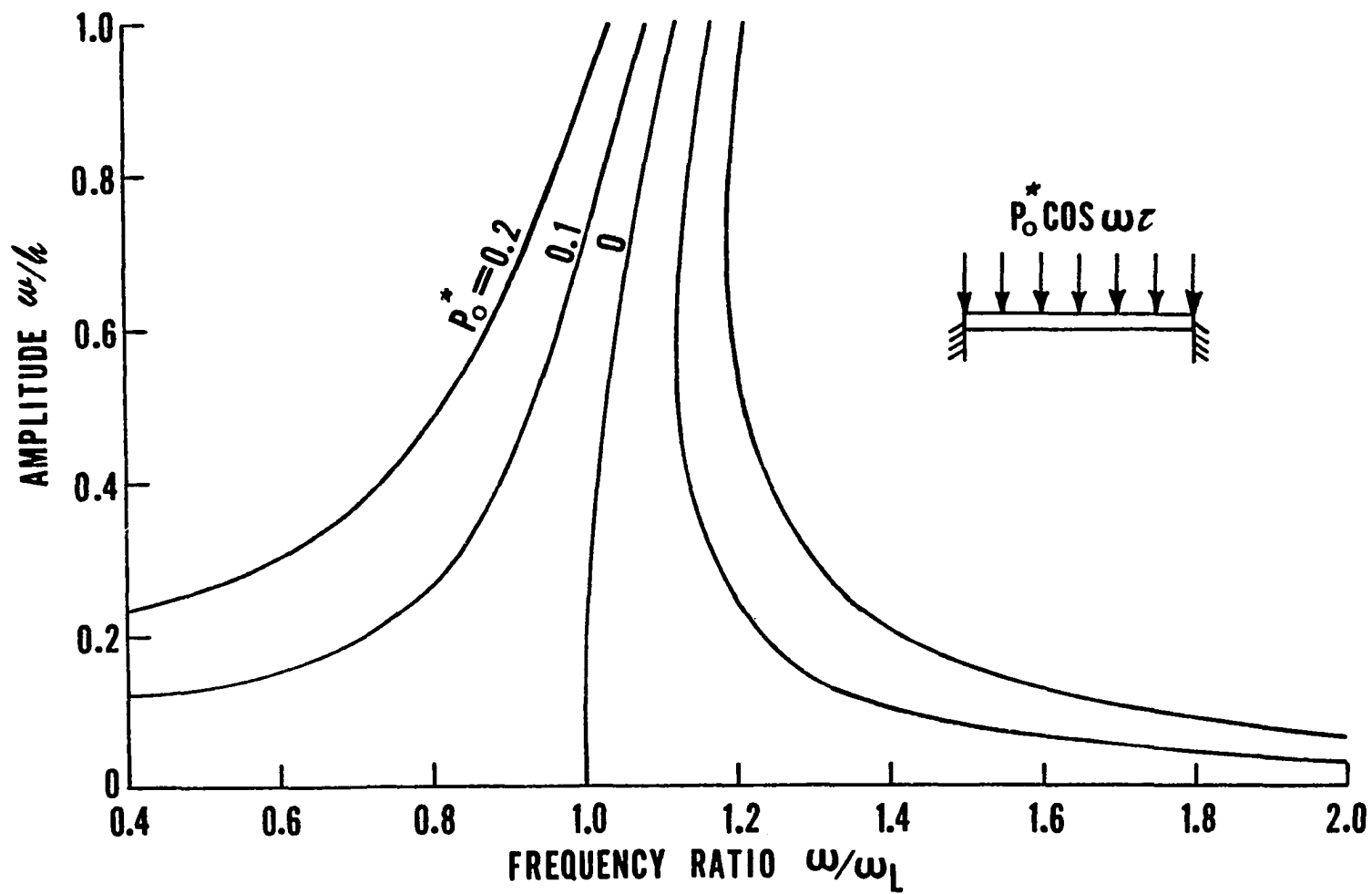Fig. 22 Amplitude versus frequency for a clamped square plate (a/h = 240) with immovable inplane edges at P_o^* = 0, 0.1 and 0.2.

Fig. 23 Amplitude versus frequency for a simply supported square plate (a/h = 240) with movable inplane edges at $P_0^* = 0$, 0.1 and 0.2.

Table 21 Convergence of Frequency Ratio ω/ω_L with Loaded Area for a Simply Supported Square Plate (a/h = 240) with Immovable Inplane Edges Subjected to a Concentrated Force Corresponds to $F_0 = 45.74 \ (a/d)^2$ N/m^2 at the Center.

$\bar{A}_0 = \dfrac{w_{max}}{h}$	Elliptic Function Result	Finite Element Result at $(d/a)^2$ %				
		Without IDI		With IDI		
		1	16	4	1	0.25
- 0.2	1.5078	1.4097	1.4402	1.4692	1.4866	1.4967
± 0.4	0.7342	0.7445	0.7652	0.7380	0.7218	0.7129
	1.3320	1.3202	1.2772	1.2940	1.3041	1.3093
± 0.6	0.9688	0.9649	0.9467	0.9330	0.9254	0.9212
	1.3280	1.3148	1.2618	1.2738	1.2811	1.2849
± 0.8	1.1449	1.1299	1.0839	1.0757	1.0719	1.0698
	1.3898	1.3711	1.3021	1.3115	1.3177	1.3209
± 1.0	1.3103	1.2831	1.2142	1.2090	1.2076	1.2068
	1.4885	1.4606	1.3747	1.3824	1.3881	1.3910

* Inplane displacement and inertia.

ω/ω_L at $(d/a)^2$ = 16.0, 4.0, 1.0 and 0.25%. It indicates that the convergence is rapid and $(d/a)^2$ = 1.0% would yield an accurate frequency response. Results obtained using earlier finite element without IDI and elliptic function (with inplane deformation but no inplane inertia) are also given. A nonlinear response of concentrated force obtained with $(d/a)^2$ = 1.0% is plotted in Fig. 24. Frequency ratios of the same plate to uniform harmonic force P_o^* = 0.2 are also given. It shows that the concentrated force is approximately two to three times as severe as the uniformly distributed force for the case studied.
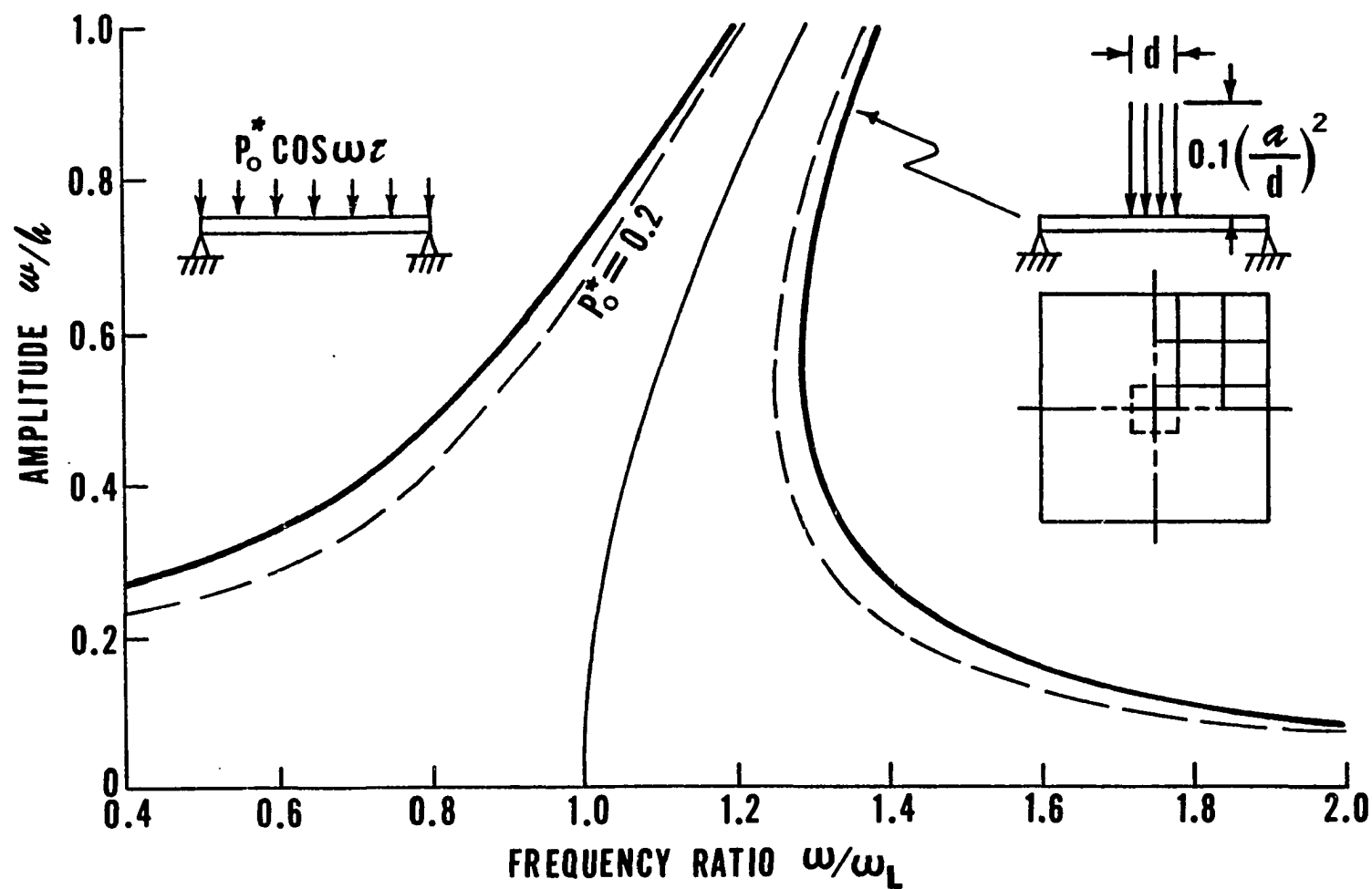
Fig. 24   Amplitude versus frequency for a simply supported square plate
(a/h = 240) with immovable inplane edges under concentrated loading.

Chapter 7

CONCLUSIONS

Finite element methodology has been developed for the nonlinear free and forced vibrations to predict both the frequency-amplitude-force relation and strains of beam and plate structures. Two finite element methods were developed, namely, the iterative single-mode method (method I) and the multiple-mode method (method II). The harmonic force matrix was developed to analyze nonlinear forced vibrations. Nonlinear free vibration can be simply treated as a special case of the general forced vibration by setting the harmonic force matrix equal to zero. The harmonic force matrix represents the external applied force in a matrix form instead of a vector form, therefore, the nonlinear forced vibration analysis can be performed as an eigenvalue problem. By solving an eigenvalue problem, the analysis can be performed efficiently to get a converged solution. The analysis is also based on the linearized nonlinear stiffness matrix and the iterative procedures. Both inplane (longitudinal) displacements and lateral deflection are included in the formulation.

The study showed that the effect of midplane stretching due to large deflection is to increase nonlinearity. However, the effects of inplane displacements and inertia (IDI) are to reduce nonlinearity. The concentrated force case yields a more severe response than the uniform distributed force case. For beams and plates with end supports

124

restrained from axial movement (immovable case), only the hardening type nonlinearity is observed. For beams with a large slenderness ratio (L/R < 100) with movable end supports, the increase in nonlinearity due to large deflection is partially compensated by the reduction in nonlinearity due to inplane displacement and inertia. This leads to a negligible hardening type nonlinearity, therefore, the small deflection linear solution can be employed. However, for beams with a small slenderness ratio (L/R = 20) with movable end supports, the softening type nonlinearity is found. The effect of the higher modes is more pronounced for the clamped supported beam than the simply supported one. The beam without inplane displacement and inertia (IDI) yields more effect from the higher modes than the beam with inplane displacement and inertia. For beams, the iterative single-mode method (method I) and the multiple-mode method (method II) converge to a true deflection shape provided the number of modes for the multiple-mode method (method II) is high enough. Similarly, both the iterative single-mode method (method I) and the multiple-mode method (method II) yields accurate strains provided the number of modes for the multiple-mode method (method II) is high enough.

The finite element method, in practice, is very suitable for analyzing modern complex structures. Nonlinear theory can be employed to obtain more accurate solutions and explain new phenomena. By combining the finite element method and nonlinear theory together, more realistic models of structural response can be analyzed easily and quickly. The nonlinear finite element method which is studied herein, may be extended to study more advanced topics, for example, the service life of a structure (S-N curve), the study of nonlinear random vibrations and the effects of sub-or super-harmonic excitations.

REFERENCES

1. Mei, C. and Wentz, K. R., "Analytical and Experimental Nonlinear Response of Rectangular Panels to Acoustic Excitation," AIAA/ASME/ASCE/AHS 23rd Structures, Structural Dynamics and Materials Conference, New Orleans, LA, May 1982, pp. 514-520.

2. Holehouse, I., "Sonic Fatigue Design Techniques for Advanced Composite Airplane Structures," Wright Patterson Air Force Base, Ohio, AFWAL-TR-80-3019, April 1980. Also Ph.D. Dissertation, University of Southampton, 1984.

3. White, R. G., "Comparison of the Statistical Properties of the Aluminum Alloy and CFRP Plates to Acoustic Excitation," Composites, October 1978, pp. 251-258.

4. Woinowsky-Krieger, S., "The Effect of an Axial Force on the Vibration of Hinged Bars," Journal of Applied Mechanics, Vol. 17, 1950, pp. 35-37.

5. Eringen, A. C., "On the Non-linear Vibration of Elastic Bars," Quarterly of Applied Mathematics, Vol. 9, 1952, pp. 361-369.

6. Burgreen, B., "Free Vibrations of a Pin-ended Column with Constant Distance Between Pin Ends," Journal of Applied Mechanics, Vol. 18, 1951, pp. 135-139.

7. Woodall, S. R., "On the Large Amplitude Oscillations of a Thin Elastic Beam," International Journal of Non-linear Mechanics, Vol. 1, 1966, pp. 217-238.

8. Raju, I. S., Rao, G. V. and Raju, K. K., "Effect of Longitudinal or Inplane Deformation and Inertia on the Large Amplitude Flexural Vibrations of Slender Beams and Thin Plates," Journal of Sound and Vibration, Vol. 49, 1976, pp. 415-422.

9. Tseng, W. Y. and Dugundji, J., "Nonlinear Vibrations of a Beam Under Harmonic Excitation," Journal of Applied Mechanics, Vol. 37, 1970, pp. 292-297.

10. Pandalai, K.A.V., "A General Conclusion Regarding the Large Amplitude Flexural Vibration of Beams and Plates," Israel Journal of Technology, Vol. 11, No. 5, 1973, pp. 321-324.

11. Atluri, S., "Nonlinear Vibrations of a Hinged Beam Including Nonlinear Inertia Effects," Journal of Applied Mechanics, Vol. 40, 1973, pp. 121-126.

12. McDonald, P. H., "Nonlinear Dynamic Coupling in a Beam Vibration," Journal of Applied Mechanics, Vol. 22, 1955, pp. 573-578.

13. Bennett, J. A. and Eisley, J. G., "A Multiple Degree-of-Freedom Approach to Nonlinear Beam Vibrations," AIAA Journal, Vol. 8, 1970, pp. 734-739.

14. Bennett, J. A., "Ultraharmonic Motion of a Viscously Damped Nonlinear Beam," AIAA Journal, Vol. 11, 1973, pp. 710-715.

15. Tseng, W. Y. and Dugundji, J., "Nonlinear Vibrations of a Buckled Beam Under Harmonic Excitation," Journal of Applied Mechanics, Vol. 38, 1971, pp. 467-476.

16. Srinivasan, A. V., "Non-linear Vibrations of Beams and Plates," International Journal of Non-linear Mechanics, Vol. 1, 1966, pp. 179-191.

17. Nayfeh, A. H., Mook, D. T. and Lobitz, D. W., "A Numerical-Perturbation Method for the Non-linear Analysis of Structural Vibrations," AIAA Journal, Vol. 12, 1974, pp. 1222-1228.

18. Van Dooren, R. and Bouc, R., "Two Mode Sub-harmonic and Harmonic Vibrations of a Non-linear Beam Forced by a Two Mode Harmonic Load," International Journal of Non-linear Mechanics, Vol. 10, 1975, pp. 271-280.

19. Takahashi, K., "Non-linear Free Vibrations of Inextensible Beams," Journal of Sound and Vibration, Vol. 64, 1979, pp. 31-34.

20. Yamaki, N. and Mori, A., "Non-linear Vibrations of a Clamped Beam with Initial Deflection and Initial Axial Displacement, Part I: Theory," Journal of Sound and Vibration, Vol. 71, 1980, pp. 333-346.

21. Yamaki, N., Otomo, K. and Mori, A. "Non-linear Vibrations of a Clamped Beam with Initial Deflection and Initial Axial Displacement, Part II: Experiment," Journal of Sound and Vibration, Vol. 71, 1980, pp. 347-360.

22. Herrmann, G., "Influence of Large Amplitudes on Flexural Motion of Elastic Plates," NACA TN 3578, 1956.

23. Chu, H. N. and Herrmann, G., "Influence of Large Amplitudes on Free Flexural Vibrations of Rectangular Elastic Plates," Journal of Applied Mechanics, Vol. 23, 1956, pp. 532-540.

24. Eisley, J. G., "Nonlinear Vibration of Beams and Rectangular Plates," Zeitschrift fur angewandte Mathematik and Physik, Vol. 15, 1964, pp. 167-175.

25. Yamaki, N., "Influence of Large Amplitude on Flexural Vibrations of Elastic Plates," Zeitschrift fur angewandte Mathematik and Mechanik, Vol. 41, 1961, pp. 501-510.

26. Lin, Y. K., "Response of a Nonlinear Flat Panel to Periodic and Randomly-Varying Loadings," Journal of Aerospace Science, Vol. 29, 1962, pp. 1029-1034, 1066.

27. Kung, G. C. and Pao, Y. H., "Nonlinear Flexural Vibrations of a Clamped Circular Plate," Journal of Applied Mechanics, Vol. E-39, 1972, pp. 1050-1054.

28. Yamaki, N., Otomo, K. and Chilea, M., "Nonlinear Vibrations of a Clamped Circular Plate with Initial Deflection and Initial Edge Displacement, Part I: Theory," Journal of Sound and Vibration, Vol. 79, 1981, pp. 23-42.

29. Huang, C. L. and Sandman, B. E., "Large Amplitude Vibrations of a Rigidly Clamped Circular Plate," International Journal of Non-linear Mechanics, Vol. 6, 1971, pp. 451-468.

30. Huang, C. L. and Al-khattat, "Finite Amplitude Vibrations of a Circular Plate," International Journal of Non-linear Mechanics, Vol. 12, 1977, pp. 297-306.

31. Rehfield, L. W., "Large Amplitude Forced Vibrations of Elastic Structures," AIAA Journal, Vol. 12, 1974, pp. 388-390.

32. Sridhar, S., Mook, D. T. and Nayfeh, A. H., "Non-linear Resonances in the Forced Responses of Plates, Part I: Symmetrical Responses of Circular Plates," Journal of Sound and Vibration, Vol. 41, 1975, pp. 359-373.

33. Lobitz, D. W., Nayfeh, A. H. and Mook, D. T., "Non-linear Analysis of Vibration of Irregular Plates," Journal of Sound and Vibration, Vol. 50, 1977, pp. 203-217.

34. Sridhar, S., Mook, D. T. and Nayfeh, A. H., "Non-linear Responses in the Forced Responses of Plates, Part II: Asymmetric Responses in Circular Plates," Journal of Sound and Vibration, Vol. 59, 1978, pp. 159-170.

35. Lau, S. L., Cheng, Y. K. and Wu, S. Y., "Amplitude Incremental Finite Element for Nonlinear Vibration of Thin Plate," Proceeding International Conference on Finite Element Methods, Guangquian, H. and Cheung, Y. K., eds., 1982, pp. 184-190.

36. Berger, H. M., "A New Approach to the Analysis of Large Deflections of Plates," Journal of Applied Mechanics, Vol. 22, 1955, pp. 465-472.

37. Wah, T., "Large Amplitude Flexural Vibration of Rectangular Plates, "International Journal of Mechanical Sciences, Vol. 5, 1963, pp. 3-16.

38. Ramachandran, J., "Non-linear Vibrations of Circular Plates with Linearly Varying Thickness," Journal of Sound and Vibration, Vol. 38, 1975, pp. 225-232.

39. Mei, C., "Non-linear Vibrations of Beams by Matrix Displacement Method," AIAA Journal, Vol. 10, 1972, pp. 355-357.

40. Rao, G. V., Raju, K. K. and Raju, I. S., "Finite Element Formulation for Large Amplitude Free Vibrations of Beams and Orthotropic Circular Plates," Computers and Structures, Vol. 6, 1976, pp. 169-172.

41. Reddy, J. N. and Singh, I. R., "Large Deflections and Large-Amplitude Free Vibrations of Straight and Curved Beams," International Journal for Numerical Methods in Engineering, Vol. 17, 1981, pp. 829-852.

42. Mei, C. and Decha-Umphai, K., "A Finite Element Method for Nonlinear Forced Vibrations of Beams," Journal of Sound and Vibration, Vol. 102, 1985, pp. 369-380.

43. Mei, C. and Decha-Umphai, K., "A Finite Element Method for Nonlinear Forced Vibrations of Rectangular Plates," AIAA Journal, Vol. 23, 1985, pp. 1104-1110.

44. Decha-Umphai, K. and Mei, C., "Finite Element Method for Non-linear Forced Vibrations of Circular Plates," International Journal for Numerical Methods in Engineering, Vol. 23, 1986, pp. 1715-1726.

45. Zienkiewicz, O. C., The Finite Element Method in Engineering Science, McGraw Hill Book Co., 1971, p. 421.

46. Busby, H. R. and Weingarten, V. I., "Non-linear Response of a Beam to Periodic Loading," International Journal of Non-linear Mechanics, Vol. 7, 1972, pp. 289-303.

47. Cheung, Y. K. and Lau, S. L., "Incremental Time-Space Finite Strip Method for Non-linear Structural Vibrations," Earthquake Engineering and Structural Dynamics, Vol. 10, 1982, pp. 239-253.

48. Mei, C., "Finite Element Displacement Method for Large Amplitude Free Flexural Vibrations of Beams and Plates," Computers and Structures, Vol. 3, 1973, pp. 163-174.

49. Rao, G. V., Raju, I. S. and Raju, K. K., "Finite Element Formulation for the Large Amplitude Free Vibrations of Beams and Orthotropic Circular Plates," Computers and Structures, Vol. 6, 1976, pp. 169-172.

50. Rao, G. V., Raju, I. S., and Raju, K. K., "A Finite Element Formulation for Large Amplitude Flexural Vibrations of Thin Rectangular Plates," Computers and Structures, Vol. 6, 1976, pp. 163-167.

51. Raju, K. K. and Rao, G. V., "Nonlinear Vibrations of Orthotropic Plates by a Finite Element Method," Journal of Sound and Vibration, Vol. 48, 1976, pp. 301-303.

52. Rao, G. V., Raju, I. S. and Raju, K. K., "Nonlinear Vibrations of Beams Considering Shear Deformation and Rotary Inertia," AIAA Journal, Vol. 14, 1976, pp. 685-687.

53. Raju, K. K. and Rao, G. V., "Axisymmetric Vibrations of Circular Plates Including the Effects of Geometric Non-Linearity, Shear Deformation and Rotary Inertia," Journal of Sound and Vibration, Vol. 47, 1976, pp. 179-184.

54. Reddy, J. N. and Stricklin, J. D., "Large Deflection and Large Amplitude Free Vibrations of Thin Rectangular Plates Using Mixed Isoparametric Elements," Symposium on Applications of Computer Methods in Engineering, Univ. of California, Los Angeles, August 23-26, 1977.

55. Mei, C. and Rogers, J. L., Jr., "Applications of the TRIPLTI Element to Large Amplitude Free Vibrations of Plates," NASA CP-2018, 1977, pp. 275-298.

56. Narayanaswami, R. and Mei, C., "Addition of Higher-Order Plate Elements to NASTRAN," NASA TM X-3428, 1976, pp. 439-477.

57. Mei, C., Narayanaswami, R. and Rao, G. V., "Large Amplitude Free Flexural Vibrations of Plates of Arbitrary Shape," Computers and Structures, Vol. 10, 1979, pp. 675-681.

58. Cowper, G. R., Kosko, E., Lindberg, G. M. and Olson, M. D., "Static and Dynamic Applications of a High-Precision Triangular Bending Element," AIAA Journal, Vol. 7, 1969, pp. 1957-1965.

59. Reddy, J. N. and Chao, W. C., "Large-Deflection and Large-Amplitude Free Vibrations of Laminated Composite-Material Plates," Computers and Structures, Vol. 13, 1981, pp. 341-347.

60. Reddy, J. N. and Chao, W. C., "A Comparison of Closed-Form and Finite Element Solutions of Thick Laminated Anisotropic Rectangular Plates," Nuclear Engineering and Design, Vol. 64, 1981, pp. 153-157.

61. Mei, C., Shen, M. H. and Cunningham, F. M., "Large Amplitude Vibration of Laminated Composite Plates of Arbitrary Shape," AIAA 24th Structures, Structural Dynamics, and Materials Conference, Part 2, Lake Tahoe, May 1983, pp. 685-692.

62. Bhashyan, G. R. and Prathap, G., "Galerkin Finite Element Method for Nonlinear Beam Vibrations," Journal of Sound and Vibration, Vol. 72, 1980, pp. 191-203.

63. Sarma, B. S. and Varadan, T. K., "Certain Discussions in the Finite Element Formulation of Nonlinear Vibration Analysis," Computers and Structures, Vol. 15, 1982, pp. 643-646.

64. Sarma, B. S. and Varadan, T. K., "Lagrange-Type Formulation for Finite Element Analysis of Nonlinear Beam Vibrations," Journal of Sound and Vibration, Vol. 86, 1983, pp. 61-70.

65. Prathap, G. and Varadan, T. K., "The Large Amplitude Vibration of Hinged Beams," Computers and Structures, Vol. 9, 1978, pp. 219-222.

66. Prathap, G. and Varadan, T. K., "The Large Amplitude Vibration of Tapered Clamped Beams," Journal of Sound and Vibration, Vol. 58, 1978, pp. 87-94.

67. Evensen, D. A., "Nonlinear Vibrations of Beams with Various Boundary Conditions," AIAA Journal, Vol. 6, 1968, pp. 370-372.

68. Mei, C., "Comments on the Lagrange-Type Formulation for Finite Element Analysis of Nonlinear Beam Vibrations," Journal of Sound and Vibration, Vol. 94, 1984, pp. 445-447.

69. Eisley, J. G., "Nonlinear Deformation of Elastic Beams, Rings and Strings," Applied Mechanic Review, Vol. 16, 1963, pp. 677-680.

70. Sathyamoorthy, M., "Nonlinear Analysis of Beams, Part I: A Survey of Recent Advances," The Shock and Vibration Digest, Vol. 14, No. 8, 1982, pp. 7-18.

71. Sathyamoorthy, M., "Nonlinear Analysis of Beams, Part II: Finite Element Methods," The Shock and Vibration Digest, Vol. 14, No. 8, 1982, pp. 19-35.

72. Chia, C. Y., Nonlinear Analysis of Plates, McGraw Hill Book Co., 1980.

73. Sathyamoorthy, M., "Nonlinear Vibrations of Plates - A Review," Shock and Vibration Digest, Vol. 15, 1983, pp. 3-16.

74. Abramowitz, M. and Stegun, I. A., Handbook of Mathematical Functions, Dover Publications, Inc., 1970, pp. 886.

75. Guyan, R. J., "Reduction of Stiffness and Mass Matrices," AIAA Journal, Vol. 3, No. 2, 1965, p. 380.

76. Bergan, P. G. and Clough, R. W., "Convergence Criteria for Iterative Process," AIAA Journal, Vol. 10, 1972, pp. 1107-1108.

77. Hsu, C. S., "On the Application of Elliptic Functions in Non-linear Forced Oscillations," Quarterly Applied Mathematics, Vol. 17, 1966, pp. 393-407.

78. Bogner, F. K., Fox, R. L. and Schmit, L. A., "The Generation of Inter-element Compatible Stiffness and Mass Matrices by the Use of Interpolation Formulas," AFFDL-TR-66-80, Wright Patterson AFB, OH, November 1966, pp. 396-443.

APPENDICES

APPENDIX A

CONVERGENCE CRITERIA

Three displacement convergence criteria (norms) used by Bergan and Clough[76] for multiple-mode nonlinear free and forced vibrations by the finite element method are employed. These three norms are the maximum norm, the modified absolute norm and the modified Euclidean norm.

The maximum norm is defined as

$$||\epsilon||_M = \max_j \left|\frac{\Delta v_j}{v_{j,ref}}\right| .$$ (A.1)

The modified absolute norm is defined as

$$||\epsilon||_A = \frac{1}{N} \sum_{j=1}^{N} \left|\frac{\Delta v_j}{v_{j,ref}}\right| .$$ (A.2)

The modified Euclidean norm is defined as

$$||\epsilon||_E = \left(\frac{1}{N} \sum_{j=1}^{N} \left|\frac{\Delta v_j}{v_{j,ref}}\right|^2\right)^{1/2} .$$ (A.3)

In these expressions, Δv_j is the change in displacement component j during iterative cycle n, and $v_{j,ref}$ is the reference displacement which is the largest displacement component of the corresponding "type". For instance in a nonlinear vibration problem involving deflections w and rotations $w_{,x}$, the reference displacements are the largest deflection and the largest rotation of the corresponding type.

APPENDIX B

TRANSFORMATION MATRIX FOR A BEAM ELEMENT

The transformation matrix for a beam element is expressed as

$$[T] = \begin{bmatrix}
1 & 0 & 0 & 0 & 0 & 0 & 0 & 0 \\
0 & 1 & 0 & 0 & 0 & 0 & 0 & 0 \\
\dfrac{-3}{\ell^2} & \dfrac{-2}{\ell} & \dfrac{3}{\ell^2} & \dfrac{-1}{\ell} & 0 & 0 & 0 & 0 \\
\dfrac{2}{\ell^3} & \dfrac{1}{\ell^2} & \dfrac{-2}{\ell^3} & \dfrac{1}{\ell^2} & 0 & 0 & 0 & 0 \\
0 & 0 & 0 & 0 & 1 & 0 & 0 & 0 \\
0 & 0 & 0 & 0 & 0 & 1 & 0 & 0 \\
0 & 0 & 0 & 0 & \dfrac{-3}{\ell^2} & \dfrac{-2}{\ell} & \dfrac{3}{\ell^2} & \dfrac{-1}{\ell} \\
0 & 0 & 0 & 0 & \dfrac{2}{\ell^3} & \dfrac{1}{\ell^2} & \dfrac{-2}{\ell^3} & \dfrac{1}{\ell^2}
\end{bmatrix} \quad (B1)$$

APPENDIX C

TRANSFORMATION MATRIX FOR A PLATE ELEMENT

The inverse of matrix $[T_b]$ in Eq. (5.24) is expressed as

$$
[\bar{T}_b]^{-1} =
\begin{array}{cccccccc}
\alpha_1 & & & \alpha_4 & & & & \alpha_8 \\
\end{array}
$$

$$
[\bar{T}_b]^{-1} =
\left[
\begin{array}{cccccccc}
1 & 0 & 0 & 0 & 0 & 0 & 0 & 0 \\
1 & \bar{a} & 0 & \bar{a}^{-2} & 0 & 0 & \bar{a}^{-3} & 0 \\
1 & \bar{a} & \bar{b} & \bar{a}^{-2} & \overline{ab} & \bar{b}^{-2} & \bar{a}^{-3} & \bar{a}^{-2}\bar{b} \\
1 & 0 & \bar{b} & 0 & 0 & \bar{b}^{-2} & 0 & 0 \\
0 & 1 & 0 & 0 & 0 & 0 & 0 & 0 \\
0 & 1 & 0 & 2\bar{a} & 0 & 0 & 3\bar{a}^{-2} & 0 \\
0 & 1 & 0 & 2\bar{a} & \bar{b} & 0 & 3\bar{a}^{-2} & 2\overline{ab} \\
0 & 1 & 0 & 0 & \bar{b} & 0 & 0 & 0 \\
0 & 0 & 1 & 0 & 0 & 0 & 0 & 0 \\
0 & 0 & 1 & 0 & \bar{a} & 0 & 0 & \bar{a}^{-2} \\
0 & 0 & 1 & 0 & \bar{a} & 2\bar{b} & 0 & \bar{a}^{-2} \\
0 & 0 & 1 & 0 & 0 & 2\bar{b} & 0 & 0 \\
0 & 0 & 0 & 0 & 1 & 0 & 0 & 0 \\
0 & 0 & 0 & 0 & 1 & 0 & 0 & 2\bar{a} \\
0 & 0 & 0 & 0 & 1 & 0 & 0 & 2\bar{a} \\
0 & 0 & 0 & 0 & 1 & 0 & 0 & 0 \\
\end{array}
\right]
$$

$$
\begin{array}{ccc}
\alpha_9 & \alpha_{12} & \alpha_{16}
\end{array}
$$

$$
\left[
\begin{array}{cccccccc}
0 & 0 & 0 & 0 & 0 & 0 & 0 & 0 \\
0 & 0 & 0 & 0 & 0 & 0 & 0 & 0 \\
\bar{a}\bar{b}^2 & \bar{b}^3 & \bar{a}^3\bar{b} & \bar{a}^2\bar{b}^2 & \bar{a}\bar{b}^3 & \bar{a}^3\bar{b}^2 & \bar{a}^2\bar{b}^3 & \bar{a}^3\bar{b}^3 \\
0 & \bar{b}^3 & 0 & 0 & 0 & 0 & 0 & 0 \\
0 & 0 & 0 & 0 & 0 & 0 & 0 & 0 \\
0 & 0 & 0 & 0 & 0 & 0 & 0 & 0 \\
\bar{b}^2 & 0 & 3\bar{a}^2\bar{b} & 2\bar{a}\bar{b}^2 & \bar{b}^3 & 3\bar{a}^2\bar{b}^2 & 2\bar{a}\bar{b}^3 & 3\bar{a}^2\bar{b}^3 \\
\bar{b}^2 & 0 & 0 & 0 & \bar{b}^3 & 0 & 0 & 0 \\
0 & 0 & 0 & 0 & 0 & 0 & 0 & 0 \\
0 & 0 & \bar{a}^3 & 0 & 0 & 0 & 0 & 0 \\
2\bar{a}\bar{b} & 3\bar{b}^2 & \bar{a}^3 & 2\bar{a}^2\bar{b} & 3\bar{a}\bar{b}^2 & 2\bar{a}^3\bar{b} & 3\bar{a}^2\bar{b}^2 & 3\bar{a}^3\bar{b}^2 \\
0 & 3\bar{b}^2 & 0 & 0 & 0 & 0 & 0 & 0 \\
0 & 0 & 0 & 0 & 0 & 0 & 0 & 0 \\
0 & 0 & 3\bar{a}^2 & 0 & 0 & 0 & 0 & 0 \\
2\bar{b} & 0 & 3\bar{a}^2 & 4\bar{a}\bar{b} & 3\bar{b}^2 & 6\bar{a}^2\bar{b} & 6\bar{a}\bar{b}^2 & 9\bar{a}^2\bar{b}^2 \\
2\bar{b} & 0 & 0 & 0 & 3\bar{b}^2 & 0 & 0 & 0
\end{array}
\right] \tag{C1}
$$

where $\bar{a}$ and $\bar{b}$ are the length and width of rectangular plate element.

Matrix $[T_S]$ in Eq. (5.25) is expressed as

$$[\bar{T}_S] = \begin{bmatrix}
\overset{U_1}{1} & 0 & 0 & \overset{U_4 \quad V_1}{0} & & & & \overset{V_4}{} \\
-a^* & a^* & 0 & 0 & & & 0 & \\
-b^* & 0 & 0 & b^* & & & & \\
a^*b^* & -a^*b^* & a^*b^* & -a^*b^* & & & & \\
 & & & & 1 & 0 & 0 & 0 \\
 & & & & -a^* & a^* & 0 & 0 \\
 & & 0 & & -b^* & 0 & 0 & b^* \\
 & & & & a^*b^* & -a^*b^* & a^*b^* & -a^*b^*
\end{bmatrix} \qquad (C2)$$

where $a^* = 1/\bar{a}$ and $b^* = 1/\bar{b}$.

Matrix $[\bar{H}]$ in Eq. (5.29) is expressed as

$$[\bar{H}] = - \begin{bmatrix}
\overset{\alpha_1}{0} & 0 & 0 & \overset{\alpha_4}{2} & 0 & 0 & 6x & \overset{\alpha_8}{2y} \\
0 & 0 & 0 & 0 & 0 & 2 & 0 & 0 \\
0 & 0 & 0 & 0 & 2 & 0 & 0 & 4x
\end{bmatrix}$$

$$\begin{bmatrix}
\overset{\alpha_9}{0} & 0 & 6xy & \overset{\alpha_{12}}{2y^2} & 0 & 6xy^2 & 2y^3 & \overset{\alpha_{16}}{6xy^3} \\
2x & 6y & 0 & 2x^2 & 6xy & 2x^3 & 6x^2y & 6x^3y \\
4y & 0 & 6x^2 & 8xy & 6y^2 & 12x^2y & 12xy^2 & 18x^2y^2
\end{bmatrix} \qquad (C3)$$

Matrix $[\bar{Q}]$ in Eq. (5.31) is expressed as

$$[\bar{Q}] = \begin{matrix} \overset{\alpha_1}{} & & & \overset{\alpha_4}{} & & & \overset{\alpha_8}{} & \\ 0 & 1 & 0 & 2x & y & 0 & 3x^2 & 2xy \\ 0 & 0 & 1 & 0 & x & 2y & 0 & x^2 \end{matrix}$$

$$\begin{matrix} \overset{\alpha_9}{} & & & \overset{\alpha_{12}}{} & & & & \overset{\alpha_{16}}{} \\ y^2 & 0 & 3x^2y & 2xy^2 & y^3 & 3x^2y^2 & 2xy^3 & 3x^2y^3 \\ 2xy & 3y^2 & x^3 & 2x^2y & 3xy^2 & 2x^3y & 3x^2y^2 & 3x^3y^2 \end{matrix} \quad (C4)$$

Matrix $[\bar{G}]$ in Eq. (5.48) is expressed as

$$[\bar{G}] = \begin{matrix} \overset{\beta_1}{} & & & \overset{\beta_4}{} & & & & \overset{\beta_8}{} \\ 0 & 1 & 0 & y & 0 & 0 & 0 & 0 \\ 0 & 0 & 0 & 0 & 0 & 0 & 1 & X \\ 0 & 0 & 1 & X & 0 & 1 & 0 & y \end{matrix} \quad (C5)$$

BIOGRAPHY

Kamolphan Decha-Umphai was born in Bangkok, Thailand, on April 1, 1956. In March 1979, he graduated from Khon Kaen University, Thailand, with a Bachelor of Science in Mechanical Engineering. He commenced full-time graduate study with Old Dominion University in Norfolk, Virginia, and graduated with a Master of Science degree in Mechanical Engineering in 1981. He then pursued his graduate study with Old Dominion University and became a candidate for the Doctor of Philosophy degree in Mechanical Engineering in 1986. During his graduate study, he was assigned to work in the National Aeronautics and Space Administration (NASA) at the Langley Research Center, Hampton, Virginia, as a graduate research assistant. He has published the following articles:

CONFERENCE PUBLICATIONS:

1. "A Finite Element Method for Nonlinear Forced Vibrations of Beams," with C. Mei, Proceedings of the Second International Conference on Recent Advances in Structural Dynamics, April 9-13, 1984, University of Southampton, England.

2. "Large Deflection, Large Amplitude Vibrations and Random Response of Symmetrically Laminated Rectangular Plates," with C. E. Gray and C. Mei, Proceedings of the 25th Structures, Structural Dynamics and Material Conference: Part 1, May 14-16, 1984, Palm Springs, California.

3. A Finite Element Method for Nonlinear Forced Vibrations of Rectangular Plates," with C. Mei, Proceedings of the 25th Structures, Structural Dynamics and Material Conference: Part 2, May 14-16, 1984, Palm Springs, California.

4. "Finite Element Method for Nonlinear Forced Vibrations of Circular Plates," Proceedings of the 26th Structures, Structural Dynamics and Material Conference: Part 2, April 15-17, 1985, Orlando, Florida.

5. "Multiple-Mode Nonlinear Free and Forced Vibrations of Beams Using Finite Element Method," with C. Mei, Proceedings of the 28th Structures, Structural Dynamics and Material Conference (to appear), April 6-8, 1987, Monterey, California.

JOURNAL PUBLICATIONS:

6. "A Finite Element Method for Nonlinear Forced Vibration of Beams," with C. Mei, Journal of Sound and Vibrations, Vol. 102, 1985, pp. 369-380.

7. "A Finite Element Method for Nonlinear Forced Vibrations of Rectangular Plate," with C. Mei, AIAA Journal, Vol. 23, 1985, pp. 1104-1110.

8. "Large Deflection, Large Amplitude Vibration and Random Response of Symmetrically Laminated Plates," with C. E. Gray, Jr. and C. Mei, Journal of Aircraft, Vol. 22, No. 11, 1985, pp. 929-930.

9. "Finite Element Method for Non-linear Forced Vibrations of Circular Plates," with C. Mei, International Journal of Numerical Methods in Engineering, Vol. 23, 1986, pp. 1715-1726.

He received "The Jefferson Goblet Award" at the 26th Structures, Structural Dynamics and Material Conference sponsored by AIAA, ASME, ASCE and AHS in April 1985, Orlando, Florida.